Copyright Warning & Restrictions

The copyright law of the United States (Title 17, United States Code) governs the making of photocopies or other reproductions of copyrighted material.

Under certain conditions specified in the law, libraries and archives are authorized to furnish a photocopy or other reproduction. One of these specified conditions is that the photocopy or reproduction is not to be "used for any purpose other than private study, scholarship, or research." If a, user makes a request for, or later uses, a photocopy or reproduction for purposes in excess of "fair use" that user may be liable for copyright infringement,

This institution reserves the right to refuse to accept a copying order if, in its judgment, fulfillment of the order would involve violation of copyright law.

Please Note: The author retains the copyright while the New Jersey Institute of Technology reserves the right to distribute this thesis or dissertation

Printing note: If you do not wish to print this page, then select "Pages from: first page # to: last page #" on the print dialog screen

FLUID FLOW AND GAS ABSORPTION

IN AN

EJECTOR VENTURI SCRUBBER

BY

ICLAL ATAY

Dissertation submitted to the Faculty of the Graduate School of the New Jersey Institute of Technology in partial fulfillment of the requirements for the degree of Doctor of Engineering Science

1986

APPROVAL SHEET

TITLE OF DISSERTATION: Fluid Flow and Gas Absorption in an Ejector Venturi Scrubber

NAME OF CANDIDATE: Iclal Atay
Doctor of Engineering Science, 1986

DISSERTAITON AND ABSTRACT APPROVED:

Dr. Gordon Lewandowski Associate Professor Department of Chemical Engineering and Chemistry	Date
Dr. Richard Trattner Professor Department of Chemical Engineering and Chemistry	Date
Dr. John McCormick Professor Department of Chemical Engineering and Chemistry	Date
Dr. Wing Wong Assistant Professor Department of Chemical Engineering and Chemistry	Date
Professor Paul Cheremisinoff Professor Department of Civil and Environmental Engineering	Date

VITA

NAME: Iclal Atay

DEGREE AND DATE
TO BE CONFERRED: Doctor Engineering Science, 1986

SECONDARY SCHOOL: Saint Benoit Lycee, 1972

COLLEGIATE INSTITUTIONS ATTENDED	DATES	DEGREE	DATE OF DEGREE
New Jersey Institute of Technology	1980-86	D. Eng. Sc.	1986
New Jersey Institute of Technology	1979-80	M.S. En. E.	1980
Middle East Technical University	1973-78	B.S. Chem. E.	1978

MAJOR: Chemical Engineering

PUBLICATIONS:

"Surfactant Enhanced Scrubbing of Hydrocarbon Vapors from Air Exhaust Streams in an Ejector Venturi Scrubber." M. S. Thesis, New Jersey Institute of Technology, 1980

"Various Methods of Controlling Sulfur Dioxide Emissions." Environmental News Journal, University of Bosphorous, Istanbul, Turkey, No. 5, p. 45-50 (1980)

ABSTRACT

TITLE OF DISSERTATION: Fluid Flow and Gas Absorption in an Ejector Venturi Scrubber

ICLAL ATAY, Doctor of Engineering Science, 1986

DISSERTATION DIRECTED BY: Dr. Gordon Lewandowski, Associate Professor of Chemical Engineering

Dr. Richard Trattner, Professor of Chemistry

Empirical models were developed to describe the fluid flow characteristics and gas absorption efficiency of an ejector venturi scrubber. The empirical constants were determined experimentally using stop action photographs of the spray, static pressure measurements, and sulfur dioxide absorption efficiencies.

To take photographs of the spray, a 2 foot high, clear plastic ejector venturi scrubber was used, with a 4 inch diameter gas entrance port. Photographic equipment included a Hasselblad camera, Xenon flash lamp, and Polaroid 667 ASA 3000 film. Exposure duration was about 1 microsecond, resulting in complete stop-action of the spray droplets at liquid rates up to 6 gpm. Droplet size ranged from 34 to 563 microns, with a volume mean diameter of 155 microns, at a liquid rate of 6 gpm.

The sulfur dioxide mass transfer coefficient ($K_g a$) varied from 0.6 to 796 lb-moles/hr-ft^3 as the liquid delivery rate was varied from 1 to 8 gpm (i.e. from no atomization to complete atomization).

To my husband Erhan Atay
and my son Atahan Atay

ACKNOWLEDGEMENTS

I wish to express my gratitude to the following people who contributed towards the completion of this dissertation:

Dr. Gordon Lewandowski, my advisor, whose advice, patience and suggestions were fundamental to the success of this work.

Dr. Richard Trattner, my advisor, for his interest and help throughout the course of the project.

Dr. Joseph Bozzelli for lending me his manometer and the dry gas meters, and for his patience.

Dr. William R. Schowalter, Princeton University, for lending me the Xenon flash lamp.

Mr. Edward Karan, for his assistance in the construction of the experimental apparatus.

Dr. Dana Knox for his advice on use of the IBM-PC.

Mrs. Donna Olsen, my friend, for typing this dissertation.

Mr. Erhan Atay, my husband, for helping me do the experimental work and for supporting and pushing me through my ups and downs.

And finally, Mr. Atahan Atay, my four year old son, for his understanding.

TABLE OF CONTENTS

LIST OF TABLES

LIST OF FIGURES

I. INTRODUCTION

The Ejector Venturi Scrubber is a wet type of contactor, which utilizes a liquid media to absorb objectionable gases and particulates from a flue gas discharge stream. Venturi type scrubbers utilize a high velocity section for bringing the liquid and gas into intimate contact with each other. They basically fall into two groups: (1) Those using a mechanical blower to draw a high velocity gas stream through the system. The liquid is originally at rest and is accelerated by the gas, which also disrupts the liquid into droplets. Gases and particulate are then captured by the slower moving (relatively) droplets. This is called a "high energy" venturi scrubber. (2) Those using a mechanical pump to impart a high velocity to the liquid, which accelerates the slower moving (relatively) gas stream. The liquid is disrupted into droplets as it passes through an atomizing nozzle. The gas is drawn through the system by transfer of momentum from the liquid. This type is called an "ejector" venturi scrubber. The two types of venturi scrubber have entirely different energy consumption, atomization, and scrubbing efficiency characteristics. This study focuses on the ejector type.

The ejector venturi scrubber uses the high velocity energy of the liquid jet stream to (1) breakup and distribute the liquid stream into a multitude of small drops, and (2) to pump the gas through the scrubbing system and connecting ductwork. This is a highly efficient way of atomizing the liquid and a less efficient way of pumping gas. However,

it eliminates the need for a separate blower and for having moving mechanical parts in contact with the gas stream. By comparison, the high energy venturi scrubber which uses a blower to move the gas, atomizes the liquid pneumatically by contact in the venturi throat. This is a highly efficient way of pumping gas through the system, and a less efficient way of atomizing liquid.

The ejector venturi scrubber is illustrated in Figure 1.1 and is usually used in series with a gravity or inertial impact separator to remove the scrubbing liquid from the gas stream.

Ejector venturi's also have been widely used in industry for purposes other than scrubbing (see Table 1.1). They are known by various names, which are usually associated with the application. Among such names are injector, ejector, eductor and water jet heat exchanger. The steam injector, for example, is a jet pump designed to supply feed water to a steam boiler, the driving fluid being a proportion of the steam generated by the boiler. The water jet ejector, on the other hand, is designed to draw leakage air and other non-condensible gases from the exhaust of a steam turbine plant. The water jet heat exchanger is essentially the same as a steam jet injector, the name signifying that the pump supplies heat to the feed water.

There are four basic forms of ejectors: gas-gas, liquid-liquid, gas-liquid, and liquid-gas (the first mentioned fluid in each case being the motivating fluid). Ejectors may also be classified in

accordance with the fluid components and fluid phases. For example, a steam jet water injector is a two phase, one component ejector since steam and water are two different phases of the same fluid. A water jet air ejector on the other hand, is a two component two phase ejector.

A literature search was performed of the Compendex Database using the Dialog Information Retrieval Service. The Compendex Database is the machine readable version of the Engineering Index which provides abstracted information from the world's significant engineering and technological literature. It provides world-wide coverage of approximately 3500 journals, publications of engineering societies and organizations, papers from the proceedings of conferences, and selected government reports and books. A Total of 131 papers have been reviewed, covering the period from 1968 through present. The state of the art review of Bonnington and King (1972) on jet pumps and ejectors has been used for the period from 1922 through 1972. The review includes more than 300 papers. Also a literature search of the Dissertation Abstracts has been conducted for the period 1975 to 1985, for any unpublished work.

Although there is a considerable body of information available on the theory and performance of high energy venturi scrubbers, there is almost no information available on ejector venturi scrubbers. Hence, the purpose of this thesis was: (1) to develop an empirical model of

ejector scrubber performance, and (2) to develop the experimental techniques needed to evaluate the model.

II. MECHANISMS BY WHICH A LIQUID JET, INJECTED THROUGH A NOZZLE INTO A CHAMBER OF GAS, BREAKS UP INTO DROPLETS

Jet breakup is a complex process which is dependent upon the physical properties of both the liquid and gas phases, the velocities and temperatures of the fluids and the nozzle geometry.

Due to the importance of sprays in technological applications, a vast amount of literature has accumulated on the subject, including several extensive reviews [Tate (1969), Lapple et. al. (1967), Ranz (1956), DeJuhasz (1960)] and books dealing with the subject of sprays [Giffen and Muraszew (1953), Orr (1966), Levich (1962)]. In spite of this profusion of literature, many important aspects of spray formation are poorly understood.

Recent publications have attempted to categorize the jet breakup phenomena in terms of the operating conditions. Grant and Middleman (1966) reviewed the behavior of low speed jets and reported the results in the form of a "breakup curve" which describes the length of the coherent portion of the liquid jet from the nozzle tip (breakup length X_B) as a function of jet velocity V_o. This is shown in Figure 2.1. The jet breakup length at first increases linearly with increasing jet velocity, reaches a maximum, and then decreases. Beyond this point there remains confusion over the true shape of the breakup curve. Haenlein (1932) reported that the jet breakup length in this region increases slightly with increasing jet velocity and then abruptly

reduces to zero. McCarthy and Molloy (1974) report that there is some evidence that the breakup length continually increases.

Reitz (1978) summarized that there are at least four regimes of jet breakup which reflect the action of different forces on the jet causing changes in the jet breakup length. The regime classification presented by him is consistent with the suggestions of Lee and Spencer (1933), Haenlein (1932), and Giffen and Muraszew (1953).

These four regimes in the order of increasing velocity are as follows:

1. Rayleigh Jet Breakup

In this regime, jet velocities range from 0 up to 500 meters per second. The breakup occurs many jet diameters downstream of the nozzle, yielding drops whose diameter exceeds that of the growth of axisymmetric oscillations of the jet surface, induced by surface tension effects. (Figure 2.2)

2. First Wind Induced Breakup Regime

In this regime, jet velocities range from 500 up to 1000 meters per second. The breakup occurs many jet diameters downstream of the nozzle, yielding drops whose diameter is of the order of the jet diameter. In this case, the surface tension effect is

augmented by the relative motion of the liquid and gas which produces a static pressure distribution across the jet, thereby accelerating the breakup process. (Figure 2.2)

3. Second Wind Induced Breakup Regime

In this regime, jet velocities range from 1000 up to 1800 meters per second. The breakup occurs some jet diameters downstream of the nozzle, yielding drops whose average diameter is very much less than the jet diameter. Droplet formation results from the unstable growth of short wavelength perturbations on the jet surface, caused by the relative motion between the liquid and gas. Here surface tension opposes the wave growth. (Figure 2.2)

4. Atomization Regime

In this regime jet velocities are higher than 1800 meters per second. The breakup occurs as the liquid exits from the nozzle, and results in a complete and immediate disruption of the liquid jet. Droplets are formed whose average diameter is very much less than the nozzle diameter. (Figure 2.2)

However, one must keep in mind that velocity is not the only criteria that determines the regime boundaries. The physical properties of the liquid, the nozzle geometry, the surrounding gas (stagnant or moving, atmospheric or pressurized) are all factors affecting the

breakup regime. Ranz (1956) developed such criteria by balancing inertial forces with surface tension forces and neglecting the effect of viscous shear stress. However, Reitz (1978) determined in his experimental studies that those criteria are not applicable in the atomization regime.

Much progress has been made toward an understanding of the fundamental breakup forces for low velocity jets. Reitz (1978) presented an analysis of stability of liquid jets, based on the equations of motion, to give a unified theory of the breakup of liquid jets in the first three regimes. This analysis is valuable towards an understanding of jet breakup in the atomization regime, which is the regime of interest in the present study.

Due to the importance of atomized sprays in practical applications, a considerable amount of literature has emerged over the last six decades, particularly in the 1930's. The most notable body of work is of an experimental nature, examining gross properties of the spray itself (penetration of spray into surrounding medium, uniformity of mass distribution over a given cross section, and drop size distribution within the spray envelope). Although such experiments have helped lead to a qualitative understanding of the behavior of sprays, little is known about the droplet formation mechanism itself, and therefore, the current characterization of the spray cannot be as quantitiative as needed.

The basic feature of liquid disintegration in the atomization regime is that the coherent length of the jet approaches zero, in which case the spray takes the form of a cone with the orifice as vortex. There exists, however, controversy about the magnitude of the jet breakup length, as some authors claim that the breakup occurs some jet diameters from the orifice [Castleman (1931)], while others claim that disintegration begins within the nozzle itself [DeJuhasz (1931)].

Figure 2.3 illustrates the breakup of a fan spray. The formation of liquid sheets, followed by filaments which further breakup into droplets, is clearly observed. A recent review and discussion of the factors affecting the breakup of droplets is given in Collins and Charwat (1971).

A. AERODYNAMIC JET BREAKUP HYPOTHESIS

Castleman (1931) postulated that jet breakup in this regime is due to aerodynamic interaction between the liquid and gas phases. He argued that this interaction leads to formation of ligaments, or liquid columns, which have one end still attached to the surface of the jet. Once formed, these ligaments rupture according to Rayleigh's classical breakup theory. The diameter of these columns was postulated to be of the order of the diameter of the drops found in the sprays. He proposed that the formation of the ligaments was due to the relative gas liquid motion, and he observed from the experimental results of Sauter (1929) that the size of the ligaments, and hence their lifetimes,

decreased (producing smaller drops) as the relative velocity increased. He argued that a lower limit on the drop size would be reached when the ligaments collapse as soon as they are formed.

Ranz (1956) analyzed the forces involved and the energy expended in the ligament model of breakup. He considered the ligament to be stretched by the action of the relative motion of the gas and liquid flows and found that the surface energy creation rate was comparable to the viscous dissipation rate [Monk (1952)], and that the surface tension forces and viscous forces opposing the stretching process were approximately equal. He postulated that the ligament diameters, and thus the drop sizes, were related to the wavelengths of unstable aerodynamicallly induced surface waves growing on the core of the surface.

The ligament model of jet atomization can be thought of as a limiting case of the Second Wind Induced Breakup regime. Various authors have objected to this jet atomization model by arguing that photographs of atomized jets show that the jet breakup process occurs immediately as the jet enters the chamber gas. They reasoned that aerodynamically induced wave growth takes time to develop and thus the model cannot explain the photographic results. However, the photograph of a fan spray in Figure 2.3 clearly shows filament formation.

B. LIQUID TURBULENCE AND JET BREAKUP

DeJuhasz (1931) proposed that the jet breakup process possibly occurs within the nozzle itself, after observing the apparent complete disintegration of the liquid jet at the nozzle exit in photographs. He suggested that liquid turbulence plays a dominant role in the jet breakup process.

Holroyd (1933) used dimensional reasoning to postulate that a balance between the centrifugal force (arising from angular turbulent velocity components) and the opposing surface tension force may account for the jet breakup process.

Schweitzer (1937) noted the existence of a radial component of velocity in turbulent pipe flow and argued that this radial flow could cause the disruption of the jet surface as soon as the jet emerged from the nozzle. This led him to reason that the effect of turbulence in the liquid flow is to disturb the jet/gas interface and to augment the aerodynamic jet breakup effects. He proposed that if the emerging jet were truly laminar, no immediate breakup would occur, and hence liquid turbulence is essential to the jet breakup mechanism. Conversely, Bergwerk (1959) discredited the effects of liquid turbulence by arguing that the turbulent velocity components in the Reynolds number range of interest in fuel injection applications are not of sufficient magnitude to explain the observed phenomena.

C. LIQUID CAVITATION AND JET BREAKUP

Berwerk (1959) paid particular attention to the liquid flow field within the injection nozzle and its influence on the jet breakup process. He observed the presence of liquid cavitation regions within the nozzles he tested, and this led him to suspect that the liquid cavitation phenomena may play a role in the jet atomization mechanism. He also found that nozzles with short L/d_o ratios, and sharp edged inlet sections, allowed complete detachment of the liquid flow from the nozzle walls under certain conditions. The jets obtained showed no tendency to disintegrate. In the case of attached flows, the experiments (made using transparent nozzles) revealed local cavitation regions within the nozzles. The emerging jets, injected into atmospheric air, now had a ruffled appearance. This behavior has also been noted by Nurick (1976) and Northrup (1951). Bergwerk (1959) surmised that the reattachment of the flow beyond the cavitation zone created large amplitude turbulent disturbances which were responsible for the waviness of the jet surface seen in the vicinity of the nozzle exit.

Sadek (1959) hypothesized that cavitation bubbles which are formed in the cavitation region and swept along with the flow may influence the jet breakup process.

D. VELOCITY PROFILE REARRANGEMENT AND JET BREAKUP

The kinetic energy per unit mass of the discharged liquid is dependent on the initial fluid velocity profile at the nozzle exit. In pipe flow, with a parabolic velocity profile, the kinetic energy of the

fluid is twice what it would be if the fluid had a uniform velocity profile with the same average velocity. In the course of the passage of the jets into the chamber gas, the profile relaxes to a nearly flat profile. Rupe (1962) suggested that the excess kinetic energy is redistributed and converted into potential energy within the jet. Since the kinetic energy is concentrated along the core of the jet, this produces a radial pressure gradient, and hence radial velocities within the jet. He postulated that these radial velocity components could disrupt the jet, leading to the formation of ligaments which could then be broken up by aerodynamic forces. To support his theory he conducted experiments with high velocity liquid jets injected into air. He found that jets from nozzles with large L/d_o ratios (L/d_o 200; i.e fully developed turbulent flows), as well as detached jets from a sharp edged orifice in a thin flat plate (L/d_o 1/10) (both of which have relatively flat exit velocity profiles), showed more stability than jets with parabolic exit velocity profiles.

E. OTHER MECHANIMS OF JET BREAKUP

Giffen and Muraszew (1953) considered the effect of the physical properties of the fluids, nozzle geometry and operating conditions, on the size of the drops found far downstream of the nozzle, by examining the sequence of events which constitute the atomization process. They noted that liquid supply pressure oscillations can have an important effect on the jet breakup process.

Shkadov (1970) described the liquid flow using boundary layer theory with a prescribed tangential stress at the interface. For the case of constant shear stress, the analysis revealed the existence of unstable short wavelength surface waves, which could contribute to jet atomization.

In summary, the atomization process is a very complex phenomenon. None of the above mentioned hypotheses alone could fully explain the mechanisms of atomization. Most of the hypotheses are contradictory to someone elses work. Most of the work in the literature was on fuel injection systems with low liquid volumetric flow rates (0.1 gallons per minute) into a chamber of quiescent gas. When considering (as in the present study) atomization of liquid sprays of high volumetric flow rates ($\sim$ 6 gallons per minute), injected into an ejector venturi scrubber, where the walls of the scrubber limit the expansion of the spray along the axis, where large volumes of gas are entrained by the liquid, and where the static pressure varies along the length of the scrubber, the evaluation of the mechanisms of atomization becomes much more complex. Therefore, the atomization theory is still uncertain even after more than 100 years of analysis, begun by Rayleigh in 1878.

III. DROP SIZE DISTRIBUTION

The breakup of liquid jets is achieved through a large variety of atomizers and for an even larger variety of applications [Giffen and Muraszew (1953), Dombrowski and Mundy (1968)]. Its purpose is to increase the surface to volume ratio of the liquid thus increasing the specific rates of mass and heat transfer and the vaporization rate.

When a liquid is forced through a cylindrical hole into a gas many modes of breakup are observed. The regime of interest in this study is the atomization regime which is reached at high injection velocities (100 ft/sec).

Because of their practical importance, many aspects of atomizing jets have been studied extensively. As summarized by Giffen and Muraszew (1953), Taylor (1968), and Obert (1973), in the 1930's significant data were collected on downstream drop sizes, tip penetration rates, and average spray angles.

A. DROP BREAKUP MODES

The breakup of the liquid drops by the convective gas flow has been shown to be important in combustion, rain erosion, and other two phase phenomena. When a spherical liquid drop is subjected to a convective gase flow, it will initially become flattened due to pressure difference between the stagnation points at the front and rear of

the drop and the lower pressure at the drop center. In addition to this distortion, the dynamic pressure exerted on the drop by gas flow also causes the drop to vibrate, and may cause it to breakup. Four rather distinct breakup modes have been observed; vibrational, bag, stripping, and chaotic.

Vibrational breakup occurs at very low convective flow speeds and results from the buildup of oscillations at the drop's natural frequency. If the gas flow interacts with the drop in such a way that the magnitude of these oscillations is amplified, then the drop will typically break into two smaller drops. Blanchard (1950) has published stroboscopic pictures of drops undergoing vibrational breakup. This type of breakup typically occurs on the order of seconds or even tens of seconds, and is consequently usually observed in a vertical wind tunnel or in free fall.

At slightly higher flow speeds, and consequently higher dynamic pressure, a drop typically exhibits the "bag" type of breakup which was observed by Lane (1951). When the drop is first exposed to gas flow it becomes flattened and then the center bows out in the downstream direction, such that the drop assumes a "bag" shape with the open end attached to a toroidal rim. The bag eventually shatters into many tiny drops, leaving the toroidal ring which persists for a short time before it too breaks up, but into much larger drops than those provided from the "bag". This type of breakup has been explained in two ways in the literature. The most common explanation, as advanced by Hinze (1949),

Gordon (1959), and Hass (1964) is that the breakup is due entirely to the pressure difference which develops between the front and back of the drop. The other explanation, due to O'Brien (1961), and also discussed by Blanchard (1962) is that the breakup is due to vortex instability; ie., that circulation is generated within the drop, which results in the development of the toroidal ring which then becomes unstable. Pictures of bag breakup, which typically occurs in milliseconds, have been published by Batchelor and Davis (1956).

The stripping mode of breakup is typically observed in the transient convective flow behind shock waves, with a typical breakup time being on the order of hundreds of microseconds. Investigations of this flow regime were first conducted by Lane (1951), and later by Engel (1958), Ranger and Nicholls (1969), and Krauss (1970). A drop exposed to the dynamic pressure created by flow speeds in this regime becomes flattened, but the front of the drop becomes convex, while the rear of the drop is almost flat (just the opposite of the "bag" type distortion). Liquid is observed continuously leaving the equator of the drop in the form of a micro-mist, which is then swept downstream and mixed in the wake.

The fourth breakup mode, the chaotic type, is observed at very high dynamic pressure with breakup typically occurring in tens of microseconds. Investigations of this mode have determined that when a drop is accelerated extremely rapidly, large waves develop on its surface, and it appears to suddenly disintegrate into a cloud of small droplets.

According to Taylor (1968), if two fluids of different density are accelerated perpendicular to their interface, the interface is unstable if the acceleration vector is directed toward the higher density fluid. The front surface of the drop is just this type of unstable gas liquid interface. Thus when the drop is accelerated very rapidly, waves develop on its surface and when the amplitude of these waves becomes comparable to the drop thickness, the drop completely shatters.

Most investigators of drop breakup attempt to find the critical value for a non-dimensional parameter corresponding to the point of transition between breakup modes, or to determine a method for calculating the time for a drop to breakup in a particular mode. The non-dimensional number most often mentioned in studies of drop breakup is the Weber Number, which is defined as the ratio of the dynamic pressure force to the surface tension force. This is an important parameter since the external pressure exerted by the gas flow is the driving force that causes a drop to become distorted, and the liquid surface tension is the principal force resisting this distortion. The role of several important non-dimensional numbers associated with drop breakup has been disputed by Reinecke and Waldman (1975).

B. FACTORS EFFECTING DROP SIZE DISTRIBUTION:

Giffen and Muraszew (1953) found experimentally that an important parameter in the determination of the drop size is the effective injection pressure, Δp (this is shown in Figures 3.1 and 3.2). An

examination of the drop size distribution (see Figure 3.2) shows that the effect of the increased injection pressure is to reduce the size of the large drops in the spray. Both figures indicate that an increase of the injection pressure beyond about 500 psia (330 atm) seems to have very little effect on the droplet size, setting a limit on the magnitude of the injection pressure for use in practical applications. The data of Retel (1938) and Mehlig (1934), however, indicate an increase in the droplet size when the injection pressure is further increased, and it has been postulated that this effect is due to coalescence of the spray droplets due to collisions within the spray envelope, (since the spray cone angle, which generally increases with increasing injection pressure, changes very little in this regime).

As can be seen in Figure 3.1, the effect of increased gas density in the spray chamber is to reduce the measured drop size. Giffen and Muraszew (1953) found that at high gas densities, or high injection pressures, the effect of small changes in the nozzle design (L/d_o ratio) on the droplet size is also small.

In general, the effect of the liquid viscosity is to delay and damp any tendency for deformation of a liquid surface. This contention is supported by the experimental finding that droplet size increases with increasing liquid viscosity.

The effect of gas viscosity (which increases slightly with increasing chamber pressure and temperature) and surface tension on

droplet size is not clear. While droplets are being formed from a continuous liquid jet, surface tension would tend to oppose any surface deformation and, in general, it is found that a low value of surface tension promotes the formation of a finer spray.

Hinze (1949) considered the forces involved in the drop formation process and by dimensional analyses recommended the use of three independent dimensionless products in any description of the droplet size:

$$\frac{r}{d_o} = f\left(\frac{\rho_l V_o^2 d_o}{\sigma}, \frac{\sigma \rho_l d_o}{\mu_l^2}, \frac{\rho_l}{\rho_g}\right)$$

Empirical droplet size correlations are presented in Table 3.1 [summarized in Lapple et al. (1967)], where it is seen that various discrepancies, particularly with respect to the effects of surface tension and gas viscosity, are found between results obtained by different authors.

Dombrowski and Hooper (1962) made a study of the stability and disintegration of flat sheets produced by single hole spray nozzles at various densities of the surrounding air. They showed that a flat laminar sheet injected in vacuo is stable, and that drops are formed only at its edges. At higher air densities the sheet is destroyed by aerodynamic waves, and previous theories predicting their wavelength and growth have been extended to show that the form of this controlling equation is critically dependent on the operating conditions. They

also demonstrated that the drop size decreases, passing through a minimum, and then increases with increasing gas density.

Bayvel and Veziroglu (1980) determined the droplet size distribution in a venturi scrubber by using a device based on light scattering. The throat and a diverging section of the venturi tube were transilluminated by a laser beam and the scattering patterns were measured. From their data they determined the mass drop size distributions. They did not observe any dependence of the drop size distribution on the liquid-to-gas ratio. Comparison of their results with those of Nukiyama and Tanasawa (1938), using the Sauter mean drop radius, is shown in Figure 3.3.

C. METHODS OF DROP SIZE MEASUREMENT AND RELATED THEORIES

The methods used in the determination of droplet size in the early studies of atomization are well documented by Giffen and Muraszew (1953). The most common techniques involved the collection of spray samples in specially prepared receptacles, and their subsequent microscopic or photographic analysis. Optical techniques relying on absorption [Sauter (1929)], diffraction [Dobbins, et al. (1963) and Swithenbank (1975)], holography [Pavitt et, al. (1970) and Trolinger (1975)], and direct photography [Borman et al. (1972)] have been used for dilute sprays.

In the majority of spray applications, a quantitative knowledge of the surface-to-volume relationship is essential.

Fraser and Eisenklam (1956) captured water drops in an oil bath. They than photographed, measured, and counted the drops. The properties of the collecting oil medium relative to the sprayed liquid were such that the drops remained suspended under the surface of the medium and coalescence is prevented, sphericity preserved, and evaporation eliminated. The collecting bath was a microscope slide surrounded by a frame, and containing Shell Cornea Oil 69(BF3) mixed with 3.5% by weight aniline, 2.0% benzene, and 8% vaseline. This mixture has low mutual solubility with the drops, but similar density and surface properties, such that the submersion of the drops is as complete as possible. Sampling was carried out in a draft-free chamber, having a relative humidity of at least 95%, so that the effect of evaporation during spraying was minimized. Droplets were collected near the region of disintegration of liquid sheets, i.e. about 1.5 feet from the nozzle, and the spray was directed vertically downwards. The slide containing the mixture was passed through the spray at a uniform speed. The photograph was taken immediately after sampling with a diameter magnification of ten. The analysis of the record was carried out on a 10x magnification of the negative, so that a drop with diameter of 10 μm appeared 1 mm in diameter.

Clark and Dombrowski (1973) made a critical assessment of the commonly accepted weighting procedure for analyzing photographs of

sprays. They demonstrated that because of the periodic nature of drop formation, unsteady state conditions may persist near the atomizer which give rise to unpredictable errors. They stated that the processes of drop formation occur in a periodic manner to an extent dependent upon the way in which energy is imparted to the liquid, as well as the physical properties of the liquid and ambient atmosphere. Fragments are periodically detached from the liquid stream and suffer continuous breakdown from their free edges as they move through the atmosphere. Consequently, when atomization is complete, diffuse bands of drops with a large range of velocities are produced. They further stated that the spatial droplet distribution, as represented by the first discrete band of drops, will be identical to the actual distribution of the spray, and that it would be incorrect to the use weighted size distribution even though the drops may be travelling at different speeds. They analyzed by statistical techniques the relationship between the true and weighted drop size distributions. For this purpose they used the particle density equation of Cox and Miller (1970), and the root-normal distribution function of Tate and Marshall (1953). They assumed that fragments are detached from the spray at regular intervals, and subsequent drop formation occurs only at the front of each fragment and moves progressively to the rear. The plane in which drop formation takes place is at a fixed distance from the nozzle. They further assumed that for a given drop size, the number of drops generated per unit area is constant, and that all drops are projected downstream with the same initial velocity. They calculated that very accurate results

can be expected from spatial distributions near the region of disintegration (Figure 3.4 and 3.5).

Boll et al. (1974) determined the mean drop size in a full scale venturi scrubber using a transmissometer. They conducted their experiments in a rectangular venturi scrubber with four nozzles. By their techniques they claim D_{32} can be determined to within $\pm$ 15%. However, to be able to know the liquid concentration, it was essential to place the transmissometer at the point in the venturi where the liquid and gas velocities were equal. The location was determined using a model developed by Boll (1973), and was found to vary between 4.5 and 61 inches below the throat.

Light scattering offers advantages over techniques for particle size analysis because the system can be observed "in situ" without perturbing the spray and the measurements are almost instantaneous. The scattered light can be recorded continuously and unsteady processes may be studied.

The main difficulty in the use of light scattering arises because of the insensitivity of the scattering data with respect to the particle size distributions. For a polydispersed system, there can be many size distributions that lead to a particular set of data, at least within the experimental uncertainty. In particle size analysis, it is usually assumed that the scattering by a cloud of particles is incoherent so that the cumulative effect is obtained by adding the intensity

scattered by each particle. In order for these conditions to apply, the particles must be randomly positioned in space, and the system must be sufficiently dilute. When the particles are very close to each other, their polarization fields interact and the scattering functions are different from those of the isolated particles and are difficult to evaluate. Even when the particles are more than several diameters apart so that mutual polarization is absent, some of the radiation scattered by a particular particle will be incident upon a second particle, which then rescatters it. This is called multiple scattering. It is significant in any particle cloud transmitting less than about 90% of the incident radiation [Kerker (1969)].

Recently, the availability of laser sources, photodetector arrays, and computers has made it possible to determine the drop size distribution from a measurement of the diffracted light intensity. Many approaches can be found in the litertaure , but two methods are most widely used. The first method was developed by Swithenbank et al. (1976) and uses measurements of light energy distribution in the Fraunhofer pattern. A special detector is used which is divided into a set of circular rings, each of which is sensitive to a particular particle size. The size distribution of the drops must be approximated by a discrete distribution of a finite number of size ranges, equal to the number of rings of the detector. The total light energy distribution is the sum of the product of the energy distribution for each size range and the mass fraction in that range. The second method is based on the measurement of the diffracted intensity distribution given by the Fraunhofer formula, [Boyvel and Jones (1981)]. The scattered

intensity distribution is measured at small angles ($\theta_s < 10^o$), because the forward lobe in the scattering diagram can be calculated reasonably well from Fraunhofer theory.

D. MATHEMATICAL EXPRESSIONS FOR MEAN DROP SIZE AND DROP SIZE DISTRIBUTIONS

The size of the drops found in sprays covers a broad range due to the process of atomization, collisions and coalescence between drops, secondary breakup of drops, and evaporation. A distribution function is usually employed to represent the various sizes. Drops are counted (from photographs, as in the present study, or from sampling cells) and divided in groups according to their diameter. Let ΔN be the number of drops with diameters in the range $D-\Delta D/2$ and $D+\Delta D/2$ and let D range from 0 to infinity in practice to some upper value. Therefore, the drop size distribution functions f_N and f_V can be constructed as [Ko-Jen Wu (1983)]:

$$f_N dD = dN$$

and

$$f_V dD = dV = \frac{\pi}{6} D^3 dN$$

The total number N and total volume V of all the drops sampled can be calculated by integration over the drop diameter as

$$N = \int_0^\infty f_N dD$$

and

$$V = \int_0^\infty f_V dD$$

The normalized distribution functions are defined as

$$f_N^* dD = f_N/N \; dD$$

and

$$f_V^* dD = f_V/V \; dD$$

and give the number and volume fractions contributed by drops with diameters between D-dD/2 and D+dD/2. In many applications it is found convenient to express the drop size distribution function in cumulative forms,

$$N^* = \int_0^D f_N^* dD$$

representing the cumulative number fraction of drops smaller than D, and

$$V^* = \int_0^D f_N^* \; dD$$

the cumulative volume fraction of drops smaller than D. Drop mean diameters Dpq are often used to describe the quality of atomization and are defined by

$$D_{pq} = \left(\frac{\int f_N^* \; D^p dD}{\int f_N^* \; D^q dD} \right)^{\frac{1}{p-q}}$$

where p and q vary according to the application.

Various mathematical expressions for the distributions have been proposed according to their ability to fit the data. These

correlations were obtained from different types of atomizers under different operating conditions. Consequently, they are applicable within a certain range of operating conditions and properties of fluids, as summarized in Table 3.2.

Most investigators [Nukiyama and Tanasawa (1938-1940), Lewis et al. (1948), Hrubecky, (1958), Gretzinger and Marshall (1961)] performed the experiments on pneumatic atomization using nozzles of very small size at very high relative velocity. Liquid injection was either parallel or opposite to the gas flow. It is questionable whether these correlations can be applied to a full size venturi scrubber with a mechanical swirl nozzle as used in the present work.

Among these correlations, the most widely quoted correlation is that of Nukiyama and Tanasawa (1938) which has been used extensively in estimating drop size in high energy venturi scrubbers. They performed extensive experiments on pneumatic atomization in which various liquids were injected in a direction parallel to a high velocity air stream. They found that the mean droplet diameter was not affected by the shape of air or water nozzles, and presented an empirical correlation to predict the mean droplet size (as a Sauter mean diameter) in the case of pneumatic atomization, as shown in Table 3.2. Analysis of this correlation show that its applicability is limited to the range of high relative velocities and low liquid-to-gas (L/G) ratios.

In addition, Nukiyama-Tanasawa also studied the effects of position and shape of liquid nozzles on the atomization of liquids normal to the air jet. This method of atomization was observed to be inferior to that obtained with parallel flow [which was confirmed later by Hrubecky (1958)].

The Nukiyama-Tanasawa equation was tested by Lewis et al. (1948) and Hrubecky (1958) who performed atomization tests in which liquid injection was parallel to the air flow. Lewis et al. (1948) studied the atomization of oil (ρ_L = 1.04 gm/cm^3, μ_L = 0.09 cp, σ = 34 dynes/cm) by nitrogen gas in a venturi atomizer at a velocity of 214 m/s and L/G of 0.14-1.8 liters/m^3. The experimental Sauter mean diameters were roughly one-half the values predicted by the Nukiyama-Tanasawa equation.

The atomization of water by a high-velocity air stream from convergent nozzles (velocity = 106-316 m/s, L/G = 0.04-1 liters/m^3) was performed by Hrubecky (1958). The measured mean diameters were found to be in good agreement (about 85% - 120%) with those estimated by the Nukiyama-Tanasawa equation. The experimental results also indicated that water injection into the region of maximum gas velocity, parallel to the air flow, gave the highest degree of atomization under similar conditions.

Mugele (1960) developed an expression for estimating the maximum and mean drop sizes by dimensional analysis. The correlations related

the drop sizes as functions of the interfacial tension and Reynolds number groups as shown in Table 3.1. A, B, C are constants which were evaluated from experimental data for a number of different atomizer types. A similar correlation subsequently derived by Gretzinger and Marshall (1961) consists of dimensionless groups. Both correlations cover almost the same range of applicability as that of Nukiyama-Tanasawa.

Kim and Marshall (1971) performed experiments similar to those of Nukiyama-Tanasawa, but covering a wider range of variables and employing an improved technique for measuring the drop sizes. The correlations for estimating the mean size and size distribution of drops (described later) were obtained from their study. The correlation for estimating the mean drop size has a form similar to the Nukiyama-Tanasawa equation. However, it was noted that the Nukiyama-Tanasawa equation predicted larger drop sizes under similar operating conditions. The Nukiyama-Tanasawa equation was based on data obtained by physical sampling techniques which were probably liable to be non-representative due to evaporation and target effects. Kim and Marshall (1971) also reported that a modified form of their equation for estimating the mean size can be used to correlate Gretzinger and Marshall's (1961) data, as well as Wetzel's (1951) drop size data obtained by venturi atomization.

Boll et al. (1974) measured the Sauter mean size of drops in an experimental venturi by means of a transmissometer. Drops were

produced by injection through a series of nozzles located upstream of the throat. The venturi had a throat flow cross-section of 30.5 cm by 35.6 cm and overall length in the flow direction was 4.6 meters. The range of throat velocity studied was 30 to 122 m/s, with L/G of 0.6 to 2.4 liter/m^3. Their results were correlated by the empirical equation shown in Table 3.2. They also reported that the Nukiyama-Tanasawa equation underpredicted the drop size for venturi scrubbers at low gas velocities and overpredicted at high gas velocities.

The application of Boll et al.'s (1974) equation for predicting the mean diameter of water drops in a venturi scrubber was confirmed by Atkinson and Strauss (1978) who studied the effect of surface tension on droplet sizes in a venturi scrubber. They measured the distribution of spray droplets using water, water and detergent, and water propanol mixtures by means of a stroboscopic-photographic method. Their experimental results showed a significant decrease in drop size when water-propanol mixtures were used, but an insignificant difference between droplet sizes for water and water-detergent systems. They did not present the size distribution data, but calculated the Sauter mean diameter and compared it with those predicted by Nukiyama-Tanasawa's and Boll et al.'s equations. The equation of Boll et al. (1974) was found to be the most accurate for estimating the mean size of water drops in a venturi scrubber, while the Nukiyama-Tanasawa equation predicted a larger size (approximately 43%) than the measured Sauter means. However, it is noted that Nukiyama-Tanasawa included the effect of surface tension in their equation while Boll et al. (1974) did not.

Another simple approach to predict the mean drop size (d_o) is to use the fact that liquid will shatter at a critical Weber number (Mugele, 1960; Calvert, 1970), which is defined as

$$W_{eg} = \frac{\rho_g V_r^2 \bar{d}_o}{\sigma}$$

The values of $W_{eg\ crit}$, ranging from 6 to 11 have been reported, based on the experiments on the drop shatter of several liquids (Goldschmid and Calvert, (1963). Licht and Radhakrishnan (1976) found that W_{eg} of 5 can be used to approximate the Sauter mean drop size as measured by Boll (1974) in cases where Q_g/Q_l is in the range of 500-750 (or L/G ratio of 1.4 to 2.0 liter/m^3) and gas velocity of 46-91 m/s. It is noted that Weber's equation gives the correlation between the drop size and air velocity only, but ignores the effect of L/G. Therefore, this estimate is quite approximate.

There are a number of semi-empirical equations which can be used to represent the size distribution of particles and aerosols, for example, the log-normal distribution, Rosin-Rammler distribution, Weibull probability distribution, and Roller distribution. The details of these distributions are summarized by Licht (1979). Some correlations of the size distribution of sprays which were produced by pneumatic atomization were described by Nukiyama-Tanasawa (1938), Mugele

and Evans (1951), Kim and Marshall (1971), but no data on the size distribution of atomized drops in venturi scrubbers has been found.

The empirical equation for size-distribution of sprays obtained from Nukiyama-Tanasawa's experiments was expressed as

$$\frac{dn}{dx} = ax^2 \exp(-bx^q)$$

where n = number of particles with diameter between zero and

x = diameter of drops

a,b,q are experimentally determined parameters.

The application of this function was shown to be somewhat limited as discussed by Mugele and Evans (1951).

Mugele and Evans (1951) applied various size distribution functions to a variety of experimental data on sprays and dispersoids. They proposed the modified "upper-limit" function as a standard for describing droplet size distribution in sprays since it gave a better fit in every case than the Rosin-Rammler, Nukiyama-Tanasawa and log-probability equations. The upper-limit function uses the maximum stable drop diameter as a significant parameter.

The study of pneumatic atomization performed by Kim and Marshall (1971) led to a generalized correlation for drop-size distribution by volume as

$$\phi_V' = \frac{1.15}{1+6.67\exp(-2.18x^*)} - 0.0150$$

Where ϕ_V' = cumulative volume fraction less than size d

x^* = reduced diameter = $\frac{d}{d_m}$

d_m = mass median diameter

The above correlation was found to well fit the size-distribution of sprays from pneumatic atomizers investigated by Gretzinger and Marshall (1961) and Wetzel (1951).

Licht (1974) analyzed the data of Kim and Marshall (1971) and found that the data fitted an upper-limit distribution function with the maximum dimensionless drop size as 2.97. The dimensionless size was defined as the ratio of the actual diameter to the mass median diameter. The function can be expressed as

$$\phi_V' = \tfrac{1}{2}\left(1+\operatorname{erf}\frac{\ln(u'/0.52)}{\sqrt{2}\ \ln 2.94}\right.$$

where

$$u' = \frac{d}{d_{max}-d} = \frac{x^*}{x^*_{max}-x^*}$$

d_{max} = maximum drop diameter in spray = 2.97 d_m

IV. PHOTOGRAPHIC METHODS FOR DROP SIZE ANALYSIS IN AN ATOMIZING SPRAY

As noted above, several methods have been developed for analyzing spray droplet size distributions. Of these methods, freezing the droplets and sieving them into size fractions [Longwell (1943)], or collecting droplets on slides [Frazer and Eisenklam (1956)], are impractial for the high liquid flow rates encountered in scrubber operation. Also, the measurement of light transmittance [Boll et al. (1974)] is only an indirect method of droplet size analysis, and is therefore inferior for our purposes to a more direct method such as photographic analysis.

The purpose of photography in analyzing objects in motion, as distinct from simple recording methods, is to "slow" down or "still" the motion so that both the form of the object while moving and also the progress of the motion can be measured and examined.

A. THE PHOTOGRAPHIC PROCESS

The photographic process comprises first a physical and then a chemical step. It consists in recording the image or shadow of an illuminated object on a photo sensitive surface and developing the latent image by a chemical process to obtain a permanent image. This image is usually silver or another metal in gelatine.

It is important to realise that at every stage of this process the image details can be accentuated or diminished according to the control of the operator. Therefore, before scientific evidence is deduced from the photograph, consideration must be given to the purely photographic results.

The recorded image is influenced by:

a) the intensity, duration, and spectral composition of the light source;

b) the optical system or focusing of the image on the light sensitive surface;

c) the characteristics of the light sensitive material or emulsion;

d) the manner in which the light sensitive material is processed.

Distortions or false accentuations may be created during any of these steps. For example:

(i) the incorrect mating of sensitive material to the spectral composition of the light source may accentuate or completely eliminate image formation;

(ii) the optical system may be focused with so little depth of field as to allow an interpretation in one plane only;

(iii) a dimensional error may be made by inaccurate measurement of the optical magnification;

(iv) the chemical development of the image may be carried out to give extreme accentuations of regions of highest brightness and diminish or eliminate regions of shadow.

Thus many combinations of technique may give a resulting photographic record which is false to a high degree. On the other hand purposeful accentuation may be required to discover a particular detail of a phenomenon.

Objects are illuminated by utilizing one or other band of the radiation spectrum. Visible light only covers a very small section of electromagnetic spectrum, but for photographic purposes other sections can be employed directly or indirectly. An emulsion can be made sensitive throughout a wide range of wavelenghts from the long infared to the short ultra-violet. X-rays, gamma rays and cosmic rays can also be made to affect the sensitive emulsion. The total range of photographic sensitivity lies between 2,000 and 14,000 A^{o}, the limits of this range being decided by the absoprtion of light by gelatine (on the one hand) and water vapor (on the other).

The radiation emitted from a particular light source has a number of characeristics:

a. the spectral distribution can vary according to the type and temperature of the light source;

b. the spectrum can be continuous, or line spectra, or a mixture of the two;

c. there can be variations in the intensity throughout its spectrum.

Within limits the emulsion can be made responsive to either wide or limited ranges of the spectrum and its sensitivity can be increased in specific areas.

The recording of objects will be considerably affected by the spectral quality of the light and the corresponding sensitivity of the emulsion. For example, although both daylight and turgsten are usually considered as white light sources, their radiation spectra differ quite appreciably, tungsten being deficient in the blue wavelengths. Thus, with a tungsten source, the full spectral sensitivity of the emulsion cannot be utilized, and its overall speed (i.e. the speed of recording the image on the photo sensitive surface) will be reduced. The speed, of course, will be reduced even further if the object reflects light primarily in the blue part of the spectrum.

B. PHYSICAL AND DYNAMIC STATE OF MATERIAL UNDER STUDY

Before applying a particular photographic technique it is necessary to define the physical and dynamic state of the material under study. In the simplest case it may be only necessary to discover the primary motion of a solid, a liquid, or a gas. This motion may be a continuous or a single event, and it may be self-initiated or controlled at the will of the operator. It is often necessary and important to discover and analyze any secondary motions which may be occurring during the primary motion. These secondary motions may be cyclic or non-cyclic and in the latter case they may be regular or irregular.

C. METHODS OF ILLUMINATION

Methods of illumination are diagrammed in Figure 4.1. Self-radiating objects, such as a flame, may be photographed by their own light. Other objects may be non-radiating but visually transparent, or translucent, or visually opaque.

Where the object requires illumination, the illumination may be from the rear, from the side, or from the front. With front lighting, i.e. recording the reflected light from the object, it may be illuminated by a diffuse source or a directional beam, which may also be directed at an angle to the surface of the object to produce specular reflection. Where the lighting is in the rear, it may also be diffuse

or a parallel beam from a point source. Each of these different methods of lighting will produce their own characteristic record and they may thus be interpreted in a number of ways.

The parallel beam or point source type of lighting can be utilized for producing direct shadowgraphs, Schlieren shadowgraphs or light interference fringes, and these methods have considerable importance.

Light interference is an important method of illumination since it provides a direct measure of the property investigated and it can be utilized in a number of ways. For example, if polarized light is passed through a stressed bi-refringent material, light interference can be made to occur and map out the lines of equal stress. The method can also be utilized to determine the thickness of thin films by arranging two adjacent rays of light reflected from the top and bottom surfaces respectively, which subsequently interfere with one another.

Although self-radiating phenomena emit their own light and therefore simplify lighting problems, it is sometimes necessary, particularly with a flame, to examine its structure in addition to its luminous characteristics. For example, gaseous detonation is associated with strong shock wave phenomena, and in order to make this visible it is necessary to take shadowgraphs with a separate light source. Techniques have to be chosen which will produce a shadowgraph without fogging the emulsion with the primary light of the flame itself. Two methods are usually employed. First, to arrange that the shadow light

source intensity is greater than that of the flame itself; and/or secondly, to filter off as completely as possible the light from the flame and choose a shadow light source in the transmission region of the filter.

In conjunction with the manner of using the light source it is necessary to consider tracer techniques, which are usually employed to make the streamlines of a transparent fluid visible. In the case of liquids, the flow may be defined by the movement of streams of dye, or the use of a bi-refringent liquid, which demonstrate velocity gradients, and in the case of gases by the trails of dense smoke. In some cases the difference of refractive index by the addition of another gas may be sufficient.

For flow visualization in wind tunnels the vaporization of lubricating oils and subsequent condensation has proven satisfactory, the color of the smoke depending upon the particle size. For large areas, it is sometimes more convenient to position small flags in a gas stream, which then indicate the direction of the flow lines. In liquids, dusts or globules or immiscible liquids, or small air bubbles can be used as visible flow indicators.

D. METHODS OF EXPOSURE

The velocity of the phenomenon to be photographed has a considerable influence on the method of exposure to be employed. The velocity

of an event is not however, the sole criterion by which to choose the correct method of exposure. If a "still" photograph is required, the permissible movement of the image before details are obscured is directly related to the object size, i.e., a large object can have a relatively longer exposure time than a small one.

Records can be made so that all movement is stopped, or alternatively, the exposure time can be extended so that image movement occurs on the photograph. The various techniques by which this can be accomplished are diagrammed in Figure 4.2.

Multiple exposures are usually made in order to make detailed examination of a rapid event. It is not always necessary to have a large number of exposures and in many cases, two or three exposures are adequate. The images may be kept separate from one another by the rapid movement of the object, by rapidly moving the emulsion, by optically moving the image, or by using a number of cameras each being operated after pre-set intervals of time. Alternatively the images may be superimposed on one another, but the number of images that can satisfactorily be examined depends on the event. The movement of single objects can permit a relatively large number of superimposed images since each can be easily distinguished. Where clouds of particles are analysed, only two superimposed images are permissible before interpretation becomes confused.

Single exposures are also useful in high speed photography for studying two types of event. First, for examining the general character of the continuous event, or for examining stationary phenomena such as standing waves or shock waves. With particular subjects and correct illumination, information can be deduced regarding flow phenomena, e.g. the presence of a shock wave or the recording of interference fringes provides information on the flow pattern in gaseous flow. Secondly, single exposures are useful for examining events of finite duration which are either cyclic or follow a regular path if non-cyclic. In this case, an experiment is repeated a number of times, and successive stages in the history of the event are recorded by taking a single photograph in each experiment at pre-set intervals of time after the event has been initiated. An example is the successive stages in the impact of a series of drops of water on a solid surface.

V. FLUID FLOW IN VENTURI SCRUBBERS

When a fluid is discharged from a nozzle into the venturi all or some of the following processes may take place:

a) Entrainment of the induced fluid by viscous friction at the periphery of the jet.

b) Expansion of the jet to a pressure below that of the induced fluid with consequent flow of induced fluid toward the exit of the jet.

c) Condensation or evaporation of the motive or induced fluids.

d) Acceleration of the particles of the induced fluid by transfer of momentum from the jet.

The theoretical analysis of an ejector in which two or more of these processes are involved is very complicated.

Most of the experimental and theoretical fluid flow studies that are found in the literature are on high energy venturi scrubbers. The studies on ejector pumps mainly concentrate on one-component-one phase systems, or two-component-one phase systems, or one-component-two phase systems. There are very few fluid flow studies on ejector venturi scrubbers that are for two component, two phase systems, such as those encountered in wet gas scrubbers.

A. HIGH ENERGY VENTURI SCRUBBERS

Calvert (1970) developed a theoretical pressure drop relationship for high energy venturi scrubbers:

$$\Delta P = 5 \times 10^{-5} V_g^2 L' \qquad 5.1$$

where: ΔP: Pressure Drop (inches of water)

L : Water Flow Rate (gallons per 1000 feet)

V_g: Gas Velocity (feet per second)

This equation does not account for the scrubber geometry, the introduction method of liquid and gas into the scrubber and the properties of the primary and secondary fluids. The experimental pressure drops are found to be much lower than those calculated by the above equation.

Hesketh (1974) developed the following empirical pressure drop equation by evaluating the data available in the literature. The pressure drop data were obtained from scrubbers of 600 cfm up to 300,000 cfm capacities.

$$\Delta P = \frac{V_t^2 \rho_g A^{0.133} L^{0.78}}{1270} \qquad 5.2$$

where: ΔP: Pressure Drop (inches of water)

L : Liquid to gas rates (gallons per 1000 af)

ρ_g: Gas Density (pounds per ft^3)

V_t: Throat Velocity of Gas (feet per second)

A : Throat Cross Sectional Area

He compared the measured pressure drop data of 40,000 acfm and larger scrubbers with the calculated pressure drops. The error of equation 5.2 ranged from 3% to 38% and was more significant at lower pressure drops. This equation is also applicable to small 1500 cfm high energy venturi scrubbers. Factors relating to the liquid properties are not included in this equation.

Placek and Peters (1981) developed a mechanical energy balance equation for a high energy venturi scrubber. They incorporated an equation of motion for single droplets (Eq. 5.3) into the mechanical energy balance equation (Eq. 5.4) in order to account for droplet size distribution.

$$\frac{du_j}{dx} = \frac{3}{4} C_{Dj} \frac{\rho (v-u_j)|v-u_j|}{u_j \rho_s D_j} - \frac{3u_j}{D_j} \frac{dD_j}{dx} \qquad 5.3$$

$$\frac{dP_T}{dx} = -\rho_v \frac{dv}{dx} - \sum_{j=1}^{j} \frac{3}{4} \frac{\rho_o}{\rho_s} \frac{\dot{m}_j}{D_j A} C_{Dj} \frac{(v-u_j)|v-u_j|}{u_j} \qquad 5.4$$

$$+ 3 \frac{\dot{m}_j u_j}{D_j A} \frac{dD_j}{dx} - \frac{\dot{m}_s + \dot{m}_g}{\dot{m}_g} \frac{f \rho v^2}{2 D_h}$$

This equation is solved by using a Milne Fourth Order Predictor - Hamming corrector numerical integration procedure.

Overcamp and Bowen (1983) investigated the effects of throat length and diffuser angle on pressure drop in venturi scrubbers. Their data showed that the pressure recovery is strongly influenced by the throat length. For a short venturi throat, a wide angle diffuser gave the best pressure recovery. For a long throat, a small angle diffuser gave the best pressure recovery.

B. ONE-PHASE, ONE-COMPONENT EJECTORS: GAS-GAS

In this type of ejector the driving fluid, which usually is supersonic, entrains and compresses the secondary fluid which can be either subsonic or supersonic. These ejectors find much use in aircraft industries. Much work has been reported on air-air ejectors. Paulon and Fabri (1958) analysed a two stream air-air ejector. They defined three operating modes for an ejector working with a secondary flow, which is initially subsonic, and a primary flow, issuing from the nozzle which is initially supersonic:

a) Upstream choking - this regime is obtained if the outlet pressure of the ejector is low, and the static pressure of the secondary

flow is low relative to the primary flow. When the secondary flow is choked at some upstream station and becomes supersonic downstream, it is called the supersonic regime. If the outlet pressure is low enough, choking takes place at the exit of the nozzle and the secondary flow is subsonic in the whole duct.

b) The saturated supersonic regime - with choking at the ejector inlet. This happens with a higher stagnation pressure of the secondary stream, whose mass flow becomes a function of ejector geometry and secondary stagnation pressure. The stagnation pressure or impact pressure is the pressure measured by a tube whose opening faces directly into the stream.

c) The mixed regime - if the outlet pressure is high enough, no choking takes place, the secondary flow remains subsonic throughout and the outlet pressure equals the external pressure. This regime is also known as the back pressure dependent mode.

Paulon and Fabri used a quasi one-dimensional approach in their treatment, but had to linearize their differential equations in order to obtain results. This limited the method to problems that did not present large variations of flow velocities along the ejector. Peters (1969) applied a numerical method of their original equations which broadened the number of applications for which solutions could be obtained, including gases with different compositions, different energetic conditions (temperature and velocity), as well as chemically

interacting gases. His approach was applied by Wright and Shahrokhi (1970) to the problem of multinozzle ejectors. Fabri and Siestrunck (1958) measured the overall pressure and mass flow ratios for the throat section for both subsonic and supersonic flow nozzles.

Only a few of the papers on ejectors deal with detailed flow field information, ejector velocity and temperature profiles, and pressure distributions [Curtet (1958), Mikhail (1960)]. Most of the mixing tubes are of constant diameter with relatively small ratios of nozzle-to-duct diameter.

Razinsky (1972) and Minner (1970) were the only authors to report turbulence measurements. Both studied imcompressible jet mixing in a constant diameter mixing section and both measured Reynold's stress and axial turbulent intensity. Minner (1970) calculated the radial and axial eddy viscosity distribution from the mean velocity and Reynold's stress profiles.

Hickman, Hill and Gilbert (1972) developed an analytical model to predict the flow behavior within axisymmetric single nozzle ejectors employing variable area mixing tubes. The primary flow may be supersonic or subsonic, and may have a different stagnation temperature than the subsonic secondary flow. Tests were performed on an ejector with an 800° F supersonic (M=2.72) primary jet to evaluate the analytical model. Good agreement was obtained between the analytical model and the measured velocity profiles, temperature profiles, and wall static

pressure distributions. The use of this type of ejector is of increasing interest for boundary layer control and lift augmentation in STOL aircraft. In one class of systems, a small mass flow of primary air at pressures up to 350 psia can be used to entrain a much larger mass flow of secondary air at ambient conditions. The use of ejectors in STOL aircraft systems places new emphasis on development of design techniques, which allow prediction of ejector performance over a broad range of operating conditions.

Later Arbel and Manheimer-Timnat (1974) calculated the performance of multinozzle air-air ejectors by means of a model using an equivalent single-nozzle device. The flow in the equivalent ejector is described by a system of integro-differential equations. These are general enough to include various combination of subsonic and supersonic flows, allow the introduction of different eddy viscosity models, and take into account the boundary layer thickness.

Hedges and Hill (1974) developed a general method for calculating two dimensional mixing of a compressible jet in variable area ducts. Their method incorporates finite-difference approximations to the conservation equations, and is applicable to a wide range of Mach numbers, mass flow ratios, and initial conditions. The model was based on mixing length approximations deduced from boundary layer and free jet mixing for the upstream portion of the flow, and a new mixing length distribution for the downstream zone which is entirely occupied by shear flow. Their finite-difference flow models, developed from

differential momentum and energy balance equations, cannot be applied to two-component, two-phase flow ejectors due to highly turbulent conditions.

Quinn (1976) made an experimental study for thrust augmenting ejectors in the wings of V/STOL aircraft. He used a convergent nozzle issuing into an axisymmetric duct that entrained from, and exhausted to, ambient conditions. The length of the ejector was varied from 12 to 0.75 diameters. Primary temperatures and pressures spanned the intervals 60 to 1000 ^{o}F and 10 to 80 psig. The mass entrainment performance usually decreased with increasing primary pressure although an aeroacoustic interaction reversed the trend over small intervals. Increasing the primary temperature decreased the performance of long ejectors, but had little effect on the performance of short ejectors.

C. LIQUID-LIQUID EJECTORS

O'Brien and Gosline (1934) developed equations for liquid-liquid jet pumps that are applicable either to one-component or two-component systems.

The phenomenon of entrainment is not clearly understood, yet it is the most important action taking place in a jet pump. Tollmien (1926) has studied the mixing problem by considering the momentum transfer taking place at a constant pressure. Through application of Prandtl's mixing length theory for turbulent flow, Tollmien obtained generalized

velocity distribution curves in a free jet issuing from a point source into initially stationary air. Kenthe (1935) extended the theoretical work of Tollmien to include the mixing of two parallel streams at different velocities but of the same density and at the same constant pressure. He also obtained experimental data under isothermal conditions to demonstrate the value of theoretical results. Goff and Coogan (1942) have extended this theoretical attack to include fluid streams of widely different densities. In all cases, the generalized velocity and temperature distributions are similar. Cleaves and Boelter (1947) have summarized the available theoretical and experimental results on jet mixing of compressible fluids and have presented new experimental data for non-isothermal flows. They concluded from their results that new theoretical investigations are necessary to describe the mechanisms of non-isothermal jet mixing.

Folsom (1948) did analytical studies on liquid-liquid and liquid-gas ejectors. He developed his equations from mass balance and energy balance relationships that are limited to straight mixing tubes of constant cross sectional area.

D. ONE-COMPONENT, TWO-PHASE FLOW EJECTOR

Levy and Brown (1972) did studies on the performance of a condensing ejector. The condensing ejector is a two phase jet pump which combines a subcooled liquid stream and a vapor stream, producing a liquid stream with a stagnation pressure which can be higher than the

stagnation pressure of either of the two inlet flows. They measured axial static and liquid-vapor stagnation pressure profiles in a constant area mixing section, using steam and water over a limited range of inlet vapor conditions and a wide range of inlet liquid velocities. They identified three flow regimes based on inlet liquid velocity. Complete vapor condensation due to a "condensation shock" occurred only in the high inlet liquid velocity regime. The presence of supersonic vapor flow was found to be a necessary but not sufficient condition for the existence of the "condensation shock". They developed a quasi one-dimensional model for an annular vapor, and rod-like liquid, flow patterns which occur in the upstream portion of the mixing section. They assumed the flow to be steady, one dimensional and axisymmetric. They assumed the jet to have a small cylindrical surface which can change radius with distance. Because of a shortage of information on interfacial heat transfer rates and shear stresses, they were not able to solve their equations of conservation directly.

Flinta, Hernborg and Stenback (1972) did performance tests on an ejector designed for pumping two-phase flow by means of a water jet. They showed that the ejector can be used over a wide range of steam quality and pumping head. They determined that the momentum transfer, in one-component, two-phase flow ejectors, is sensitive to the steam pressure and the water content in the secondary flow.

E. TWO-COMPONENT, TWO PHASE FLOW EJECTORS

This type is the focus of the present work. The two-component, two-phase ejector is a device which entrains and compresses a gas in a cylindrical mixing throat. The resulting mixture of gas and liquid is discharged through a diffuser, to increase the static pressure at the expense of the kinetic energy of the mixture. Applications might include: vacuum pump, gas compression, intimate mixing to enhance rapid chemical or biological reactions (e.g. aeration of sewage) or to scrub or clean the gas phase. Ejectors have been used in industry mostly as vacuum pumps for power plant condensers. The familiar laboratory aspirator is another example of a common application.

Ejector pumps operate on fluid power rather than electrical or mechanical devices, and in some cases this characteristic alone justifies their use. A review by Bonnington and King (1972) lists over 300 references reflecting many of the possible fluid combinations and applications.

The fluid flow in an ejector venturi scrubber can be called compressible, dispersed, two-phase flow. The complete field of compressible flow is very large, and it covers wide ranges of pressure, temperature and velocity. As with incompressible flow, the Reynolds number is also important in some applications of compressible flow. Another important parameter in compressible flow is the Mach number. The Mach number denoted by N_{Ma}, is defined as the ratio of "u", the speed of a fluid, to "a", the speed of sound in the fluid under the same flow conditions:

$$N_{ma} = \frac{u}{a}$$

For isothermal flow, an isothermal Mach number (N_i) can be defined:

$$N_i = u/a'$$

Where:

$$a' = \sqrt{\frac{g_c P}{\rho}} = \sqrt{\frac{g_c TR}{M}}$$

An isothermal process cannot pass through the limiting condition where $N_i = 1$. If the flow is initially subsonic, it must remain so. Therefore, Mach number does not appear in the mechanical energy balance equation for subsonic isothermal compressible flow.

For cocurrent flow with constant liquid/gas ratios, considerable experimental and theoretical work has been done to predict the pressure drop, volume fractions, and flow pattern. However, a reliable general correlation has not as yet been developed.

1. Design Factors Affecting the Performance of Ejectors

Mellanby (1928) experimentally determined that ejectors with cylindrical throats produced a higher maximum vacuum than ejectors which had a gradual constriction tapering off to the outlet. He also indicated that the capacity of a jet for entraining the fluid is independent of the position along the jet at which the entrained fluid enters. An explanation for possible reasons was not given.

The distance of the nozzle outlet to the diffuser throat considerably effects the performance of an ejector. Watson (1933) determined

that the maximum value of this length decreases with increasing nozzle supply pressure, and decreases with increasing vacuum. He also stated that it is important to have the nozzle centered along the axis of the throat, and that a comparatively small change in throat area makes a large difference in the amount of air entrained. If the throat is too small, choking will occur (i.e., the liquid will fill the throat and the entrained gas will not be able to pass through) and if it is too large, leakage of air back into the system will occur.

Also, a long and slowly diverging diffuser is preferred for pressure recovery. It has been determined by Engdahl and Holton (1943) that the best form for the entrance to the diffuser throat is a well-rounded bell-mouthed entry. They determined that a conical or tapered entry should have an angle larger than 20 degrees, so that the nozzle jet (which also has an angle of about 20 degrees) will not produce objectionable shock and eddy losses at the inlet.

2. Mixing Shock in the Ejector

The main pumping action of the water jet and the associated pressure increase occur in a rather short region in the mixing tube, in which intensive mixing of the two phases also takes place. This phenomenon is called "mixing shock".

Hinze and Rijnders (1971) during their investigations of the characteristics of the water jet pump, observed the following phenomena and features:

a) The pressure build-up in the mixing tube takes place over a relatively short distance (a few inches).

b) The ejector pump can operate only under certain conditions of gas flow, liquid flow, and pressure build-up. These conditions are determined by the second law of thermodynamics such that the mixing shock is accompanied by an increase in entropy.

c) Under certain conditions, the mean gas velocity in the section of the mixing tube where the gas is the continuous phase attains a higher value than the mean velocity of the liquid which constitutes the discontinuous phase. This is possible because the gas accelerates due to compression experienced while passing from the converging section into the throat.

The experiments of Hinze and Rijnders (1971) were carried out with water as the driving agent, and most of the experiments with air as the gas phase (a few with CO_2). They determined that at normal, atmospheric, pressures in the suction chamber, the structure of the mixing shock is much more homogeneous than it is at lower pressures (at which cavitation can occur due to implosion of the bubbles). Short-flash, still-camera pictures, and high speed motion pictures, showed that in mixing shock, the gas bubbles collapsed in groups or clouds. At the same time, these initially more or less spherical clouds became deformed into flat shaped clouds as they move through the mixing or cavitation shock, until they almost disappeared. Weak light

radiation was observed under conditions where cavitation shocks occurred. It was believed that this radiation of light was due to the phenomenon of sonoluminescence, which is well-known in the literature from cavitation experiments. The number and intensity of the light pulses increased with decreasing pressure in the suction chamber, i.e. with increasing degree of cavitation. This sonoluminscence was weaker with CO_2 than with air. Hinze and Rijnders further explained the origins and existence of the mixing shock by anology to the shock wave familiar in gas dynamics. They calculated the velocity of sound for the mixture upstream of the mixing shock and found it to be supersonic, whereas downstream of the mixing shock the flow is subsonic. They further stated that within the mixing shock there is no dynamic equilibrium between the two phases, and probably no thermodynamic equilibrium. Across the mixing shock, they calculated the ratio between the pressure in the liquid and gas phases, and determined that this ratio passed through a maximum mid-way along the cross-section of the mixing shock.

3. Theoretical and Experimental Analysis of Ejectors

A one dimensional analysis of the mixing process in a cylindrical throat was reported by Folsom (1948). Takashima (1952) developed a similar throat expression as well as a diffuser equation, and he also reported experimental data. Volumetric flow ratios of liquid-to-gas were on the order of five or larger, and pumping efficiencies were quite low.

Bonnington (1956) showed that measured pumping efficiencies declined with increasing jet velocities. A later paper of Bonnington (1960) made an important contribution in reporting tests with a transparent mixing throat. Best pumping performance was obtained when the mixing zone was positioned in the cylindrical throat section. A longer throat also produced better results.

Higgins (1964) presented one dimensional relations for the ejector pump including frictional losses. With a fixed water jet velocity and suction port air pressure, he found that the mixing zone could be positioned at will by controlling the back pressure. At the upper limit the pump "flooded", i.e. water flowed back through the air inlet. With the discharge valve fully open, the jet passed through the throat and mixing occured in the control diffuser. Optimum performance occcured when mixing was located just upstream of the throat exit. Betzler (1969) refined the relationship of Higgins for the diffuser section.

Harris (1965) determined that in a given ejector venturi scrubber the flow capacity can be increased by using a larger nozzle with higher liquid flow rates (Figure 5.1). Also, as illustrated in Figure 5.2, he obtained maximum pumping efficiencies of 16 to 20 percent. The family of efficiency curves shows the desirability of operating at higher liquid pressures. Like many other types of conventional pumps, the maximum capacity and maximum efficiency points do not coincide, and in practice the user has to choose between them on the basis of capital

and operating costs. Harris also calculated the energy requirements of the 12 inch S&K ejector venturi scrubber (Figure 5.3). The curves reveal the amount of additional energy required by the ejector in order to overcome the pumping losses through the connecting ducts.

In addition, the curves reveal the energy advantages of operating at the higher motive pressures when drafts above 1.5 inches of water are desired, while conversely operating at the lower motive pressures when drafts in the range of 0 to 1 inches of water are desired.

All of the above analyses were similar in the momentum continuity modelling of the throat process. Witte's (1969) analyses was the most thorough, however, particularly his study of compressibility effects. He proposed to use a dimensionless number, u, to evaluate the performance of the ejector pump.

$$u = \frac{\rho_l V_{lo}^2 A_n}{g_c A_t^2 P_o}$$

Analysis of the diffuser processes have shown less agreement with experimental results. The mixture compressibility has usually been neglected, and only Takashima (1952) and Betzler (1969) included the log term associated with isothermal gas compression.

Bhat, Mitra, and Roy (1972) studied the performance of a horizontal liquid-air ejector by employing different liquids as the motive fluid. They determined that the performance of the system was enhanced by creating mixing shock involving conversion of jet flow to bubble flow. They also made a theoretical analysis of the system on the basis of macroscopic momentum and mechanical energy balance equations. However, in their analyses, they assumed the pressures at the nozzle exit and at the entrance to the throat section were equal, and they neglected the expansion of the liquid jet in that region. These assumptions are not valid for ejector venturi scrubbers. Also, liquid film at the walls of the venturi was not taken into consideration.

Cunningham (1974), and Cunningham and Dopkin (1974), conducted experimental and theoretical studies of ejector pumps. In their experimental analysis, they determined that the pumping efficiency of the ejector venturi is very much dependent on the nozzle geometry and throat length (i.e., the optimum throat length varies with the type of nozzle used). Liquid to gas ratios used in their experiments were on the order of 0.5. In the theoretical analysis of the diffuser section, they assumed the liquid and gas formed a homogeneous, one-phase, compressible mixture, with no-slip between gas and liquid. Their relationships are applicable to horizontal ejector venturis. They also neglected the liquid film on the walls of the venturi.

Most of the prior work on ejectors involved straight liquid jets and very large liquid-to-gas volumetric ratios.

VI. GAS ABSORPTION IN THE EJECTOR VENTURI SCRUBBER

Most of the work done on venturi scrubbers has been for the capture of particulate matter rather than gas absorption. Only a few theoretical and/or experimental studies of gas absorption in venturi scrubbers were found in the literature, and all of these studies were performed on high energy venturi scrubbers.

A. THEORETICAL MASS TRANSFER STUDIES

Kuznetsov and Ortavskii (1962) presented a model for the gas absorption rate in the throat and diverging section of a high energy venturi scrubber. They considered the case of radial liquid injection at the entrance of the throat section. They began their analysis from the basic equation for the number of mass transfer units:

$$N_T = \frac{K_G a Q_{throat}}{G}$$

where the interfacial area, "a" is defined as

$$a = \frac{G_m}{D_{32} Q_{throat}} \frac{\rho_g}{\rho_l} \left(\frac{ft^2 \text{ of drop surface}}{ft^3 \text{ of flowing gas}} \right)$$

To evaluate the interfacial area, they obtained the Sauter mean diameter, D_{32}, using the Nukiyama-Tanasawa equation. This equation requires that the value of the liquid-to-gas ratio, L/G, and the relative liquid to gas velocity, V_r, be specified. To obtain a value for the relative velocity, Kuznetsov and Ortavskii assumed that the liquid velocity is negligible as compared to the gas velocity. Therefore, they take the relative velocity to be equal to the gas velocity along the length of the unit. Their assumption is justified only at the liquid injection point for a high energy venturi scrubber, but is not valid at short distances downstream. This is because the droplets are accelerated by the gas stream, and given a long enough system, Vr should approach zero. Raman (1977) has shown that a 400 micron droplet, exposed to a 300 ft/sec gas stream, is accelerated to a velocity of 200 ft/sec within a distance of 6 inches. Because of their assumption, the model of Kuznetov and Ortavskii is not applicable to ejector venturi scrubbers where the liquid is ejected through a nozzle with a sizable initial velocity. Further, Kuznetsov defined the interfacial area, a, as the ratio of the drop surface area to the volume of gas, and not as the ratio of drop surface area to the volume of the scrubber, as is conventionally reported. Therefore his $K_g a$ differs from the conventional $K_g a$ by the ratio of gas volume to scrubber volume.

Boyadzhiev (1964) used the model of Kuznetsov to optimize the operating parameters in a venturi scrubber. Although his optimization methodology is correct, the results may be questioned because of the assumptions used in Kuznetsov's model.

Downs and Atwood (1973) presented a model for gas absorption in a venturi scrubber where the liquid was introduced through a spray nozzle located near the entrance to the converger section. They divided the scrubber into two zones. The first zone extended from the nozzle to the point where the liquid first impinged on the wall. The second zone extended from the point of impingement to the scrubber exit. In the second zone the liquid flows partly as a film on the scrubber wall and partly as finely dispersed drops in the gas core. Separate sets of differential material balance equations were written for each of the two zones. The liquid phase material balance for the second zone included the mass transfer to the liquid film flowing on the scrubber walls and to the dispersed drops in the scrubber core. Their model was developed for gas phase diffusion controlled systems. They introduced the concept of an extended surface factor to account for the increase in drop surface area resulting from drop distortion. Downs concluded from his model that the diverger angle, droplet diameter, gas throat velocity, and liquid rates were the major parameters which affected scrubber absorption efficiencies.

Wen and Uchida (1973) presented a model for sulfur dioxide absorption into lime-limestone slurries in a high energy venturi scrubber. Their differential equations required trial-and-error solution by numerical techniques. Their model correlated well the experimental data of Gleason and McKenna (1971), but their model included the following assumptions:

i) Once formed, the droplets do not undergo any further atomization.

ii) Wall film flow rates are negligible. This assumption is questionable since wall film flow rates are dependent on the liquid-to-gas ratio and the gas throat velocity. As indicated by Raman (1977), under certain experimental conditions 50% of the injected liquid may be flowing as a film down the scrubber wall.

Raman (1983) developed differential mass transfer equations for high energy venturi scrubbers for: (1) gas-phase, resistance controlling systems; and (2) liquid film resistance, and reaction rate controlling systems. The equations for gas phase resistance controlling systems are similar to those of Downs and Atwood (1973). To use the model the relative velocity between gas and liquid must be known. This is generally not known for any scrubber. So he assumed the relative velocity equals the nozzle exit velocity which is clearly inaccurate. In both papers, the gas is assumed to be drawn through the scrubber with a blower, and not by draft created by a liquid jet. As a consequence the liquid-to-gas ratio is much lower than for an ejector venturi scrubber. Also these differential equations must be solved by numerical techniques.

B. EXPERIMENTAL MASS TRANSFER STUDIES:

A number of experimental gas absorption studies in high energy venturi scrubbers were found in the literature.

Johnstone, Field and Tassler (1954) studied gas phase controlling absorption of an SO_2-NaOH system. Their experiments were carried out in a Plexiglas venturi scrubber with throat diameters ranging from 1-1/8 to 1-1/2 inches and throat lengths from 1-1/2 to 3 inches. The angle of the converging section of the venturi was 25^o and the angle of the diverging section was 7^o. Gas throat velocities ranged from 350 to 600 ft/sec and the liquid rates varied from 0.03 to 0.3 gallons/min. They found that the majority of mass transfer occured at the spray nozzle, and the amount of mass transferred per unit spray volume decreased at increasing distances from the nozzle. $K_g a$'s were determined experimentally and found to vary from 90 to 700 lb moles/(hr)(atm)(ft^3 of spray volume).

Johnstone's K_g is not consistent with the normal definition of K_g. Johnstone defines $K_g a$ with units of lb moles/(hr)(ft^3 of spray volume)(atm) and defines "a" with units of ft^2 of drop surface/ft^3 of spray volume. Thus K_g has units of lb moles/(hr)(ft^2)(ft^3 of gas flowing/ft^3 of spray volume). The ratio of volumes will approach 1 only when the velocity of the liquid approaches the velocity of the gas, and only then will Johnstone's K_g have conventional units.

Gould (1952) determined experimentally the overall mass transfer coefficient, $K_g a$ for absorption of ammonia in water in a venturi

scrubber. The values of the experimentally determined overall mass transfer coefficients were around 500 lb moles/hr ft^2.

Elenkov (1964) studied SO_2 absorption by sodium carbonate in a venturi tube, with a throat diameter of 0.825 inches and a throat length of 1.9 inches. Gas throat velocities ranged from 100 to 220 ft/sec, and the liquid-to-gas ratio varied from 0.4 to 2.85 lb/lb. A sodium carbonate concentration of 1.5 gm moles/liter ensured that gas phase diffusion was the controlling resistance. Elenkov found that increasing gas throat velocities and liquid gas ratios increased the amounts of SO_2 absorbed.

Volgin (1969) studied SO_2 absorption by ammonium sulfite-bisulfite solutions in two different venturis. One had a rectangular throat 0.395 inches by 0.59 inches, and the other had a cylindrical throat with a diameter of 0.788 inches. Throat velocities ranged from 98.5 ft/sec to 197 ft/sec and the liquid-to-gas ratios varied from 0.21 to 8.2 lb/lb. He also studied the effect of throat length on the amount of SO_2 absorbed and used three throat sections: 0.394, 7.88 and 11.8 inches long. Volgin found that increasing gas throat velocities and the liquid-to-gas ratio resulted in increasing amounts of SO_2 absorbed. He also found that there was an optimum throat length which maximized the amount of SO_2 absorbed.

Sharma and Virkar's (1975) experiments were carried out in a Perspex venturi scrubber with a throat diameter of 1.6 cm and throat

length 0.9 cm. The angle of the convergent section was 35^{o} while that of the divergent section was 8^{o}. The entrance of the convergent section and the exit of the divergent section was 5 cm. Gas throat velocities ranged from 1000 ft. sec to 350 ft/sec and liquid rates varied from 1.5 to 3.8 lb/min. Two modes of liquid injection were used:

1. Pease-Anthony mode of operation, where the liquid is injected into the throat of the venturi.
2. Wet Approach mode of operation, where the liquid is introduced in a way such that the walls of the entire convergent section are wetted by the liquid phase.

They used mass transfer with chemical reaction to obtain values of the interfacial area, "a" and the mass transfer coefficients, $K_g a$ and $K_l a$, for various throat velocities and liquid-to-gas ratios. They also investigated the effect of surface tension and viscosity on the interfacial area. From their results, they concluded that the viscosity of the liquid did not affect the interfacial area, while a decrease in the surface tension of the liquid resulted in an increase in the interfacial area. A decrease in surface tension causes a decrease in drop diameter, and consequently an increase in the interfacial area. All their results were obtained for the scrubber/separator combination. Any scrubber is followed by a separator, to divide the gas-droplet mixture into separate phases. Since they did not collect any experimental data at the exit of the scrubber, it is not possible to

determine the fractions of the total absorption which occurred in the scrubber and separator, respectively. The residence times of the gas-liquid mixture in the scrubber and separator are of the same order of magnitude, and it is possible that the mass transfer in the separator could be a significant fraction of the total mass transfer.

None of the above investigators considered a material balance closure between the bulk gas and liquid phases.

Raman (1983) measured the absorption efficiencies of two percent SO_2 in NaOH, and six to ten percent CO_2 in NaOH and sodium carbonate-bicarbonate buffer solutions. Experiments were carried out in a high energy venturi scrubber, where the gas flow was introducted by a blower and the liquid was introduced through two spray nozzles. His experimental results showed that higher throat velocities and liquid rates, use of a finer nozzle, and a diverger with a smaller solid angle significantly improved the absorption of SO_2 and CO_2. The spray nozzle position and spray cone angle significantly affected gas absorption rates. With a critical Weber number of 6 (i.e. the value of Weber number at which the spray disintergrates into droplets), the experimental SO_2 absorption efficiencies were predicted to within $\pm$10%. Using a critial Weber number of 1, the CO_2 absorption efficiences were predicted to $\pm$15%. Critical Weber number was defined as:

$$W_{ec} = \frac{D_{max} V_r^2 \rho_g}{g_c \sigma_l}$$

C. GAS ABSORPTION THEORY:

The first theory of gas absorption was proposed in 1923 by Whitman (1927). His "two film concept" relates the overall transfer coefficient to the individual film transfer coefficients. The relations are:

$$\frac{1}{K_g} = \frac{1}{k_g} + \frac{H}{k_l} \qquad 6.1$$

$$\frac{1}{K_l} = \frac{1}{k_l} + \frac{1}{Hk_g} \qquad 6.2$$

where K_g and K_l, are the overall gas side and liquid side transfer coefficients, k_g and k_l, are the respective individual film coefficients, and H is the Henry's Law constant for the solute. For the case where the solute gas is very soluble in the liquid phase, small changes of solute in the gas phase will produce large solute concentration changes in the liquid phase. In that case, the gas phase resistance dominates, and $K_g \tilde{=} k_g$. Conversely, when the solute gas is relatively insoluble in the liquid phase, the liquid phase is the major resistance and $K_l \tilde{=} k_l$.

1. Gas-Side Mass Transfer Coefficient

Early investigators noted a similar dependence of mass, heat and momentum transfer upon eddy activity. The existing empirical correlations for heat, mass and momentum transfer were manipulated by Chilton and Colburn (1931) to obtain analogies between these processes in terms

of quantities designated as j-factors. The j-factor for mass transfer is defined as

$$j_D = \frac{N_{Sh}}{N_{Re} N_{Sc}^{1/3}} \qquad 6.3$$

and that for heat transfer, j_H is

$$j_H = \frac{N_{Nu}}{N_{Re} N_{Pr}^{1/3}} \qquad 6.4$$

The classical Chilton-Colburn analogy for turbulent flow through smooth tubes states that

$$j_D = j_H = \frac{f}{2} \qquad 6.5$$

where f is the friction factor.

Since then, j factor correlations for flat plates, cylinders and spheres have been published by a large number of investigators. A review of the literature in this area is presented by Skelland (1974). The j factor equalities can be used to estimate mass transfer coefficients for analogous cases where heat transfer data are available but no mass transfer data are available, and vice versa. When experimental correlations are available for evaluating the mass transfer coefficients, they should be used in preference to the j factor analogies.

A large number of experimental studies have considered mass transfer from a single sphere placed in an extensive flowing field. Rowe et al. (1965) provide an excellent review of the work done in heat and mass transfer from single spheres. They also collected extensive data using benzonic acid spheres in air. Their correlation was

$$\frac{k_g D_{sphere}}{\mathcal{D}} = 1.95 + 0.68 N_{Sc}^{0.33} N_{Re}^{0.5} \qquad 6.6$$

This is of the same form as that developed by Froessling (1938) who investigated the evaporation of nitrobenzene, aniline, water, and naphthalene in a hot air stream. The first two liquids were suspended as drops on thin glass rods, and the rate of evaporation was such that there was negligible heat transfer. The naphthalene was melted to form a spherical blob at the end of a glass stem. The drops were placed in an upward flowing wind tunnel and the mass transfer was measured by photographing the diminishing sphere. The diameters ranged from 0.1 to 2 mm. Froessling developed the following correlation for the mass transfer coefficient:

$$\frac{k_g D_{drop}}{\mathcal{D}} = 2 + 0.552 N_{Re}^{0.5} N_{Sc}^{0.33} \qquad 6.7$$

The Froessling correlation also provided a good fit to the data of Vyrubov, and of Rowe. Later experimental data collected by Houghton (1932) and Johnstone et al. (1951) were also in good agreement with the

predictions of the Froessling correlation. The Froessling correlation is widely used to predict the gas side transfer coefficient, k_g.

Vyrubov (1939) performed mass transfer studies with the intention of applying the results to analogous heat transfer problems. Roughened abonite spheres with diameters from 1 to 3 cm were coated with orthophosphoric acid and held in a 12 cm diameter vertical tube through which air was blown at a known rate. Ammonia was mixed with the air several meters upstream of the sphere and the acid coating neutralized with the formation of crystalline ammonium phosphate. The sphere was removed and ammonia estimated by titration. In the Reynold's number range of 200 to 3000, his data were correlated by

$$\frac{k_g D_{sphere}}{\mathcal{D}} = 0.54\ N_{Re}^{0.5} \qquad 6.8$$

2. Liquid-Side Mass Transfer Coefficient

In order to evaluate the liquid film coefficient, k_l, the cases of physical absorption and absorption with chemical reaction are considered below.

a. Physical Absorption

Higbie (1935) proposed the "Penetration Theory" which accounts for the transient diffusion of solute from the gas to the liquid phase. By solving the partial differential equation, he obtained the following

equation for the mass flux at a point on the liquid surface which is exposed to a solute gas:

$$N_A = \sqrt{\frac{D_A}{\pi t_e}} (C_A^* - C_{Ab}) \qquad 6.9$$

From the definition of the mass transfer coefficient:

$$k_l = \sqrt{\frac{D_A}{\pi t_e}} \qquad 6.10$$

Higbie assumed that the time of exposure, t_e, was the same for all the liquid elements brought up to the surface from the bulk liquid. The exposure time, t_e, can be estimated from the hydrodynamic conditions within the system.

The Dankcwerts (1951) surface renewal model assumes that the chance of an element of surface being replaced with fresh liquid is independent of its time of exposure. Fresh fluid elements remain in contact with the surface for variable times, t. The fractional rate of renewal, s, of the area exposed to penetration is assumed to remain constant and the surface age distribution function is.

$$\phi = Se^{-st}$$

This represents the probability that any element area will be exposed for time, t, before being replaced with fresh fluid. The average absorption rate is

and $$N_A = \sqrt{D_{As}} (C_A^* - C_{Ab}) \qquad 6.11$$

$$k_l = \sqrt{D_A s} \qquad 6.12$$

where s represents the rate of surface renewal and 1/s may be regarded as an average life of surface elements.

The Higbie and Danckwerts models both indicate that the mass transfer coefficient, k_l, is proportional to the square root of diffusivity D_A; the j factors show that K_l, is proportional to the 2/3 power of diffusivity; while the film theory predicts a linear relationship between the two.

b. Absorption with Chemical Reaction

An excellent review of the theory of absorption with chemical reaction has been presented by Danckwerts and Sharma (1966). Absorption with chemical reaction is commonly encountered in processes for the removal or recovery of acid gases. These processes include the removal of CO_2 and H_2S in natural gas distribution, the manufacture of CO_2 and sodium carbonate, and the manufacture of sodium sulfite for use in the paper and pulp industry. The absorbent is usually selected to maximize the amount of gas which will dissolve in the solvent, and to minimize the cost of regeneration of the solvent.

According to Astarita (1966) absorption with chemical reaction can be thought of as occurring in the following stepwise fashion:

i) Diffusion of gaseous reactants from the bulk of the gas to the gas liquid interface.

ii) Diffusion of gaseous reactants from the interface to the bulk of the liquid phase.

iii) Chemical reaction within the liquid phase.

iv) Diffusion toward the liquid surface of reactants initially present in the bulk liquid phase; and diffusion of reaction products away from the liquid surface.

If step (i) is rate controlling, the overall rate is not influenced by chemical reaction and the process may be regarded as a simple mass transfer phenomenon.

Van Krevelen and Hoftijzer (1968) have classified chemical absorption processes into four groups according to the rate of chemical reaction.

a) Very fast irreversible reactions (e.g. ammonia absorption in sulfuric acid) have so small a chemical resistance that the rate is determined practically by the mass transfer in the gas phase.

b) Fast reversible reactions (e.g. absorption of hydrogen sulfide in alkaline liquors) where the rate of absorption is determined by mass transfer in the gas phase, and by mass

transfer of the reactants and reaction products in the liquid phase.

c) Moderate speed reactions (e.g. absorption of CO_2 in alkaline solutions), in which the rate of absorption is determined by mass transfer of the reactants in the liquid phase.

d) For very slow reactions, rate of absorption is determined by diffusion of the reactants in the liquid phase and by the rate of reaction in the liquid phase.

A pioneering work in mass transfer with chemical reaction was that of Hatta (1928). Using the film theory, he derived an expression for the enhancement factor, E, for the case of absorption accompanied by a first-order chemical reaction. The enhancement factor corresponds to the mass transfer coefficient of non-reacting systems, but includes the effects of the chemical reaction taking place in the liquid phase. Since then, enhancement factors, have been obtained using surface renewal models. But first-order reactions are seldom encountered in practice. Common gas-liquid reactions are second-order of the type:

$$A + B \longrightarrow \text{Products}$$

The rate of disappearance of the solute gas is:

$$r_A = k_2 [A][B]$$

No analytical solutions for the case of absorption accompanied by second order reactions are available in the literature. An approximate set of solutions have been presented by Van Krevelen and Hoftijzer (1968).

In many cases, the concentration of the dissolved reactant remains uniform, and the rate of reaction of dissolved gas is proportional to its local concentration. Under these circumstances, the overall reaction can be considered to be a pseudo-first order reaction.

D. MASS TRANSFER TO DROPS UNDER JETTING CONDITIONS

The total mass transfer in the ejector venturi scrubber is a function of mass transfer to single drops, and the velocity of single drops integrated over the size distribution. Therefore, a literature search was undertaken to find any work on mass transfer to droplets under jetting conditions.

Quantitative relationships for mass transfer during drop formation under jetting conditions are non-existent. Most of the work has been done on laminar jets and did not take into consideration mass transfer into atomized jet.

Mayfield and Church (1952) experimentally determined that mass transfer under jetting conditions is higher than under non-jetting conditions.

Burkholder and Berg (1974) studied the effect of mass transfer on laminar jet breakup for liquid jets in gases, and liquid jets in liquids. For liquid jets in gases, they concluded that solute transfer out of the gas is stabilizing (produces longer jets), while transfer into the jet is destabilizing and promotes breakup.

Numerous workers employing laminar jets have checked the penetration theory quite closely without making any allowance for a surface effect for gas absorption.

Cullen and Davidson (1957) used a nozzle specially shaped to produce a uniform velocity distribution at the nozzle exit. They showed theoretically that the rate of absorption of a non-reacting gas into a tapering jet is given by

$$\phi_T = 4C^* (DQZ)^{\frac{1}{2}} \qquad 6.13$$

where ϕ_T = Theoretical average absorption rate, gm-mole/sec

Z = Axial coordinate, cm

Q = Dispersed phase flow rate cm^3/sec

C^* = Equilibrium concentration of solute in liquid, $gm\text{-}mole/cm^3$

D = Molecular diffusivity, cm^2/sec

Scriven and Pigford (1958) developed a shaped nozzle which formed a non-convergent jet of 1.5 mm in diameter. Measurements of the absorption of carbon dioxide in water agreed closely with predictions from penetration theory assuming rod-like flow. By analyzing the fluid

mechanics of the jets, they suggested that it was unlikely that predictions from penetration theory assuming rod-like flow would be more than 2-3 percent in error under most conditions employed.

Rehm, Moll, and Babb (1963) measured the rate of carbon dioxide absorption by a jet of dilute sodium hydroxide. Rates were calculated with a model based on one-dimensional diffusion occuring simultaneously with two consecutive irreversible chemical reactions. The calculated absorption rates agreed within five percent of the experimental values.

Duda and Vrentas (1968) developed a technique for determining diffusion coefficients from laminar liquid jet absorption experiments by a vigorous analysis of jet hydrodynamics. This method of analysis eliminated the need for specially designed nozzles which inhibit velocity profile development. A comparison between experimental results and the available diffusivity data indicated that the penetration theory could be applied in the calculation of liquid jet mass transfer.

In their studies of the effect of mass transfer on liquid jet breakup, Burkholder and Berg (1974) also suggested that the experimental situation is best described as penetration type mass transfer into a cylinder of initial concentration. Because the jet life times for the experiments are small, the boundary layer thickness is small relative to the jet radius, and the solute concentration profiles in

each phase are strongly non-linear. Hence, the jet itself may be considered an infinite medium.

Huang (1976) analyzed mass transfer into and out of droplets both experimentally and theoretically. He stated that there are four stages of mass transfer in the life of each drop.

a) mass transfer to liquid jet

b) mass transfer during drop breakup

c) mass transfer during drop free fall

d) mass transfer during drop coalescence

This type of staging is not applicable to ejector venturi scrubbers, because under normal operating conditions the jet atomizes soon after it exits the nozzle, and the drops do not free fall. Even though most of the previous studies found penetration theory suitable, Huang stated that prediction of mass transfer may be improved if one considers the velocity distribution inside the jet stream and solves the mass transfer problem with a Graetz-type solution.

VII. PHOTOGRAPHIC EXPERIMENTS

Photographic experiments were performed to determine the drop size distribution and the volume mean droplet diameter of the spray. The area occupied by the liquid at various cross sections of the scrubber (this area is a parameter in the fluid flow model) is a function of the average drop size. Also, the interfacial area available for gas absorption is a function of the average drop diameter of the spray. Photographic analysis of the spray was preferred to other methods of analysis (e.g., freezing the droplets and collecting them on slides, or measurement of light transmittance, etc.) because it is a direct technique applicable to the high liquid flow rates encountered in the ejector scrubber.

A. SPRAY CHARACTERISTICS

In order to interpret the photographs, it was necessary to analyze the liquid spray and understand the atomization process.

As the liquid enters the nozzle, (Figures 7.1 and 7.2) it passes through a spiral insert. This spiral imparts a tangential velocity to the liquid, which then enters a swirl chamber, and finally exits from the nozzle orifice. Since there is no longer any restraining surface when the liquid leaves the nozzle, the centrifugal force created by the swirling motion pushes the liquid outward, creating the spray cone and considerably aiding the breakup process.

The liquid first leaves the nozzle in the form of conical sheets, which slip over each other. As a result of internal viscous forces as well as shear at the liquid gas interface, holes develop in the liquid sheets. These holes grow in size as the liquid spreads out in the spray cone, and liquid filaments form where the holes meet. The filaments subsequently break into drops under the influence of drag forces.

Spray characteristics vary considerably with the nozzle pressure. For the clear plastic scrubber used in the present study, the following phenomena have been observed. At low pressures (1 -15 psi) the spray does not atomize. At pressures lower than 10 psi the spray angle is zero and the liquid falls down the scrubber in a straight line. The air flow is very low. As the pressure is increased to 15 psi and above, but lower than 30 psi, the spray angle becomes 15^{o}. The liquid reaches the walls of the venturi at the throat entrance, but no atomization is observed, since the liquid does not yet have enough energy. At higher pressures ($>$ 30 psi) atomization is observed, and the impact of the liquid spray with the walls of the venturi greatly improves turbulence, which is required for good liquid/air contact.

At increased pressures (50 psi and up) the atomization is greatly increased. The droplet formation starts as soon as the high energy liquid jet exits the nozzle. The spray is not transparent anymore, it has a white foamy appearance. The intensity of turbulence is further increased as the pressure reaches 100 psi which corresponds to a liquid

flow of 8 gpm. All of the above experiments were conducted with tap water and room air at ambient conditions. (Table 7.1)

B. APPARATUS AND PROCEDURES

The standard 4 inch AMETEK ejector venturi scrubber constructed of carbon steel was found to be unsuitable for the photographic experiments. The throat diameter was too small to build a see-through window large enough for the lens of the camera without disturbing the geometry of the scrubber, and therefore the characteristics of the flow. A clear plastic scrubber similar to the Ametek 7010 was built to order by Environmental Systems Company, Pennsylvania. The dimensions of the plastic scrubber were slightly different than the AMETEK 7010 scrubber. The dimensions of both scrubbers are compared on Figure 9.1. However, the diameters of air inlet, throat, and diffuser exit, and the length of throat were the same. Therefore, the liquid flow capacity, and the liquid-to-gas flow ratio of both scrubbers, were exactly the same. The slight dimensional differences did not affect the fluid flow characteristics between the two scrubbers (Figure 7.3).

The nozzle was a 3/8 inch, 622-L Schutte-Koerting design with a 15^{o} cone angle and 4.5 mm orifice. Delivery rates for this nozzle are given in Figure 7.4 as a function of pressure. This was the same nozzle used in the fluid flow and gas absorption experiments.

The initial photographs were taken with a Minolta SRT 201 camera with 50 mm f/1.4 MD Rokkor-x lens (Tables 7.2, 7.3), and a Vivitar 285 auto electronic flash (Table 7.4). The minimum focusing distance was 1.48 feet.

The two camera exposure control settings are lens opening and shutter speed. The size of the aperture determines the amount or volume of light reaching the film, and the shutter speed determines the length of time this light acts upon the film. The specific combination of aperture and speed depends upon the desired depth-of-field, and the need to stop the movement of the drops. A smaller aperture will increase the depth-of-field, but will require a slower shutter speed for a given light intensity. A slower shutter speed may blur the droplets.

The electronic flash can be either operated manually or automatically. It has four auto positions from shallow depth-of-field and longer focusing distance, to wider depth-of-field and shorter focusing distance. When shooting manually with the flash, the power output can be varied. Originally in the experiments the photographs were taken with the flash at manual operation to determine the best aperture and speed combination. The three variables were the flash distance, the flash power and the aperture. The camera was always 1.5 feet from the object.

When front lighting was used, the light reflected back from the Lucite surface of the scrubber. Therefore, side and back lighting were tried.

The shutter speed of the camera was set at $1/60^{th}$ of a second. The room was completely dark. Therefore, the speed of the flash light determined the exposure time, since it was much faster (1/1000 of a second at manual operation, 1/1000 to 1/30,000 of a second at auto operation) than the shutter speed of the camera.

The following films from Kodak were tried :

1. Tri-X Kodak film. It has high speed but large grain size. It is good for the stop action photographs, but the quality of image sharpness decreases when prints are enlarged.
2. Panatomic-X ASA32 Kodak film has a lower speed and smaller grain size.
3. Plus-X ASA125 Kodak film has moderately faster speed than Panatomic-X and smaller grain size than Tri-X.
4. Extachrome-X 200 Kodak film is for slide development.

With the above experimental techniques, stop-action of droplet movement was not achievable. This can be observed in Figure 7.5. Even though the motion was slowed down considerably, the individual droplets could not be distinguished. Also, the image sharpness was unsatisfactory. Therefore, it was impossible to differentiate between the droplets that are in the focusing plane and the ones that are not.

At this point it was decided to consult industrial photographers. Ms. Connie Jantzen was recommended by Photographic Analysis in Wayne, New Jersey. Upon her advice Plus-X ASA125 Kodak film with a Vivitar 285 flash at automatic yellow mode was used. The yellow mode utilizes the widest lens opening for relatively shallow depth-of-field, and provides the greatest automatic operating range (6 - 60 feet). She recommended trying the following flash distance/f-stop combinations: 1) flash at 2 ft with f/4, f/5.6, f/8; 2) flash at 1 feet with f/5.6, f/8, f/11. All combinations were tried with back lighting and side lighting. Two photographs were taken with front lighting. The quality of resulting photographs were considerably better. The speed of the electronic flash is faster at auto modes than on manual. At auto mode the flash time can be varied from 1/1000 of a second to 1/30,000 of a second. This resulted in better stop action quality. (Figures 7.6, 7.7, 7.8)

Generally large apertures gave sharper photographs due to a smaller depth of field (fewer drops). Flash distance is an important factor. From the point of view of sufficient lighting and picture sharpness, shorter flash distance with large aperature was found preferable. The uncertainty introduced during the film processing must be considered. The photographs were professionally developed and there was no control over the developing quality and consistency. When back lighting was used, the light was excessive at all f-stops and flash distances. Even though the second stage photographs were better in quality, the photographs were not clear enough to distinguish, count and size the drops.

At this point, Dr. Rolf D. Reitz from General Motors, and Professor Bracco from the Mechanical and Aerospace Engineering Department of Princeton University, were contacted. Dr. Reitz completed his Ph.D. dissertation under the supervision of Professor Bracco on the subject of atomization of fuel injection systems. In their experiments they used a Beckman and Whitley model 192 Framing camera (1.44 frames/sec) with Xenon N-789B nanolamp with 437A nanopulser and quartz lens. The size of field photographed was 500 microns by 500 microns. A visit to the Princeton University MAE laboratory revealed the fact that it is economically and physically impossible to use their system to photograph the spray in the ejector venturi scrubber.

Mr. Peter Kezios from Princeton University's Chemical Engineering Department recommended the use of a Hasselblad camera, with Xenon flash lamp and Polaroid 667 ASA 3000 film. (Mr. Kezios is presently analyzing the dispersion of gas bubbles in a liquid environment by photographic techniques, with Professor W. R. Schowalter.)

As a result of his recommendations, the following equipment was used in the final experiments:

- 500 C/M Hasselblad camera with 135 mm CF lenses and bellows system, [rented from Ken Hansen Photographic, New York (Figure 7.9)]
- Short arc, Xenon flash lamps (FX-199) with FYD-505 Lite Pac and PS-302 power supply trigger module, from EG&G Electrooptics, borrowed from Dr. Schowalter, Princeton

University, New Jersey. With this system, a flash duration of 1 microsecond can be achieved. (Figures 7.10, 7.11)

The camera was set at 10 inches from the mid-plane of the ejector venturi scrubber, and the flash lamp was installed 1.5 feet to the side. The power output of the flash was varied by using external capacitors. The liquid flow rate was varied from 3 to 9 gpm (in the atomizing range of the scrubber). Most of the photographs were taken at 6 gpm liquid flow rate with 49 cfm air flow rate. The f stops of the camera were varied from f/5.6 to f/45.

The use of Polaroid 667 ASA 3000 film allowed some control over the developing process. The recommended processing time was 30 seconds at 74 ^{o}F and above. The room temperature was between 75 to 80 ^{o}F. Therefore, by using a timer, each photograph was developed an equal amount of time (30 seconds). The results were excellent. There was no blur due to movement and the images were sharp. However, since the camera is focused at the centerline of the scrubber, spray hitting the walls of the scrubber can block the field of view. A window can be opened to exclude the wall effects, but due to the relative sizes of the throat diameter and camera, this is impossible without disturbing the fluid flow characteristics. Therefore, it was decided to determine a characteristic droplet size from the photographs where there was a clear enough image, and compare it with the manufacturer's data.

As the power of the flash lamp increased from no external capacitor to 2 μf external capacitor, and the aperture varied from lower f number (f/5.6) to higher f numbers (f/45), the image sharpness improved. However, the photographs of the throat section were too blurred because of the liquid at the walls of the scrubber. Therefore, photographs of the spray above the throat, in the converging section, were taken. With no external capacitor at higher f numbers the light was not sufficient. With no external capacitor, f/5.6 was the best f stop, but the image quality was still not satisfactory due to insufficient light. The photographs taken with flow rates above 6 gpm were too blurry because of the increased spray volume hitting the walls of the scrubber.

With a 2 μf external capacitor and lower f numbers (f/5.6 to f/22) there was excessive light. However, at f stops f/32 through f/45, and with 6 gpm liquid flow rate, good results were obtained with good image quality.

With 1 μf external capacitor mid range f numbers gave best results (f/22). At lower f numbers there was too much light and low image sharpness, and at higher f numbers also the image sharpness was also low.

In conclusion, good results were obtained at 6 gpm liquid rate with a 2 μf external capacitor and f numbers larger then f/22. (Figures 7.12, 7.13, 7.14) Figure 7.15 is the photograph of the spray at 3

gpm liquid flow rate with a 2μf external capacitor and f/22. Decreased turbulence and incomplete atomization is clearly observed.

For the purpose of acquiring a comparison between Polaroid 667 film and Kodak Plus X film, the best external capacitor and f stop combinations were also used with Plus X film. The stop action quality was the same as on Polaroid 667, but the quality of image sharpness was considerably lower.

VIII. PROPOSED FLUID FLOW MODEL FOR THE EJECTOR VENTURI SCRUBBER

In this work, the fluid flow through an ejector venturi scrubber is described by a one dimensional empirical model including frictional losses. Because of the complexity of the fluid flow, it is impossible to construct an analytical model from the Navier-Stokes equations.

In the ejector venturi scrubber, the helical vanes of the nozzle impart a tangential velocity to the liquid jet. At the exit of the nozzle the jet forms a hollow cone of spray. Due to slip between phases holes form on the spray sheets. As these holes meet the boundary between them forms liquid filaments which then disintegrate into drops. These droplets are further atomized into smaller droplets due to the drag forces.

The accelerated gas and atomized droplets mix in the throat section. During the mixing process the transfer of momentum from the liquid serves largely to compress the gas. Frictional losses occur in the nozzle, throat and diffuser. These losses are dependent on the local liquid/gas volumetric flow ratios. In the diffuser the static pressure increases at the expense of the kinetic energy of the mixture (largely that of the liquid, since the mass of the gas is relatively small). Since the liquid performs work in compressing the entrained gas, pressure recovery in the diffuser is significantly reduced. The pressure drop across the scrubber is primarily dependent on the mixing loss, as well as frictional and kinetic losses. The liquid is removed

from the bottom of the separator and returned to the nozzle via a mechanical pump which raises the drive fluid pressure.

Application of the mechanical energy balance for an isothermal system, and equations of continuity, produce the following expressions. (see Appendix A for derivation.)

(1) Mechanical Energy Balance for Liquid from Nozzle to Throat:

$$\frac{P_o - P_i}{\rho_l} + \frac{V_{li}^2}{2g_c}\left[\left(\frac{A_n}{A_{lo}}\right)^2 - 1 + K_{nz}\right] + \frac{g}{g_c}(L_o - L_i) = 0 \qquad 8.1$$

(2) Mechanical Energy Balance for Gas from Entry to Throat:

$$\frac{RT}{M_g} \ln \frac{P_o}{P_s} + \frac{V_{gs}^2}{2g_c}\left[\left(\frac{A_{gs}P_s}{A_{go}P_o}\right)^2 - 1 + K_{en}\right] + \frac{g}{g_c}(L_o - L_s) = 0 \qquad 8.2$$

(3) Mechanical Energy Balance for the Throat Section:

$$\frac{RT}{M_g} \ln \frac{P_t}{P_o} + \frac{Q_{li}}{2Q_s \frac{M_g P_s}{RT}}\left[\left(\frac{L_o - L_i}{L_t - L_i}\right)^2 + 1\right](P_t - P_o) + \left(\frac{A_{gs}P_s}{A_{go}P_o}\right)^2 \frac{V_{gs}^2}{2g_c} *$$

$$\left[\frac{P_o^2}{P_t^2} - 1 + K_{th}\right] + \frac{\rho_l Q_{li}}{\frac{P_s M_g}{RT} Q_{gs}}\left(\frac{A_n}{A_{lo}}\right)^2 \frac{V_{li}^2}{2g_c}\left[\left(\frac{L_o - L_i}{L_t - L_i}\right)^6 - 1 + K_{th}\right]$$

$$+ \frac{g}{g_c}(L_t - L_o) + \frac{g}{g_c} \frac{\rho_l Q_{li}}{\frac{P_s M_g}{RT} Q_{gs}}\left[\left(\frac{L_o - L_i}{L_t - L_i}\right)^2 L_t - L_o\right] = 0 \qquad 8.3$$

(4) Mechanical Energy Balance for the Diffuser Section:

$$\frac{RT}{M_g}\ln\frac{P_d}{P_t} + \frac{Q_{li}RT}{2Q_{gs}P_sM_g}\left(\frac{L_o-L_i}{L_t-L_i}\right)^2\left[\left(\frac{L_t-L_i}{L_d-L_i}\right)^2+1\right](P_d-P_t)+\left(\frac{A_{gs}P_s}{A_{gt}P_t}\right)^2\frac{V_{gs}^2}{2g_c}\left[\frac{P_t^2}{P_d^2}-1+K_{di}\right]$$

$$+\frac{\rho_l Q_{li}RT}{Q_{gs}P_sM_g}\left(\frac{L_o-L_i}{L_t-L_i}\right)^6\left(\frac{A_n}{A_{lo}}\right)^2\frac{V_{li}^2}{2g_c}\left[\left(\frac{L_t-L_i}{L_d-L_i}\right)^6-1+K_{di}\right] + \frac{g}{g_c}(L_d-L_t)$$

$$+\frac{g}{g_c}\frac{\rho_l Q_{li}RT}{Q_{gs}P_sM_g}\left(\frac{L_o-L_i}{L_d-L_i}\right)^2\left[\left(\frac{L_t-L_i}{L_d-L_i}\right)^2 L_d-L_t\right] = 0 \qquad 8.4$$

The above relationships are logarithmic as a result of flow compressibility. The following are the only assumptions that were made during the development of the fluid flow model:

1. The gas is isothermally compressed from the scrubber inlet to diffuser outlet. (verified by measurements)
2. Heat rejection to the liquid from the compressed gas and from dissipation of frictional energy cause a negligible rise in liquid temperature.
3. Prior to mixing in the throat, the liquid jet and the gas are separate phases.
4. Changes in gas solubility and average molecular weight between scrubber inlet and outlet are neglected.
5. Evaporation of the liquid is neglected in performing the material balances.

The only data required are the pressure and temperature, and volumetric flow rates of the liquid and the gas. The frictional loss coefficients (K_{nz}, K_{en}, K_{th}, and K_{di}) were calculated from experimental results.

The fluid flow equations are general equations applicable to any circular ejector venturi scrubber with any dimensions and any type of nozzle. The lengths of the various sections of the ejector venturi scrubber; the diameters of the throat, the diffuser, and the gas inlet; the distance of the nozzle from the throat entrance; the diameter of the nozzle orifice; the spray angle; and the liquid and gas properties appear as parameters in the fluid flow equations. These are listed in Table 8.1.

IX. FLUID FLOW EXPERIMENTS

Fluid flow experiments were planned to determine the pressure and temperature variations within the ejector venturi scrubber. The pressure and temperature distributions were than used to calculate the empirical constants in the fluid flow model.

A. APPARATUS

An AMETEK 7010 ejector venturi scrubber with baffle separator was used during the experiments. This scrubber is an industrial size, fabricated of carbon steel. The diameters of air inlet and diffuser exit are both 4 inches and the diameter of the throat section is 2 inches. The overall height of the scrubber is 24 inches. Figure 9.1 shows the dimensions of the various sections of the AMETEK 7010 scrubber. The ejector venturi is connected to an AMETEK 7040 liquid/gas separator. The separator consists of an inlet at the top, a drain at the bottom, and a clean gas outlet at the side. A separating element, which incorporates a series of baffles, is located just below the inlet. Scrubbing liquid from the separator is drained to a storage tank and recirculated through the system.

B. INSTRUMENTATION

The liquid flow rate was measured by a rotameter from Emerson Electrical Company, Brooks Instrument Division, installed on the water recycle line. The range of this rotameter is between 1 and 15 GPM. The air flow rate was measured with a Hastings meter, from Teledyne Hastings - Raydist Inc.. This air meter measures the velocity of the gas stream in feet per minute. The volumetric flow rate is calculated by multiplying the cross-sectional area of the tube by the velocity. The Hastings air meter was calibrated against a pitot tube. The calibration curve of the Hastings air meter is shown in Figure 9.2. The Hastings meter was installed on the 4 inch air inlet pipe, 10 pipe diameters downstream from the room air pick up point, and much more than 10 pipe diameters upstream of the next flow disturbance. The experimental setup is shown in Figure 9.3.

Three thermometers were installed in the air inlet pipe, and at locations i and d of the ejector venturi scrubber.

Five pressure taps were installed at locations i, s, o, t, and d. These pressure taps were connected through ¼" outside diameter plastic tubing to a water knockout chamber. An on-off valve was installed on each of the lines. A single line ran from the water knockout chamber to the manometer. Since very small pressure drops were expected, a slant type manometer from F.W.Dwyer Manufacturing Company was chosen.

The manometer readings were in inches of water and the manometer fluid was 0.826 sp. gr. red oil.

C. PROCEDURES

The water flow was set at the desired level by using a globe valve installed in the recycle line. It was varied from 1 through 8 GPM. The liquid to gas ratio through the scrubber was constant. Figure 9.4 shows liquid flow rate versus gas flow rate of the ejector venturi scrubber.

At each liquid rate setting, readings of air flow rate and temperature at various sections of the system were recorded. The pressure readings at sections i, s, o, t, d were taken by connecting one line at a time to the manometer. The above procedure was repeated four times with 10 minutes lapse between each individual reading, to assure accuracy of the data. The water knockout pot was drained as necessary.

X. GAS ABSORPTION EXPERIMENTS

Anhydrous pure SO_2 gas, purchased from MG Industries, was introduced into the air inlet pipe. Gas samples were extracted from the air inlet, diffuser exit, and separator exit of the ejector venturi scrubber system, and analysed by barium-thorin titration method. The miminum detectable limit of the method was determined to be 1.28 ppm.

A. APPARATUS

The sampling train is shown in Figure 10.1 and component parts are discussed below.

The sampling probe was ¼" plastic tubing installed through Swage-Lok fittings. The tubing was connected to a water knockout chamber, and followed by three midget impingers in series. A silica gel drying tube was installed after the midget impingers. A vacuum pump in series with a rotameter was connected to the dry gas flow meter. The flow rate of the sample gas was regulated by the valve on the rotameter.

B. PROCEDURES

The procedure is the USEPA Testing Method 6 for determination of sulfur dioxide emissions from stationary sources. However, the following modifications were made in this procedure:

1. The isopropanol bubbler that precedes the midget impingers was replaced with a water knockout chamber. The purpose of the isopropanol bubbler is to remove free ammonia or fluorides that can interfere with SO_2 sampling. Since these interferences were not present in the room air drawn through the scrubber, the isopropanol was not necessary.
2. The ice bath around the midget impingers was removed. Method 6 is developed for high temperature stack gas sampling and the ice bath is necessary to keep the temperature at ambient levels. Since our sampling was done at room temperature, the ice bath was unnecessary.

Three percent hydrogen peroxide was prepared by diluting 30 percent hydrogen peroxide 1:9 (v/v) with distilled water. Fifteen milliliters of three percent hydrogen peroxide were measured into each of the first two midget impingers. The final impinger was left dry. The sampling train was assembled as shown in Figure 10.1.

The inital dry gas meter reading was recorded, then the vacuum pump was started. The sampling flow was adjusted to a constant rate of 1.0 liter per minute as indicated by the rotameter. The sampling duration was 20 minutes. At the end of sampling the pump was turned off and the final dry gas meter reading was recorded. The system was purged by drawing clean air through the system for 15 minutes at the desired sampling rate. The samples were collected at air inlet and separator exit, or diffuser exit and separator exit, simultaneously.

After purging the impingers were disconnected and the contents were transferred into a 100 ml volumetric flask. The three midget impingers were rinsed with distilled water and the washings were added to the volumetric flask. The contents of the volumetric flask were diluted to exactly 100 milliliters with distilled water. A 20 ml aliquot of this solution was pipetted into a 250 ml Erlenmeyer flask, and 80 ml of 100 percent isopropanol (reagent grade) and four drops of thorin indicator (prepared by dissolving 0.20 g in 100 ml distilled water) were added. Barium perchlorate solution (0.0100N) was prepared by dissolving 1.22 gm of $BaCl_2.2H_2O$ in 200 ml distilled water and diluted to 1 liter with 100 percent isopropanol. Barium perchlorate solution was standardized against 25 ml of standard sulfuric acid (0.0100N) to which 100 ml of 100 percent ispropanol had been added. The sample solution was titrated to a pink end-point using the barium perchlorate solution. The titration was repeated with the rest of the sample and titration volumes were averaged.

XI. RESULTS

In this section the results of the photographic, fluid flow, and gas absorption experiments are presented. Through photographic analysis of the spray in the clear plastic replica of the 4 inch AMETEK 7010 ejector venturi scrubber, the drop size range and the median drop size were determined. The techniques of this analysis are explained with the results.

The median drop size of the spray was used to determine the area occupied by the liquid at any cross section of the scrubber. The area occupied by the liquid is a parameter of the fluid flow model. Its value along with the pressure drop and temperature variation data were used to determine the empirical frictional loss contants of the fluid flow model.

Gas absorption experiments were performed to determine the SO_2 scrubbing efficiency of the ejector venturi system. The additional scrubbing efficiency of the separator was determined separately. The relationship of the scrubbing efficiency to the drop size variation was investigated and the mass transfer coefficient $K_g a$ was calculated.

A. DROP SIZE AND SIZE RANGE

Out of the 35 photographs that were taken with the Hasselblad 500 C/M camera and the Polariod 667 film, two photographs were used for the

determination of volume mean droplet diameter and the drop size range (Figures 7.12 and 7.13). These two photographs were both taken at 6 GPM liquid flow rate with 2μf external capacitor at f/27 and f/22, respectively. In both cases, the spray was fully atomized and the image quality was satisfactory. The other photographs were either too dark or too bright, or (at higher flow rates) the pictures were blurred due to spray hitting the walls of the scrubber.

Visibility of the one inch strip on the enlargements above the throat is blurred by the spray hitting the walls of the scrubber. Therefore, a four and a half square inch area located just above that strip was arbitrarily chosen to count and size the drops.

The projected area of the liquid droplets were measured on the enlargements. For this purpose, a photocopy of the enlarged print and a transparency of a graph paper were made. The transparent graph paper was placed on the enlarged photograph. As the area of each droplet was determined, it was marked off the photocopy of the print.

There is a 7.42 enlargement factor between the original prints and the enlargements. Therefore, the area of each droplet on the enlargement was divided by 7.42 to determine the area on the original prints, and the apparent diameter of each droplet calculated from the corrected area:

$$d = \sqrt{\frac{4 \times \text{corrected area}}{\pi}} \qquad 11.1$$

Since one centimeter on the original print is actually 1.3 centimeters near the scrubber axis (determined by photographing a metric scale), the apparent diameters were multiplied by 1.3 to determine the actual diameters.

Once the actual diameters and the number of drops in each size had been determined, the volume mean diameter was calculated using the following formula:

$$D_v = \left(\frac{\sum_i n_i D_i^3}{\sum n_i} \right)^{1/3} \qquad 11.2$$

The volume mean diameter was determined to be 155 microns, and the sizes of the droplets ranged from 34 microns to 563 microns. The results were compared to the data provided by the manufacturer (Figure 11.1). In this figure the volume mean droplet diameter versus pressure drop across the nozzle for one inch and longer nozzles are graphed. By extrapolation the volume mean droplet diameter at 80 psi nozzle pressure drop for a 3/8" nozzle was found to be about 150 microns. Therefore, the volume mean droplet diameter determined by the photographic analysis is consistent with the manufacturer's data. The size distribution of the droplets is shown on Figure 11.2.

The photographs were also analysed for the degree of atomization of the spray. It was determined that at 6 GPM liquid flow rate through

the nozzle, atomization is complete. No filaments, the presence of which would be an indication of incomplete atomization, were observed on the photographs. Also it was determined that the number of smaller droplets ($< 150\mu m$) was much higher than the number of larger droplets. However, the total volume of the smaller droplets did not significantly influence the volume mean diameter for the spray.

B. AREA OCCUPIED BY THE LIQUID

The volume mean droplet diameter was used in the determination of the area occupied by the liquid at various cross sections of the scrubber. Under steady state conditions in the throat section, the droplets are distributed uniformly in a volume element of $\Delta X \Delta Y \Delta Z$ dimensions. Originally it was assumed that the number of drops per unit area in the vertical plane ($\Delta X \Delta Y$) of the photographs was equal to the number in the horizontal plan ($\Delta X \Delta Z$). And the area occupied by the liquid at the entrance to the throat was calculated by:

$$A_{lo} = NA_t(\pi D_v^2/4) \qquad 11.3$$

However, when the frictional loss constants of the fluid flow model were calculated by using the above assumption, negative values were obtained (i.e. an under-estimation of the area occupied by the liquid). By the above assumption the area occupied by the liquid would

be 0.11 percent of the total area of the throat section. From a visual observation of the throat section, such a low fractional area covered by liquid seemed improbable. Therefore, the area occupied by the liquid drops at the entrance to the throat section was calculated from volume balance relationships. In a cylindrical element with diameter equal to throat diameter and length equal to volume mean diameter, the ratio of the volume occupied by the spray (V_{lo}) to the volume occupied by the gas (V_{go}) is equal to the local liquid-to-gas volumetric flow rate ratio.

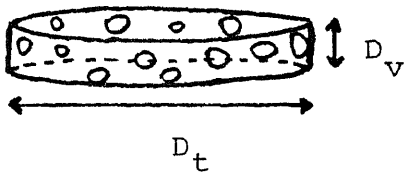

Using the following equation:

$$\frac{V_{lo}}{V_{go}} = \frac{A_{lo}D_v}{(A_t - A_{lo})D_v} = \frac{Q_{lo}}{Q_{go}} \qquad 11.4$$

A_{lo} was calculated to be 0.05112 square inches, or 1.63% of the throat area. From the photographs, the number of drops on the vertical plane were determined to be 38 drops per square inch. However, on the horizontal plane the number of drops were calculated to be 557 drops per square inch. This was much more consistent with visual observations, and resulted in positive parameters in the fluid flow model.

C. PRESSURE DISTRIBUTION

The pressure drop distribution profile was determined by measuring the static pressure at various locations along the scrubber. Also the variation of the pressure drop profile with liquid flow rate was determined. The results are shown on Figure 11.3. The overall pressure drop of the ejector venturi scrubber was determined to be zero inches of water. There was a sharp pressure drop between the nozzle tip and the throat exit (Locations i and t). Then a slower pressure recovery in the diffuser section was observed. The pressure recovery was achieved at the expense of the kinetic energy of the gas and liquid streams. It was also determined that the pressure distribution profile flattened as the liquid flow rate decreased. At 8 gallons per minute liquid flow rate, the pressure drop between nozzle tip and throat exit was determined to be 15.1 pound force per square feet. But at 2 gallons per minute liquid flow rate, the pressure drop between the same two locations was only 0.8 pound force per square feet. This is largely due to the decreased kinetic energy of the liquid jet that creates lower draft to entrain the gas.

D. FRICTIONAL LOSS CONSTANTS

The empirical frictional loss constants of the fluid flow model were calculated using the results of the photographic analysis and pressure distribution profile. The values of the various parameters and variables of the model are listed in Table 11.1.

The frictional loss constant of the liquid side entry equation K_{nz} was determined to be 0.82. This is the section where the high velocity liquid jet exits the nozzle and atomizes into droplets. The cross sectional area of the nozzle tip was 1.7×10^{-4} ft^2. The area occupied by liquid at the entrance to the throat was 3.55×10^{-4} ft^2.

The constant for the gas side entry equation was determined to be: $K_{en} = 4.41$. The gas enters through a 12.6 square inch opening into the scrubber and gradually compresses as it travels down the scrubber to pass through the 3.14 square inch throat section.

The empirical constants for the throat section, K_{th}, and the diffuser section, K_{di}, were determined to be 0.84 and 0.80 respectively. The throat section is a short straight duct with length-to- diameter ratio of 0.5, and the diffuser was tapered with a 5^{o} angle. The length of the diffuser section was 14¼ inches.

Values of the empirical frictional loss constants are listed in Table 11.2. Their order of magnitude is consistent with typical values for other fluid flow phenomena (see e.g. texts by McCabe and Smith, or Bird, Stewart, and Lightfoot).

E. SULFUR DIOXIDE ABSORPTION EFFICIENCY

Sulfur dioxide gas at 12,500 ppm inlet concentration was scrubbed with 0.0001M sodium hydroxide solution. At 7 GPM and higher liquid

flow rates, the overall scrubbing efficienty of the ejector venturi-separator system was determined to be 99.97 percent. Between 4 and 2 GPM liquid flow rate, there was a sharp decrease in the scrubbing efficiency from 98% to 10%. This is primarily due to a decrease in the interfacial area between the liquid and gas phases. At all flow rates, the liquid-to-gas ratio was constant (Q_l/Q_g=0.0164). But the interfacial area decreased at lower flow rates due to incomplete atomization and lower turbulence, hence larger drops and a multitude of filaments formed.

The droplet interfacial area in the entire scrubber, expressed in terms of square feet per cubic feet of scrubber volume, is represented by the following relationship:

$$a = \frac{1}{(1+Q_g/Q_l)} \frac{6}{D_v} \qquad 11.6$$

The derivation of equation 11.6 in Appendix E. The only variable in equation 11.6 is the volume average drop diameter. The interfacial area decreases with increasing drop diameter.

This relationship should be taken into consideration when upscaling ejector venturi scrubbers. The nozzle should be chosen such that the mean droplet diameter will provide sufficient interfacial area.

The additional scrubbing efficiency achieved in the separator was determined separately. Maximum scrubbing efficiency achieved in the separator was 48%. As the flow rates decreased, the separator efficiency slowly dropped to about 1% around 1 gpm flow rate.

The results of overall efficiency determination experiments, and separator experiments, are shown in Tables 11.3 and 11.4.

Figure 11.4 shows the variation of scrubbing efficiency with liquid flow rate. The curve has an S shape showing a sharp increase in efficiency as the liquid flow rate reaches the complete atomization regime. Figure 11.5 shows the variation of scrubbing efficiency achieved in the separator section of the system as a function of liquid flow rate.

The overall volumetric mass transfer coefficient for the SO_2 - NaOH system was calculated from experimental results, and at 99.97% efficiency it was determined to be 796 pound mole per hour per cubic foot of scrubber volume (Table 11.5). The interfacial area for gas absorption at full atomization was 47.6 square feet per cubic feet of scrubber volume. Therefore, the overall mass transfer coefficient was calculated to be 16.72 lbmoles/hr-ft^2 of interfacial area.

Raman (1983) determined the mass transfer coefficient for the SO_2 - NaOH system in a modified ejector venturi scrubber to be in the range

of 440 to 1420 pound moles per hour per cubic foot of scrubber volume. His experiments were carried out in a 1¼ inch scrubber with 0.05 or lower liquid-to-gas ratios.

As the liquid flow rate decreased the mass transfer coefficient, Kga also decreased (Figure 11.6) down to 0.6 pound moles per hour per cubic foot of scrubber volume. This also is primarily due to the decreased interfacial area at lower flow rates.

XII. CONCLUSIONS AND RECOMMENDATIONS

The empirical fluid flow model equations developed in this work for the ejector venturi scrubber are general equations applicable to any size circular ejector venturi scrubber with any nozzle. Parameters pertaining to the scrubber and nozzle geometry, as well as liquid and gas properties, are included in the model.

The model equations are in Appendix A. The values of the empirical constants are listed in Table 11.2.

Pressure drop distribution within the scrubber varied considerably with the nozzle flow rate. At 1 gpm liquid flow rate, the pressure distribution profile was flat. As the flow rate was increased, the pressure distribution profile formed a U shaped curve that deepened at higher flow rates. Above 5 gpm liquid flow rate, there was a very sharp drop in pressure between the nozzle exit and the throat exit.

The spray within the scrubber starts atomizing at around 15 psi nozzle pressure, which corresponds to 3 GPM liquid flow rate. At this flow rate, the majority of the liquid body is in the form of filaments. At 30 psi nozzle pressure, complete atomization of the spray is achieved.

The analysis of the photographs of the spray confirm the above findings. On the photographs taken at 6 GPM liquid flow rate (70 psi

nozzle pressure) no filaments were observed. The liquid phase was in the form of small liquid droplets dispersed throughout the scrubber.

The volume median droplet diameter of the 3/8" S & K 622-L nozzle was determined to be 155 microns. The droplet diameters ranged from 34 microns to 563 microns.

The sulfur dioxide scrubbing efficiency with 0.0001 M sodium hydroxide solution was 99.97%. The maximum efficiency of the separator alone was 48% under the same operating conditions. Therefore, the scrubbing efficiency of the ejector venturi alone was 99.94% in the complete atomization regime. There is a sharp decrease in the efficiency of the scrubber when the liquid flow rate decreased from 4 gpm to 2 gpm. This was primarily due to incomplete atomization of the liquid phase at 3 gpm and lower flow rate, which resulted in much lower interfacial area for gas absorption. Therefore, the performance of the ejector venturi scrubber depends mainly on the degree of atomization of the liquid spray as well as the liquid-to-gas volumetric flow ratios.

The overall volumetric mass transfer coefficient for this system was 796 pound moles per hour per cubic foot of scrubber volume. This value is comparable with the results of Raman (1983) (440 - 1420 pound moles per hour per cubic foot of scrubber volume). The interfacial area of the system at full atomization was 47.6 square feet per cubic foot of scrubber volume, calculated from the volume median droplet diameter. Therefore, the overall mass transfer coefficient was

calculated to be 16.72 lbmoles/hr-ft^2 of interfacial area. The interfacial area of the ejector venturi scrubber is a function of the gas-liquid flow ratio and volume median droplet diameter of the nozzle. When scaling up ejector venturi scrubbers of known liquid-to-gas ratio (i.e. known draft), the scrubbing efficiency can be increased by changing to a nozzle with smaller drops, hence higher interfacial area.

It is recommended that further tests be performed in scaled-up scrubbers of similar and modified geometry with S & K 622-L nozzles. The purpose would be to determine the role of scrubber size and geometry in achieving complete atomization. In such experiments, the angle of the converging section should be varied.

It is further recommended that the gas absorption efficiency be determined for scaled-up scrubbers with nozzles of different volume median diameter. The variation of the volume median diameter from nozzle to nozzle should be verified by photographic analysis. The purpose will be to determine the effect of the increase in the interfacial area on the scrubbing efficiency of the system, and compare it with the additional pumping power needed to increase the interfacial area.

NOMENCLATURE

a	liquid jet radius, ft.; speed of sound under conditions of flow, ft/sec; interfacial area for gas absorption, ft^2/ft^3.
a_T	total interfacial area in the venturi, ft^2.
A	cross section area, ft^2.
A_d	cross sectional area of diffuser exit, ft^2.
A_{dr}	projected area of the drop with volume mean diameter, ft^2.
A_{drop}	surface area of a drop with volume mean diameter, ft^2.
A_l	cross sectional area occupied by liquid ft^2.
A_n	cross sectional area of nozzle tip, ft^2.
A_g	cross sectional area of gas ft^2.
A_t	cross sectional area of throat, ft^2.
C	solute gas concentration, $lbmoles/ft^3$.
C^*	equilibrium concentration of solute in liquid, $lbmole/ft^3$.
C_A^*	concentration of dissolved gas A at interface, in equilbrium with gas at interface, $lb/moles/ft^3$.
C_{Ab}	concentration of dissolved gas in bulk of liquid $lbmoles/ft^3$.
C_m	mass concentration of drops in light beam, $lbmole/ft^3$.
C_D	drag coefficient
d_m	mass median diameter of drops, ft.
d_{max}	maximum drop diameter in spray, ft.
d_o	nozzle exit diameter, ft.
D	drop diameter, ft.
D_h	hydraulic diameter of the venturi, ft.
D_i	diameter of drop of size i, ft.

D_{max} maximum stable drop diameter, ft.

D_{pq} drop mean diameter, ft.

D_v volume mean drop diameter, ft.

D_{32} Sauter mean drop diameter, ft.

D_A diffusivity of solute gas in the liquid, ft^2/sec.

D_m diffusivity (lbmoles/ft/hr)

E enhancement factor.

f friction factor.

f_N drop size distribution function by number.

f_N^* normalized drop size distribution by number.

f_V drop size distribution function by volume.

f_V^* normalized drop size distribution function by volume.

g gravitational acceleration, ft^2/sec^2.

g_c gravitational constant, ft-lbm/lbf-sec^2.

G molar flow rate of solute free bulk gas, lbmoles/sec.

H Henry's law constant, atm.cm^3/gmmole

j_d j factor for mass transfer

j_H j factor for heat transfer

J_o zeroth order Bessel function of first kind.

J_i first order Bessel function of the first kind.

K_o zeroth order modified Bessel function of the second kind.

K_i first order modifed Bessel function of the second kind.

k_2 second order reaction rate constant, liters/gmole-sec.

K_{di} frictional loss coefficient of diffuser.

K_{en} frictional loss coefficient from gas inlet to throat.

K_{nz} liquid expansion loss coefficient from nozzle to throat.

K_{th} frictional loss coefficient of throat.

k mass transfer coefficient (lbmole/ft^2.hr)

k_g gas phase mass transfer coefficient, lbmoles/sec ft^2.

K_g overall gas side mass transfer coefficient, lbmoles/sec $ft.^2$.

K_{ga} overall gas side volumetric mass transfer coefficient, lbmoles/sec ft^3.

L nozzle passage length, ft.

L_d height of diffuser exit, ft.

L_i Height of nozzle tip, ft.

L_o height of the throat entry, ft.

L_s height of gas inlet section, ft.

L_t height of the throat exit section, ft.

M molecular weight of fluid, lbm/lbmole.

M_g molecular weight of gas, lbm/lbmole.

m mass flow rate, lb/sec.

m_s mass flow rate of spray, lb/sec.

N particle size distribution function, (drops per ft. of diameter per ft^3 of suspension), number of drops per unit, area (drops/ft^2).

Na,n instantaneous rate of absorption of solute gas, lbmoles/sec ft^3.

Na,N average rate of absorption of solute gas, lbmoles/sec ft^3.

N number of drops per unit area, drops/ft^2

N_{drop} total number of drops in the scrubber.

N_i isothermal Mach number.

n_i number of drops of size i.

N_{Ma} Mach number, (u/a)

N_{Nu}	Nusselt number ($= hD/K$)
N_{Pr}	Prandtl's number ($= C_p \mu/K$)
N_{Re}	Reynolds number ($= DV\rho/\mu$)
N_{Sc}	Schmidt number ($= \mu/\rho D$)
N_{Sh}	Sherwood number ($= KD/Dm$)
P	static pressure lbf/ft^2.
P_d	static pressure at diffuser exit, lbf/ft^2.
P_i	static pressure at nozzle tip, lbf/ft^2.
P_o	static pressure at throat inlet, lbf/ft^2.
P_s	static pressure at gas inlet, lbf/ft^2.
P_t	static pressure at throat exit, lbf/ft^2.
Q	volumetric flow rate, ft^3/sec.
Q_g	volumetric flow rate of gas, ft^3/sec.
Q_l	volumetric flow rate of liquid, ft^3/sec.
R	gas constant, psi $ft^3/lbmole\ ^oR$.
r	radius of nozzle, ft.
$r_{t,o}$	radius of spray at locations t and o, ft.
T	Temperature, ^oR.
t	time, sec.
te	exposure time, sec.
u	axial velocity component, ft.
V_o	jet velocity, ft/sec.
V_g	gas velocity, ft/sec.
V_l	liquid velocity, ft/sec.
v_r	relative velocity of liquid and gas, ft/sec.
V	volume, ft^3.
V_{liq}	liquid hold up, ft^3.

V_T total volume of scrubber, ft^3.

W disturbance growth rate

W_e Weber number $(= \rho V_r^2 D/\sigma)$

W_j mass fraction in the jth size range.

X distance measured along asix, ft.

X^* reduced diameter, d/dm.

X_B distance from nozzle exit where liquid jet is no longer continuous (breakup length), ft.

Y_1 first order Bessel function of second kind.

Y_A solute gas concentration in bulk gas, moles solute gas/moles inertgas.

$Y_{i,o}$ solute gas concentation inlet or outlet, moles solute gas/moles inertgas.

Y_{lm} log mean solute gas concentration.

Z Ohnesorge number; axial coordinate, ft.

SUBSCRIPTS OF FLUID FLOW MODEL

c	critical
d	diffuser exit
g	gas
i	nozzle exit
l	liquid
o	throat inlet
s	gas inlet
st,sd,so	spray at location t, d and o.
t	throat exit

GREEK LETTERS

θ	spray angle, degree.
μ_g	gas viscosity, centipoise
μ_l	liquid viscosity, centipoise
ρ_g	gas density, lbm/ft^3.
ρ_{gs}	density of gas at gas inlet location, lbm/ft^3.
ρ_l	liquid density lbm/ft^3.
ρ_o	gas density at entrance to throat conditions, lbm/ft^3.
ρ_s	spray phase density, lbm/ft^3 ( ).
σ	gas/liquid surface tension, dyne/cm.

ϕ specific extinction cross section of the drops, ft^3/lb; volumetric flow ratio of gas to liquid, Q_g/Q_l.

ϕ_T theoretical average absorption rate, lbmole/sec.

$\sim\!\Omega\!\sim$ coefficient in Froesling's equation (1938), lb/moles/sec,ft.

APPENDICES

A. DERIVATION OF FLUID FLOW MODEL

LIQUID-SIDE ENTRY EQUATION

Assumptions:

(1) the liquid pressure equals the gas pressure at entry to the scrubber and throat.

(2) Liquid is incompressible.

$$\frac{P_o - P_i}{\rho_l} + \frac{V_{lo}^2 - V_{li}^2}{2g_c} + \frac{g}{g_c}(L_o - L_i) + K_{nz}\frac{V_{li}^2}{2g_c} = 0$$

$$V_{lo} = \frac{A_n}{A_{lo}} V_{li}$$

$$\frac{P_o - P_i}{\rho_l} + \frac{V_{li}^2}{2g_c}\left[\left(\frac{A_n}{A_{lo}}\right)^2 - 1 + K_{nz}\right] + \frac{g}{g_c}(L_o - L_i) = 0$$

GAS-SIDE ENTRY EQUATION

$$\int_s^o \frac{dP}{\left(\frac{PM_g}{RT}\right)} + \frac{V_{go}^2 - V_{gs}^2}{2g_c} + \frac{g}{g_c}(L_o - L_s) + K_{en}\frac{V_{gs}^2}{2g_c} = 0$$

$$\frac{RT}{M_g} \ln \frac{P_o}{P_s} + \frac{V_{gs}^2}{2g_c}\left[\left(\frac{A_{gs}P_s}{A_{go}P_o}\right)^2 - 1 + K_{en}\right] + \frac{g}{g_c}(L_o - L_s) = 0$$

where $A_{go} = A_t - A_{lo}$

Assumptions:

(1) No mixing

(2) Isothermal expansion

MIXING THROAT MOMENTUM EQUATION

$$\int_o^t m_g \frac{dP}{\rho_g} + \int_o^t m_l \frac{dP}{\rho_l} + m_g \frac{\left(V_{gt}^2 - V_{go}^2\right)}{2g_c} + \frac{m_{lt}V_{lt}^2 - m_{lo}V_{lo}^2}{2g_c}$$

$$+ \left[(m_g+m_{lt})L_t - (m_g+m_{lo})L_o\right] \frac{g}{g_c} + \left[m_g \frac{V_{go}^2}{2g_c} + m_{lo} \frac{V_{lo}^2}{2g_c}\right] K_{th} = 0$$

$$\frac{RT}{M_g} \ln \frac{P_t}{P_o} + \left(\frac{m_{lt}+m_{lo}}{2m_g}\right)\left(\frac{P_t - P_o}{\rho_l}\right) + \frac{V_{go}^2}{2g_c}\left[\frac{P_o^2}{P_t^2} - 1 + K_{th}\right]$$

$$+ \frac{m_{lo}V_{lo}^2}{2g_c m_g}\left[\frac{m_{lt}V_{lt}^2}{m_{lo}V_{lo}^2} - 1 + K_{th}\right] + \frac{g}{g_c}(L_t - L_o) + \frac{g}{g_c}\frac{m_{lo}}{m_g}\left(\frac{m_{lt}}{m_{lo}}L_t - L_o\right) = 0$$

Where

$$V_{go} = \frac{A_{gs}P_s}{A_{go}P_o} V_{gs} \quad , \quad m_{lo} = m_{li} \quad , \quad m_g = \frac{P_s M_g}{RT} Q_{gs} \ ,$$

$$V_{lt}A_{lt} = V_{lo}A_{lo} \ , \quad m_{lt} = m_{lo} \frac{A_{lo}}{A_{lt}}$$

$$A_{lt} = A_{lo} \frac{\pi r_t^2}{\pi r_o^2} = A_{lo} \frac{\pi\left[\tan(\theta/2)\,(L_t - L_i)\right]^2}{\pi\left[\tan(\theta/2)\,(L_o - L_i)\right]^2} = A_{lo}\left(\frac{L_t - L_i}{L_o - L_i}\right)^2$$

$$m_{lt} = m_{li}\left(\frac{L_o - L_i}{L_t - L_i}\right)^2$$

Therefore

$$\frac{RT}{M_g}\ln\frac{P_t}{P_o} + \frac{Q_{li}}{2Q_{gs}\,\frac{M_g P_s}{RT}}\left(\left(\frac{L_o-L_i}{L_t-L_i}\right)^2 + 1\right)(P_t-P_o) + \left(\frac{A_{gs}P_s}{A_{go}P_o}\right)^2 \frac{V_{gs}^2}{2g_c} *$$

$$\left[\frac{P_0^2}{P_t^2} - 1 + K_{th}\right] + \frac{\rho_l Q_{li}}{\left(\frac{P_s M_g}{RT}\right) Q_{gs}}\left(\frac{A_n}{A_{lo}}\right)^2 \frac{V_{li}^2}{2g_c}\left[\left(\frac{L_o-L_i}{L_t-L_i}\right)^6 - 1 + K_{th}\right]$$

$$\frac{g}{g_c}(L_t-L_o) + \frac{g}{g_c}\,\frac{\rho_l Q_{li}}{\left(\frac{P_s M_g}{RT}\right) Q_{gs}}\left[\left(\frac{L_o-L_i}{L_t-L_i}\right)^2 L_t - L_o\right] = 0$$

Assumptions:

(1) Isothermal system

(2) Incompressible liquid

(3) No change in m_g

DIFFUSER FLOW EQUATION

$$\int_t^d m_g \frac{dP}{\rho_g} + \int_t^d m_l \frac{dP}{\rho_l} + m_g \left(\frac{V_{gd}^2 - V_{go}^2}{2g_c} \right) + \frac{m_{ld} V_{ld}^2 - m_{lt} V_{lt}^2}{2g_c}$$

$$+ \left[(m_g + m_{ld}) L_d - (m_g + m_{lt}) L_t \right] \frac{g}{g_c} + \left[m_g \frac{V_{gt}^2}{2g_c} + m_{lt} \frac{V_{lt}^2}{2g_c} \right] K_{di} = 0$$

$$\frac{RT}{M_g} \ln \frac{P_d}{P_t} + \left(\frac{m_{ld} + m_{lt}}{2m_g} \right) \frac{P_d - P_t}{\rho_l} + \frac{V_{gt}^2}{2g_c} \left[\frac{P_t^2}{P_d^2} - 1 + K_{di} \right]$$

$$+ \frac{m_{lt} V_{lt}^2}{m_g 2g_c} \left[\frac{m_{ld} V_{ld}^2}{m_{lt} V_{lt}^2} - 1 + K_{di} \right] + \frac{g}{g_c} (L_d - L_t) + \frac{g}{g_c} \frac{m_{lt}}{m_g} \left(\frac{m_{ld}}{m_{lt}} L_d - L_t \right) = 0$$

where

$$V_{gt} = \frac{A_{gs} P_s}{A_{gt} P_t} V_{gs} \ , \quad V_{ld} = \frac{A_n}{A_{ld}} V_{li} = \frac{A_n}{A_{lo}} \left(\frac{L_o - L_i}{L_t - L_i} \right)^2 \left(\frac{L_t - L_i}{L_d - L_i} \right)^2 V_{li}$$

$$m_{ld} = m_{lt} \left(\frac{L_t - L_i}{L_d - L_i} \right)^2 \ , \quad A_{gt} = A_t - A_{lt}$$

Therefore

$$\frac{RT}{M_g} \ln \frac{P_d}{P_t} + \frac{Q_{1i}RT}{2Q_{gs}P_sM_g}\left(\frac{L_o-L_i}{L_t-L_i}\right)^2\left[\left(\frac{L_t-L_i}{L_d-L_i}\right)^2+1\right](P_d-P_t)$$

$$+\left(\frac{A_{gs}P_s}{A_{gt}P_t}\right)^2 \frac{V_{gs}^2}{2g_c}\left[\frac{P_t^2}{P_d^2}-1+K_{di}\right]+\frac{\rho_l Q_{1i}RT}{Q_{gs}P_sM_g}\left(\frac{L_o-L_i}{L_t-L_i}\right)^6\left(\frac{A_n}{A_{lo}}\right)^2\frac{V_{1i}^2}{2g_c}*$$

$$\left[\left(\frac{L_t-L_i}{L_d-L_i}\right)^6-1+K_{di}\right]+\frac{g}{g_c}(L_d-L_t)$$

$$+\frac{g}{g_c}\frac{\rho_l Q_{1i}RT}{Q_{gs}P_sM_g}\left(\frac{L_o-L_i}{L_t-L_i}\right)^2\left[\left(\frac{L_t-L_i}{L_d-L_i}\right)^2 L_d-L_t\right] = 0$$

Assumptions:

(1) Isothermal system

(2) No change in m_g

(3) incompressible liquid

B. DETERMINATION OF MASS TRANSFER COEFFICIENT

DETERMINATION OF THE MASS TRANSFER COEFFICIENT

When SO_2 is absorbed into aqueous sodium hydroxide the following reactions take place:

$$SO_2 + NaOH \rightleftharpoons NaHSO_3 \qquad (1)$$

$$NaHSO_3 + NaOH \rightleftharpoons Na_2SO_3 + H_2O \qquad (2)$$

The equilibrium constants for reaction (1) and (2) are (Johnstone, Field, and Tassler, 1954):

$$K_1 = \frac{[NaHSO_3]}{[SO_2][NaOH]} = 1.7 \times 10^{12} \text{ liters/gmmole}$$

$$K_2 = \frac{[Na_2SO_3]}{[NaHSO_3][NaOH]} = 6.2 \times 10^{6} \text{ liters/gmmole}$$

Reaction (1) is very fast with a forward rate constant exceeding 10^9 liters/(gm mole) (sec). Reaction (2) is a proton transfer reaction and has a much higher forward rate constants, both the reactions are essentially irreversible and the overall reaction is:

$$SO_2 + 2NaOH \longrightarrow Na_2SO_3 + H_2O$$

Which is an instantaneous irreversible reaction.

Therefore, the local, SO_2 absorption rate (n) is:

$$n = K_g a(Y_A)$$

The overall SO_2 absorption rate (N) is given by:

$$N = K_g a Y_{lm}$$

Where Y_{lm} is the logmean concentration driving force and is determined from the inlet and outlet solute gas mole fractions, Y_i and Y_o:

$$Y_{lm} = \frac{Y_i - Y_o}{\ln(Y_i/Y_o)}$$

N can be calculated from the inlet and outlet SO_2 concentrations:

$$N = \frac{Q_{gs}(Y_i - Y_o)}{V_T} \frac{P_s}{RT} = K_g a \, Y_{lm}$$

Therefore,

$$K_g a = \frac{Q_{gs} P_s}{RTV_T} \ln \frac{Y_i}{Y_o}$$

C. DETERMINATION OF SULFUR DIOXIDE CONCENTRATIONS

CALCULATION OF SULFUR DIOXIDE CONCENTRATIONS

The samples collected during gas absorption experiments were analyzed by barium thoring titration method, and the sulfur dioxide concentration in the gas samples were calculated as follows:

$$C_{SO2} = K_2 \frac{(V_t - V_{tb}) \quad N(V_{soln}/V_o)}{V_{m(std)}}$$

where:

C_{SO2} = concentration of SO_2 lbs/dscf

$K_2 = 7.061 \times 10^{-5}$ lb/meq

V_t = Volume of Barium perchlorate titrant used for sample, ml

V_{tb} = Volume of Barium perchlorate titrant used for blank, ml

N = Normality of Barium perchlorate titrant milliequivalents per milliliter

V_{soln} = Total volume of solution in which the sulfur dioxide sample is contained, 100 ml

V_o = Volume of sample aliquot titrated, ml

$$V_{m(std)} = V_m(y) \ (T_{std}/T_m) \ (P/Pstd)$$

where:

V_m = dry gas volume, dsf

y = dry gas meter calibration factor

$$= \frac{\text{wet test meter calibration volume}}{\text{dry gas volume}} \text{ at same T and P}$$

T = temperature, ^oK

P = atm

Calculation of solute gas mole fraction from SO_2 concentration:

$$Y = \frac{(C/M_g) \ 387}{1-(C/M_g)387}$$

D. DERIVATION OF INTERFACIAL AREA FOR GAS ABSORPTION

DERIVATION OF INTERFACIAL AREA FOR GAS ABSORPTION

$$a_T = N_{drop} x A_{drop}$$

$$N_{drop} = \frac{V_{liq}}{V_{drop}}$$

$$\frac{V_{liq}}{V_T - V_{liq}} = \frac{Q_l}{Q_g}$$

$$V_{liq} = \frac{Q_l}{Q_g} (V_T - V_{liq})$$

$$(1 + \frac{Q_l}{Q_g}) V_{liq} = \frac{Q_l}{Q_g} V_T$$

$$V_{liq} = \frac{1}{1+(Q_g/Q_l)} V_T$$

$$N_{drop} = \frac{1}{1+(Q_g/Q_l)} \frac{V_T}{V_{drop}}$$

$$a_T = \frac{1}{1+(Q_g/Q_l)} \frac{V_T}{V_{drop}} A_{drop}$$

$$a = \frac{a_T}{V_T} = \frac{1}{1+(Q_g/Q_l)} \frac{\pi D_v^2}{1/6 \pi D_v^3}$$

Therefore,

$$a = \frac{1}{1+(Q_g/Q_l)} \frac{6}{D_v}$$

TABLES

TABLE I.1

Functions of Ejectors and the Types of Equipment Available

PUMPING AND LIFTING LIQUIDS

Using steam as the motive fluid

- Steam Jet Syphons
- Steam Jet Exhauster
- Single-Stage Vacuum Pumps

Using air as the motive fluid

- Air Jet Syphons
- Air Jet Exhausters

Using liquids as the motive fluid

- Water Jet Eductors
- Water Jet Exhausters

HEATING LIQUID (BY DIRECT CONTACT)

Tank Type Heaters

- Steam Jet Heaters

Pipeline Type Heaters

- Steam Jet Heaters
- Steam Jet Heaters (large capacity)
- Steam Jet Syphons

Open Type Heaters

- Steam Jet Heaters (large capacity)

MOVING AIR AND GASES (AND PUMP PRIMING)

Using steam as the motive fluid

- Steam Jet Blowers
- Steam Jet Exhausters
- Steam Jet Thermo-Compressors
- Single-Stage Vacuum Pumps
- Multi-Stage Vacuum Pumps

TABLE I.1 CONTINUED

Using air as the motive fluid

Air Jet Blowers
Air Jet Exhausters
Single-Stage Vacuum Pumps
Air Jet Compressors

Using gas as the motive fluid

Gas Jet Compressors

Using liquid as the motive fluid

Water Jet Exhausters
Barometric Condensers
Low Level Condensers
Water Jet Eductors (small capacities)

HANDLING SLURRIES AND GRANULAR SOLIDS

Using steam as the motive fluid

Steam Jet Syphons
Steam Jet Slurry Heater
Single-Stage Vacuum Pumps

Using air as the motive fluid

Air Jet Exhausters

Using liquid as the motive fluid

Water Jet Eductors

MIXING AND AGITATING LIQUIDS

Water Jet Eductors
Water Jet Exhausters

MIXING GASES

Steam Jet Exhausters
Jet Compressors

TABLE I.1 CONTINUED

GAS COOLING

Gas Coolers
Spray Nozzles (as equipment components)

CONDENSING

Steam Jet Syphons
Steam Jet Heaters
Steam Jet Heaters (large capacities)
Barometric Condensers
Low Level Condensers
Spray Nozzles (as equipment components)

PRODUCING VACUUM

Using steam as the motive fluid

Steam Jet Exhausters
Single-Stage Vacuum Pumps
Multi-Stage Vacuum Pumps

Using air as the motive fluid

Air Jet Exhausters
Single-Stage Vacuum Pumps

Using liquids as the motive fluid

Water Jet Exhausters
Barometric Condensers
Low Level Condensers

TABLE 3.1

DROPLET SIZE CORRELATIONS

AUTHOR	CORRELATION
Harmon (1955)	$d_{32} = 3330\ d_o^{0.3}\ \mu_L^{0.07}\ \mu_g^{0.78}\ U_o^{-0.55}\ \rho_L^{-0.648}\ \rho_g^{-0.052}\ \sigma^{-0.15}$
Merrington and Richardson (1947)	$d_{ave} = 500\ d_o^{1.2}\ \mu_l^{0.2}\ U_o^{-1}\ \rho_l^{-0.2}$
Panasenkov (1951)	$d_{30} = 6\ d_o^{0.85}\ \mu_L^{0.15}\ U_o^{-0.15}\ \rho_L^{-0.15}$
Popov (1961	$d_{ave} = 0.083\ d_o^{1.15}\ \mu_L^{1.22}\ \mu_g^{0.08}\ U_o^{-1}\ \rho_L^{0.55}\ \rho_g^{-0.4}\ \sigma^{1.15}$
Tanasawa and Toyoda (1956)	$d_{32} = 47\ d_o U_o^{-1}\ \rho_g^{-0.25}\ \sigma^{0.25}\ (1+331\ Z)$

TABLE 3.2

EMPIRICAL EQUATIONS FOR DROP SIZE AND THEIR APPLICATION RANGES

Investigators	Equations	APPLICABLE RANGES			
		v_r, cm/s	m_g/m_l	μ_l poise	σ; dyne/cm
Nukiyama and Tanasawa (1938-40)	$d_{3,2}=58500\frac{\sqrt{\sigma}}{v_r\sqrt{\rho_l}}+597\left(\frac{\mu_l}{\sqrt{\sigma\rho_l}}\right)^{0.45}1000\left(\frac{Q_l}{Q_g}\right)^{1.5}$	10^4 to sonic velocity	1.8-15	0.01-0.3	30-73
Mugele (1960)	$\frac{d_{3,2}}{d_n}$ or $\frac{d_{max}}{d_n}=A\left(\frac{d_n\rho_l v_r}{\mu_l}\right)^B\left(\frac{\mu_l v_r}{\sigma}\right)^C$ A,B,C are constants	10^4 sonic velocity	1.8-15		
Gretzinger and Marshall (1961)	$d_m=2600\left[\left(\frac{m_l}{m_g}\right)\left(\frac{\mu_g}{G_a L}\right)\right]^{0.4}$	10^4 to sonic velocity	1-15	0.01-0.3	50
Kim and Marshall (1971)	$d_m=2600\frac{\sigma^{0.41}\mu_l^{0.32}}{(v_r^2\rho_g)^{0.57}A^{0.36}\rho_l^{0.16}}+18900\left(\frac{\mu_l^2}{\rho_l\sigma}\right)^{0.17}\frac{1}{v_r^{0.54}}\left(\frac{m_g}{m_l}\right)^m$ $m=-1$ for $\frac{m_g}{m_l}<3$; $m=0.5$ for $\frac{m_g}{m_l}>3$ and $d_{3,2}=0.83\,d_m$	7.5×10^3 to sonic velocity	0.06-40	0.01-0.5	29.6-31.2
Boll et al. (1974)	$d_{3,2}=\frac{6.75\times10^7+5.28\times10^{12}\left(Q_l/Q_g\right)}{v_i^{1.602}}1.922$	3×10^3 to 10^4	0.5-2.0	0.01	73

-----(6)

TABLE 7.1

SPRAY CHARACTERISTICS

0 - 10 psi	no cone, no atomization
10 - 15 psi	15° cone, no atomization (sheets)
15 - 30 psi	15° cone, partial atomization (filaments)
$\geq$ 30 psi	15° cone, complete atomization (drops)

Kinetic Energy of jet exiting the nozzle at 100 psi = 5.87 $\frac{\text{lbf - ft}}{\text{sec}}$

Total Surface Energy of the droplets = 0.16 $\frac{\text{lbf - ft}}{\text{sec}}$

TABLE 7.2

MINOLTA SRT-201

CAMERA SPECIFICATIONS

Type:	35mm single-lens reflexes with match-neddle/manual exposure control
Lens mount:	Minolta SLR bayonet, 54° rotating angle; coupling for aperture metering and automatic diaphrahm control with "MD" or "MC" lense (stop-down metering used for other lenses); buttion for depth-of-field preview and stop-down meetering. (Standard lenses: 45mm f/2 MD Rokkor-X for SR-T200; 50mm f/1/7 or 50mm f/1.4 MD Rokkor-X or 50mm f/1.2 MD Rokkor-X for SR-T 201
Light metering:	Full-aperture ıTL type with overlapping readings taken by 2 CdS cells mounted on pentaprism and circuited to provide optimum exposure in both flat and most contrast lighted situations; stop-down metering also possible. Film range: ASA 6 to 6400 set by selector on shutter-speed dial Power: One 1.35v mercury cell, contained in camera base
Exposure control:	Turning shutter-speed dial and/or lens aperture ring to align follower with meter neddle visible in finder yields proper exposure according to metering system indication at the film speed set. Alignment may be disregarded for exposure adjustment or full manual control. Metering and match-needle exposure range: EV 3 to EV 17 (e.g. 1/4 sec. at f/1.4 to 1/1000 at f/11) at ASA 100 with f/1.4 lens
Shutter:	Horizontal-traverse mechanically controlled focal-plane type; speeds 1, 1/2, 1/4, 1/8, 1/15, 1/30, 1/60, 1/125, 1/500, and 1/1000 sec. plus "bulb" setting
Mirror:	Oversize quick return type (PO value: 138 mm; finder image cutoff negligible even with 1600mm f/11 RF Rokkor-X extreme telephoto)
Finder:	Eye-level pentaprism type showing 94% of 24 x 36mm film-frame area: Magnification: 0.86x with 50mm lens focused at infinity Mat-Fresnel-field focusing screen with centered focusing aid: 2.5mm horizontal split-image spot surrounded by 1.5mm microprism band Meter needle and circle-tipped follower for match-needle exposure control, coupled metering-range limits, and battery-check indication all sihouetted within the viewfield; shutter-speed scale and setting indicator visible below the fram in SR-T-201
Flash sync:	X delay; electronic flash synchronizes at 1/60 sec. and all slower settings including B through single PC terminal or hot shoe
Film advance:	Lever type, single or multiple-stroke, 150° winding angle 20° unengaged movement to allow offsetting from body Advancing type frame counter reset automatically when camera back is opened

continued

TABLE 7.2

Self-timer:	On SR-T-201 only; lever-type approximately 10 sec. maximum delay
Other:	4 slot take-up spool; ASA/DIN conversion scale on back cover; conversion scale surrounded by memo holder
Dimensions:	145 x 47.5 x 95mm (5 3/4 x 1 7/8 x 3 3/4 inches) without lens

TABLE 7.3

MINOLTA SRT-201

STANDARD LENS SPECIFICATIONS

Camera Model:	SRT-201		
Lens:	50mm f/1.7 MD Rokkor-X	50mm f/1.4 MD Rokkor-X	50mm f/1.2 MD Rokkor-X
Type:	Meter-coupled Gauss type standard lens		
Construction:	6 elements in 5 groups	7 elements in 6 groups	7 elements in 6 groups
Angle of View:	47°	47°	47°
Coating:	Minolta Achromatic		
Min. Focusing Dist.:	0.45m (1.43 ft.)	0.45m (1.48 ft.)	0.45m (1.48 ft.)
Diaphragm:	Fully automatic, meter-coupled		
Aperture Scale:	1.7,2.8,4,5,6,8,11,16	1.4,2,2.8,4,5.6,8,11,16	1.2,2,2.8,4,5.6,8,11,16
	Each with full and half-click-stops		
Filter Thread Diam:	55mm		
Dimensions:	64mm x 40mm (2.½" x 1.9/16")	64mm x 40mm (2.½" x 1.9/10")	65.5mm x 46.5mm (2.9/16 x 1.13/16")
Weight:	185g (5½ oz.)	230g (8 1/8 oz.)	315g (11 1/8 oz.)

TABLE 7.4

VIVITAR 285 FLASH:

AUTOMATIC f-STOP SETTINGS AND GENERAL SPECIFICATIONS

	Film Speed								Zoom Flash Head Position			
ASA DIN	25 15	64 19	80 20	100 21	125 22	160 23	200 24	400 27	Super Wide 28mm	Wide 35mm	Normal 50mm	Tele 105mm
YELLOW Mode f-Stop	1.0	1.4	2.0	2.0	2.0	2.8	2.8	4.0	4-35 ft. (1.2-10.6m)	5-50 ft. (1.5-15.1m)	6-60 ft. (1.8-18.3m)	7-70 ft. (2.1-2.13m)
RED Mode f-Stop	2.0	2.8	4.0	4.0	4.0	5.6	5.6	8.0	3-18 ft. (1.0-5.5m)	5-25 ft. (1.5-7.5m)	5-30 ft. (1.5-9.1m)	6-35 ft. (1.8-10.6m)
BLUE Mode f-Stop	4.0	5.6	8.0	8.0	8.0	11.0	11.0	16.0	2-9 ft. (0.7-2.6m)	2-12 ft. (0.7-3.7m)	2-15 ft. (0.7-4.4m)	2-18 ft. (0.7-5.5m)
PURPLE Mode f-Stop	5.6	8.0	11.0	11.0	11.0	16.0	16.0	22.0	2-6 ft. (0.7-1.8m)	2-9 ft. (0.7-2.6m)	2-11 ft. (0.7-3.3m)	2-12 ft. (0.7-3.7m)

General Specifications
Flash Duration (Approx.)
Auto--1/1000 to 1/30,000 of a second
Manual--1/1000 of a second
Angles of Illumination:

Focal Length	Horizontal	Vertical
Super Wide (28mm) w/wide angle flash lens inserted	70°	53°
Wide (35mm)	60°	45°
Normal (50mm)	46°	34°
Tele (105mm)	27°	20°

Color Temperature: 6,000 °K
Camera/Flash Synchronization
Connections: Hot Shoe
Shutter Cord
Weight(without batteries): 14.9 oz. (423 g)
Diminsions (Head in 0° position): 4"W x 5.2"H x 4.2"D
(100mm W x 130mm H x 105mm D)
Accessories Included: 28mm Wide Angle Flash Lens °C-1 Shutter Cord

TABLE 8.1

LIST OF THE VARIABLES AND PARAMETERS IN THE FLUID FLOW MODEL

LIQUID & GAS PROPERTIES	SCRUBBER GEOMETRY	CONSTANTS	PRESSURE	FRICTIONAL LOSS CONSTANTS	NOZZLE GEOMETRY	CALCULATED VARIABLES
l	L_i	g	P_i	K_{nz}	0	A_{lo}
gs	L_o	g_c	P_s	K_{en}	A_n	$V_{li} = \frac{Q_{li}}{A_n}$
Q_{li}	L_t		P_o	K_{th}		$V_{gs} = \frac{Q_{gs}}{A_{gs}}$
Q_{gs}	L_d		P_t	K_{di}		$A_{go} = A_t - A_{lo}$
	L_s		P_d			$A_{gt} = A_t - A_{lt}$
	A_n					
	A_t					
	A_s					
	A_d					

TABLE 11.1

Static Pressure Data (4" AMETEK 7010 Ejector Venturi Scrubber with 3/8" S&K 622-L Nozzle)

Q_{li} (ft^3/sec)	Q_{gs} (ft^3/sec)	V_{li} (ft/sec)	V_{gs} (ft/sec)
0.018	1.073	105.26	12.29
0.016	0.943	93.57	10.80
0.013	0.812	76.02	9.30
0.011	0.674	64.32	7.72
0.009	0.537	52.63	6.15
0.007	0.406	40.94	4.65
0.004	0.261	23.39	2.99
0.002	0.131	11.69	1.50

P_i (lbf/ft^2)	P_s (lbs/ft^2)	P_o (lbf/ft^2)	P_t (lbf/ft^2)	P_d (lbf/ft^2)
2117.01	2109.51	2106.51	2101.71	2116.54
2117.01	2111.33	2108.7	2105.41	2116.81
2117.01	2113.16	2111.2	2108.21	2116.96
2116.99	2114.01	2112.7	2109.78	2116.72
2116.97	2114.88	2114.0	2112.85	2116.81
2116.95	2115.71	2115.2	2113.99	2116.87
2116.90	2116.59	2116.42	2115.72	2116.96
2116.81	2116.81	2116.77	2116.68	2116.93

TABLE 11.2

Empirical Frictional Loss Constants of the Fluid Flow Model

Q_l	Q_g	K_{nz}	K_{en}	K_{th}	K_{di}
0.018	1.073	0.777	1.940	0.854	0.361
0.016	0.943	0.778	4.280	0.895	0.299
0.013	0.812	0.780	4.410	0.672	0.175
0.011	0.674	0.782	3.904	0.753	0.209
0.009	0.537	0.786	5.167	0.680	0.440
0.007	0.406	0.794	5.749	0.779	0.415
0.004	0.261	0.835	2.879	1.051	0.704
0.002	0.131	1.020	7.195	1.48	3.808
Averages		0.819	4.44	0.838	0.801

TABLE 11.3

SO_2 Absorption Data with 0.0001 M NaOH solutions

Q_1 (gpm)	SO_2 Concentration in inlet air (ppm)	SO_2 Concentration in outlet air (ppm)	Overall Removal Efficiency (Percent)
8	12940	3.86	99.97
7	12335	3.48	99.97
6	12408	61.8	99.5
5	12275	245.1	98.0
4	12232	735.3	94.00
3	12178	6089	50
2	12221	10340	15.4
1	12190	11610	4.75

TABLE 11.4

SO_2 Absorption Data with 0.0001 M NaOH solutions in AMETEK 7040 Separator

Q_1 (gpm)	SO_2 Concentration in inlet air (ppm)	SO_2 Concentration in outlet air (ppm)	Efficiency Percent
8	7.5	3.85	48.3
7	7.0	3.76	46.4
6	79.8	56.24	29.54
5	350.7	266.67	23.96
4	1009.8	810.3	19.76
3	6167.8	5551.03	10.0
2	11428.59	11126.25	1.0
1	10098.28	9916.88	1.8

TABLE 11.5

Values of Mass Transfer Coefficient

Q_l (gpm)	$K_g a$ ($\frac{lb\ moles}{hr\ ft^3}$)
8	796
7	719
6	399
5	240
4	138
3	25.53
2	4.09
1	0.6

FIGURES

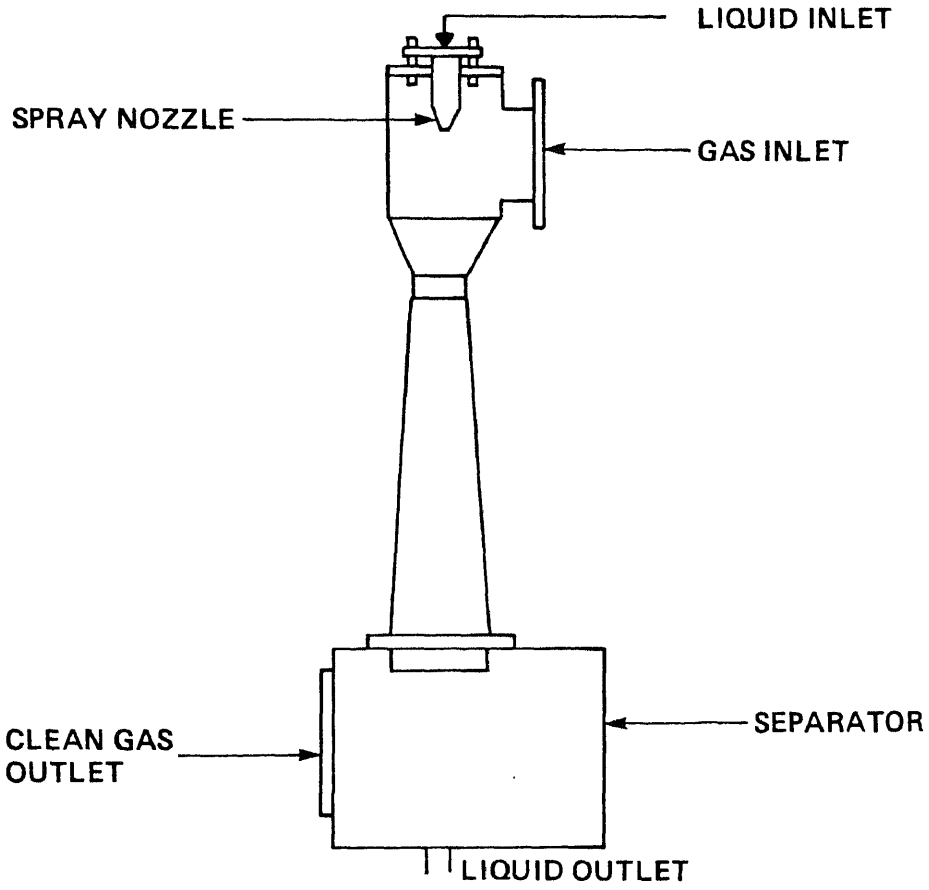

FIGURE 1.1.
4 INCH AMETEK 7010 EJECTOR VENTURI SCRUBBER

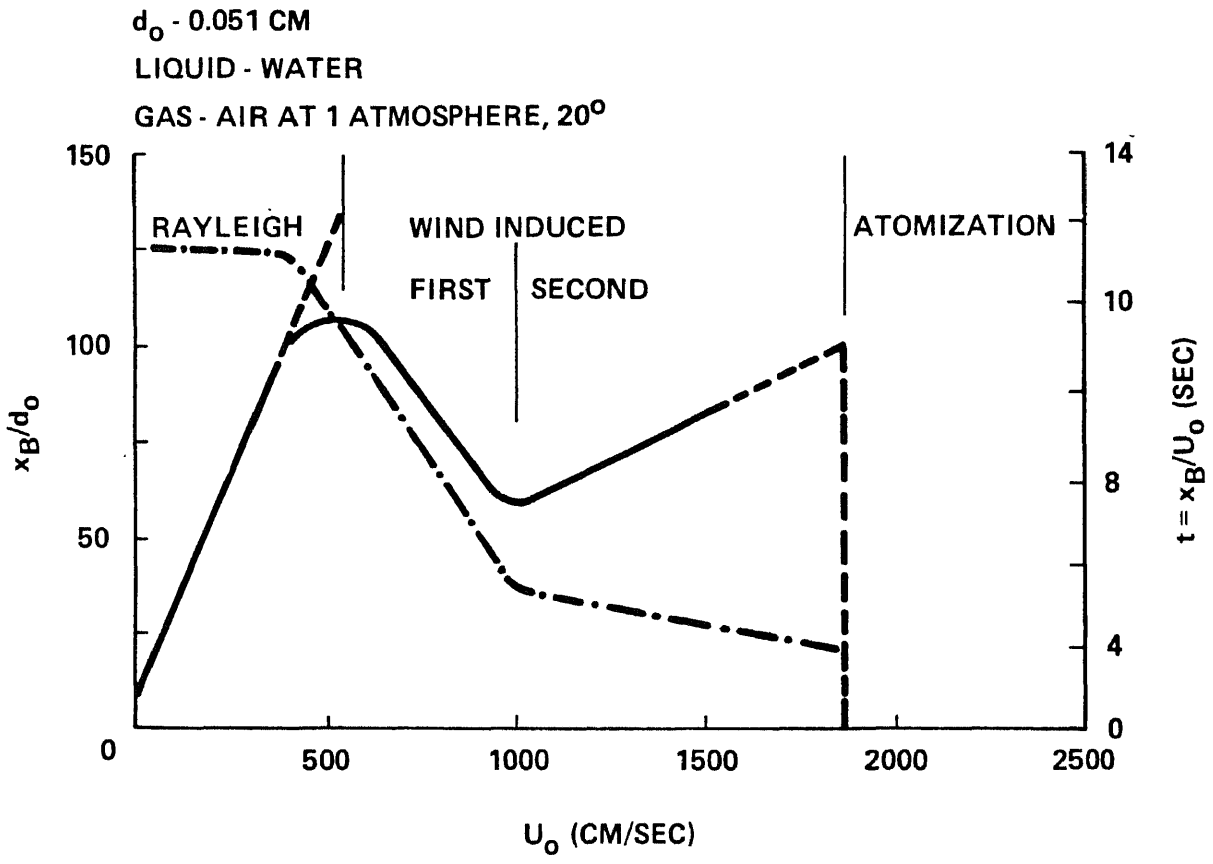

FIGURE 2.1.
JET BREAKUP LENGTH AND BREAKUP TIME AS A FUNCTION OF JET VELOCITY [FROM HAENLEIN (1932)]

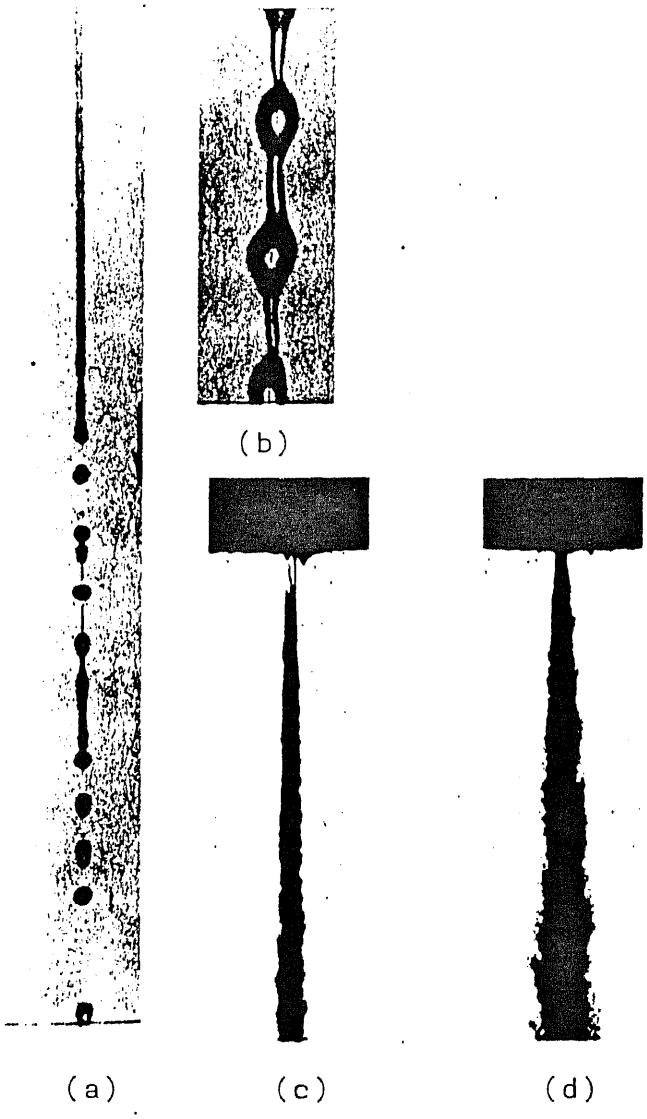

FIGURE 2.2 Examples of the Four Breakup Regimes
(from Reitz (1978))

(a) Rayleigh
(b) First Wind Induced
(c) Second Wind Induced
(d) Atomization

FIGURE 2.3
PROCESS OF DROP FORMATION FROM
A FLAT LIQUID SHEET

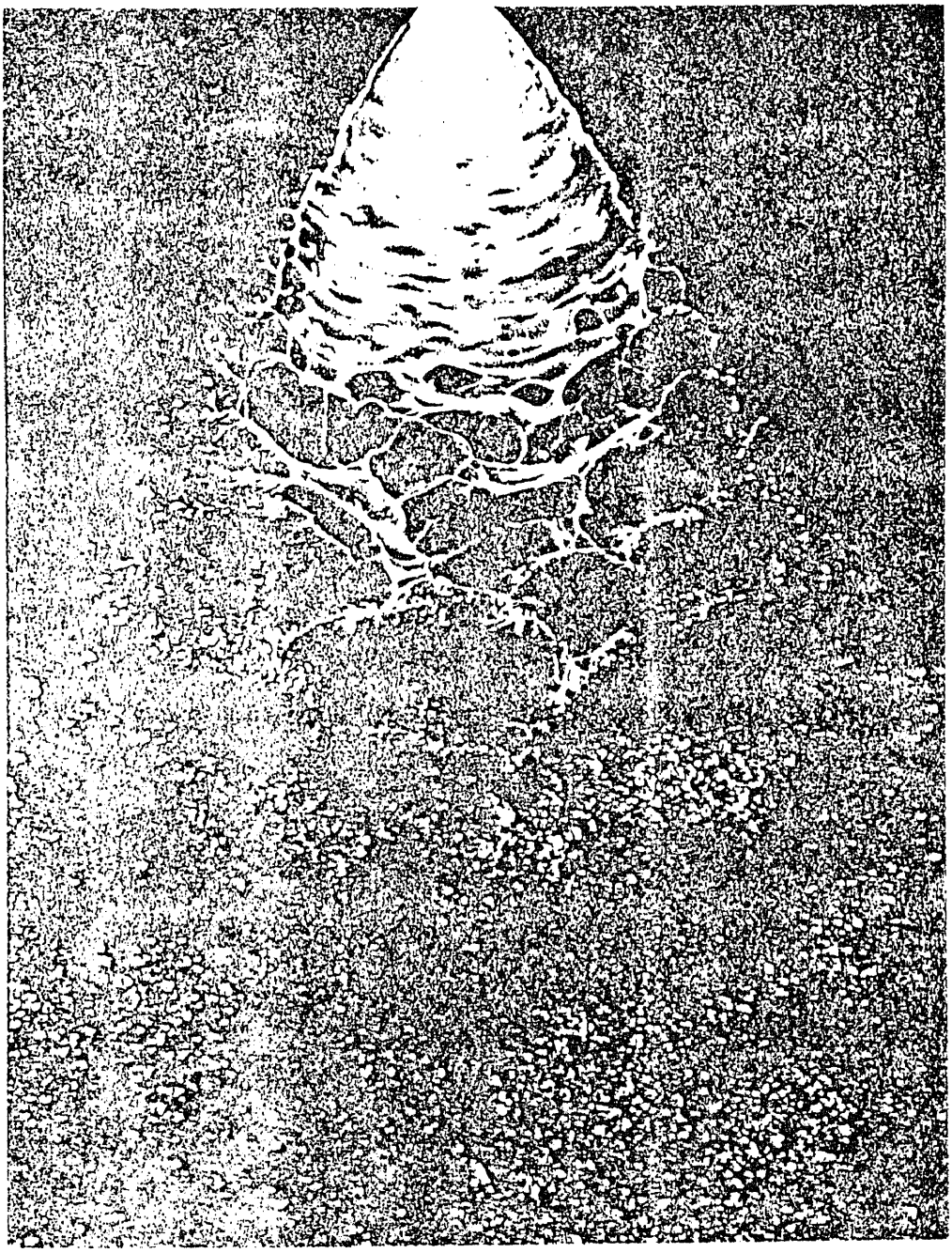

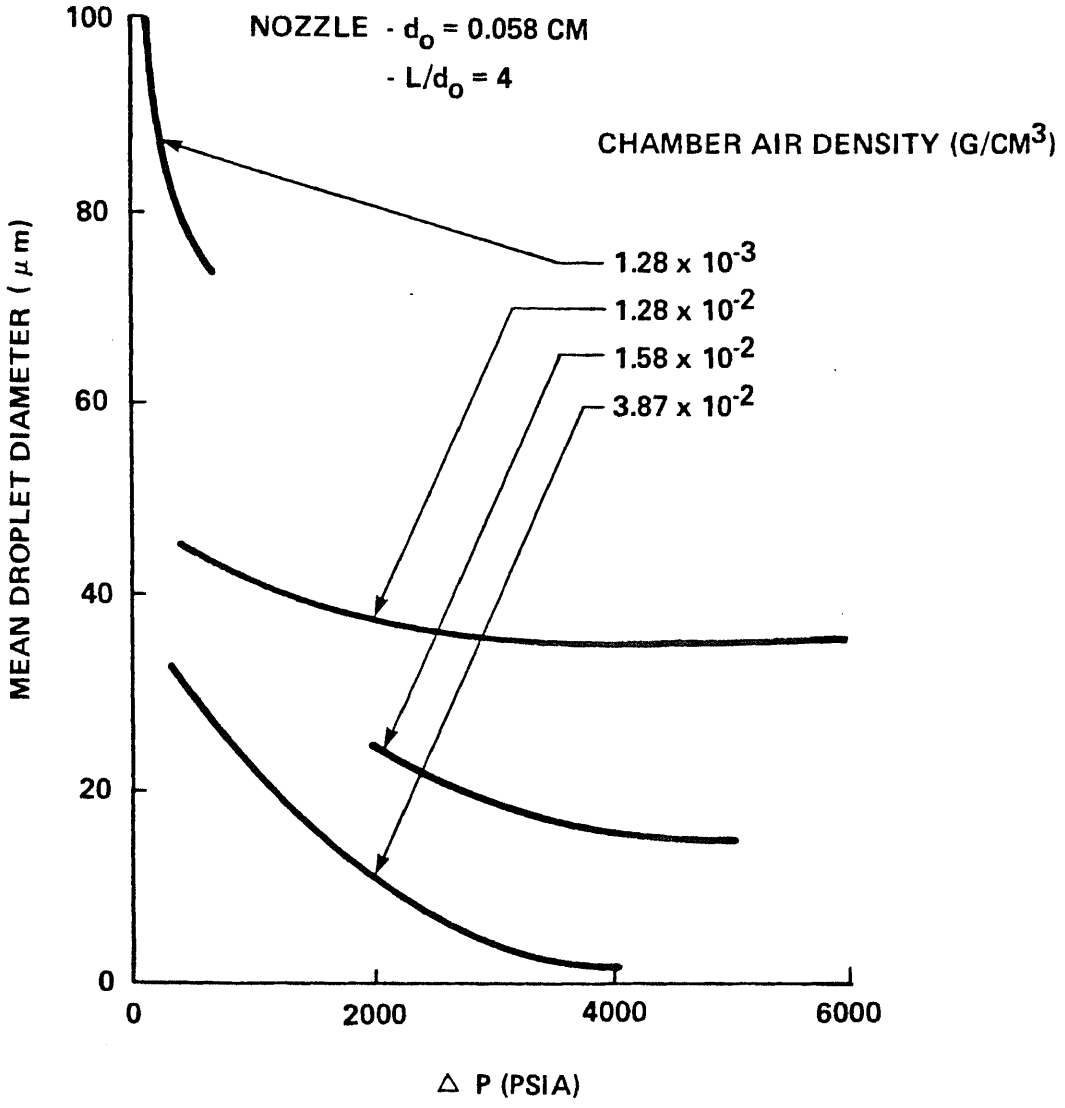

FIGURE 3.1.
EFFECT OF INJECTION PRESSURE ON MEAN DROP SIZE
[FROM GIFFEN AND MURASZEW (1953)]

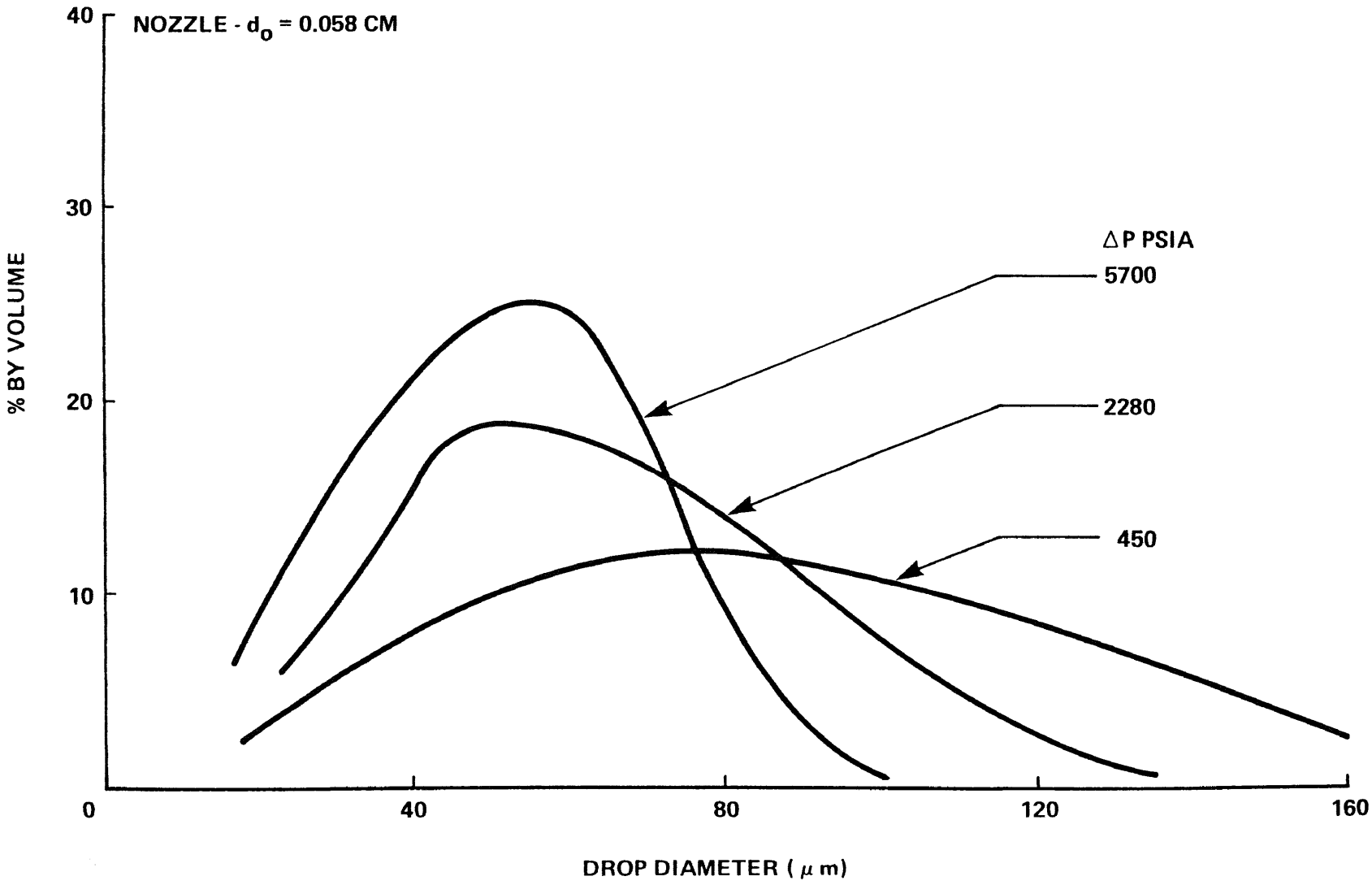

FIGURE 3.2
EFFECT OF INJECTION PRESSURE ON DROP SIZE DISTRIBUTION
[FROM GIFFEN AND MURASZEW (1953)]

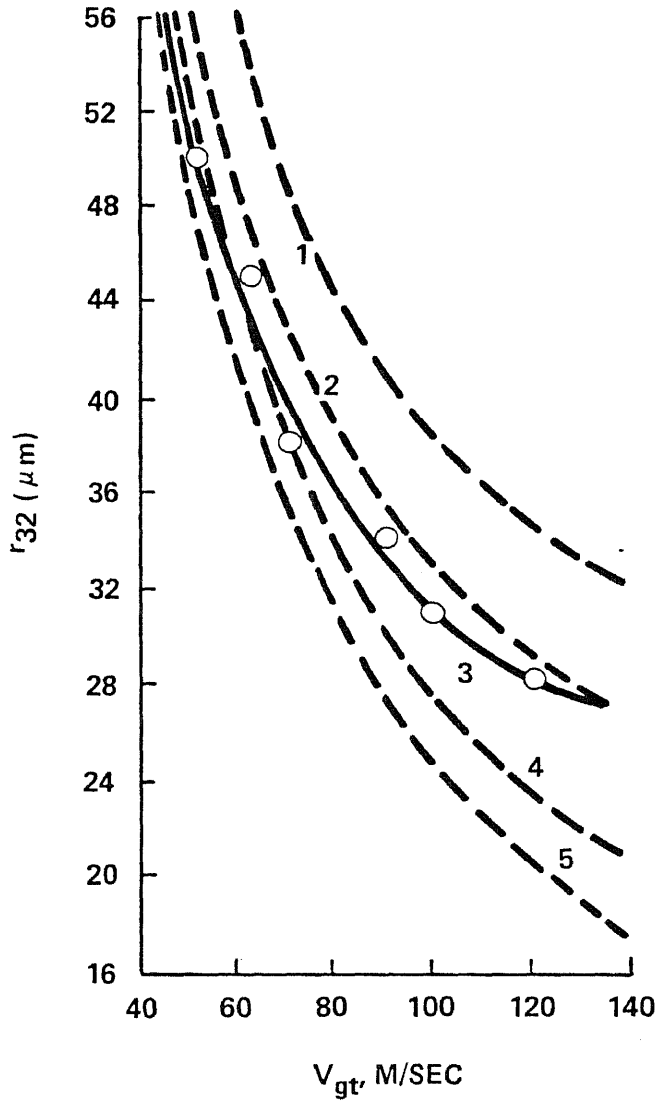

FIGURE 3.3.
DEPENDENCE OF DROP SAUTER RADIUS ON GAS VELOCITY
CURVES 1, 2, 4, 5 CALCULATED USING THE NUKIYAMA-TANASAWA EQUATION WITH ϕ = 0.8; 0.4; 0.2; 0.1 LITERS m^{-3} RESPECTIVELY
CURVE 3 IS FROM THE EXPERIMENTAL DATA OF BAYVEL AND VEZIROGLU (1980), WITH ϕ = 0.1 TO 0.81 m^{-3}

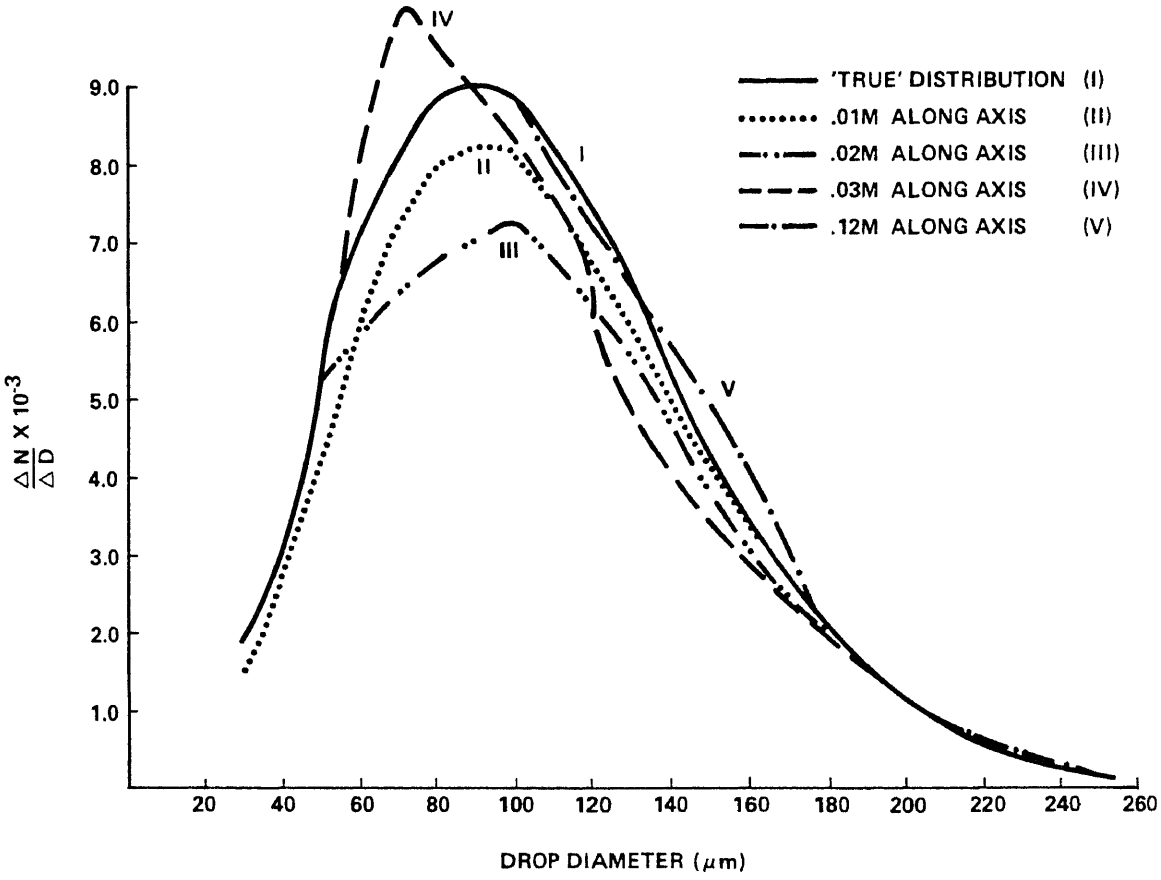

FIGURE 3.4
VARIATION OF "WEIGHTED" SIZE-FREQUENCY DISTRIBUTION
ALONG SPRAY AXIS [FROM CLARK AND DOMBROWSKI (1973)]

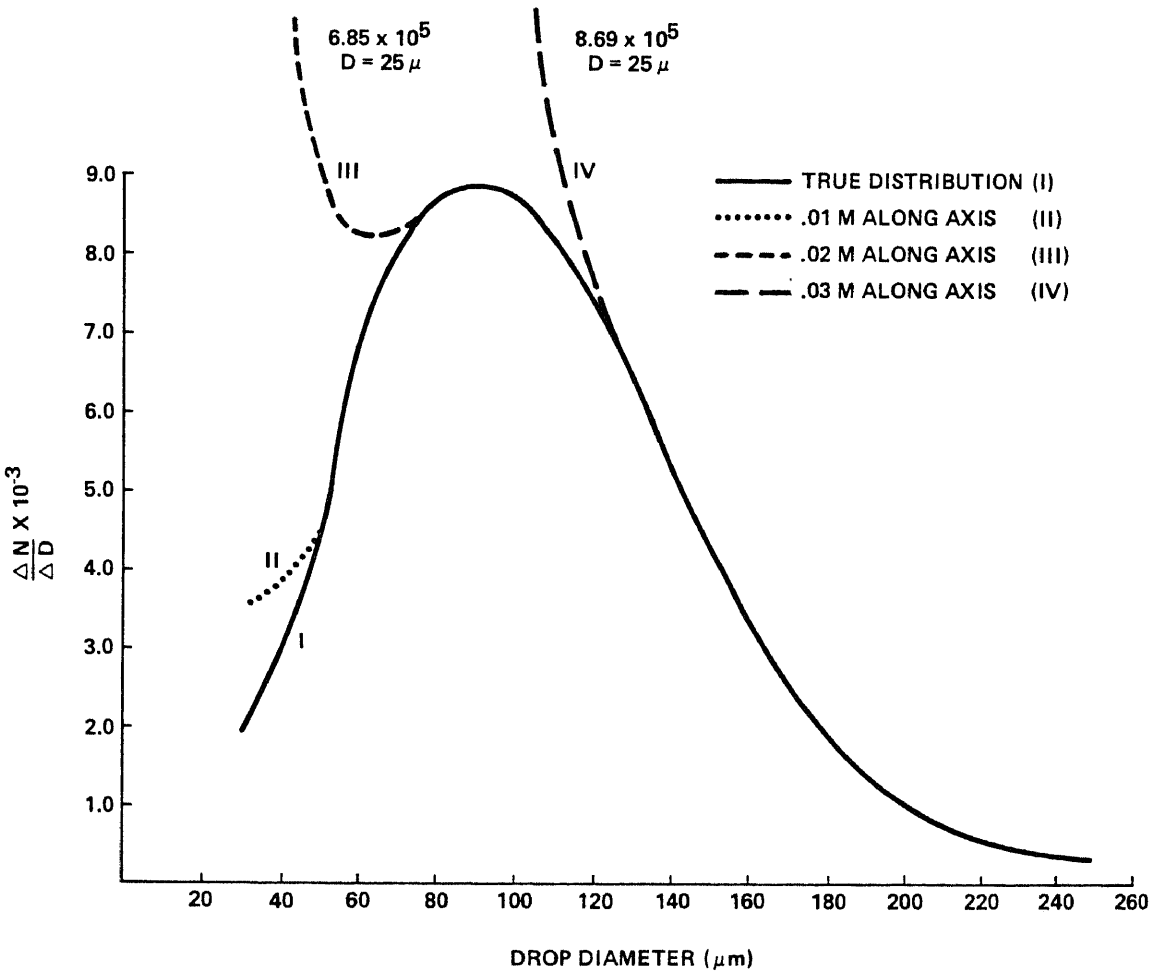

FIGURE 3.5
VARIATION OF SPATIAL SIZE FREQUENCY DISTRIBUTION ALONG SPRAY AXIS, [FROM CLARK AND DOMBROWSKI (1973)]

FIGURE 4.1

METHODS OF ILLUMINATION

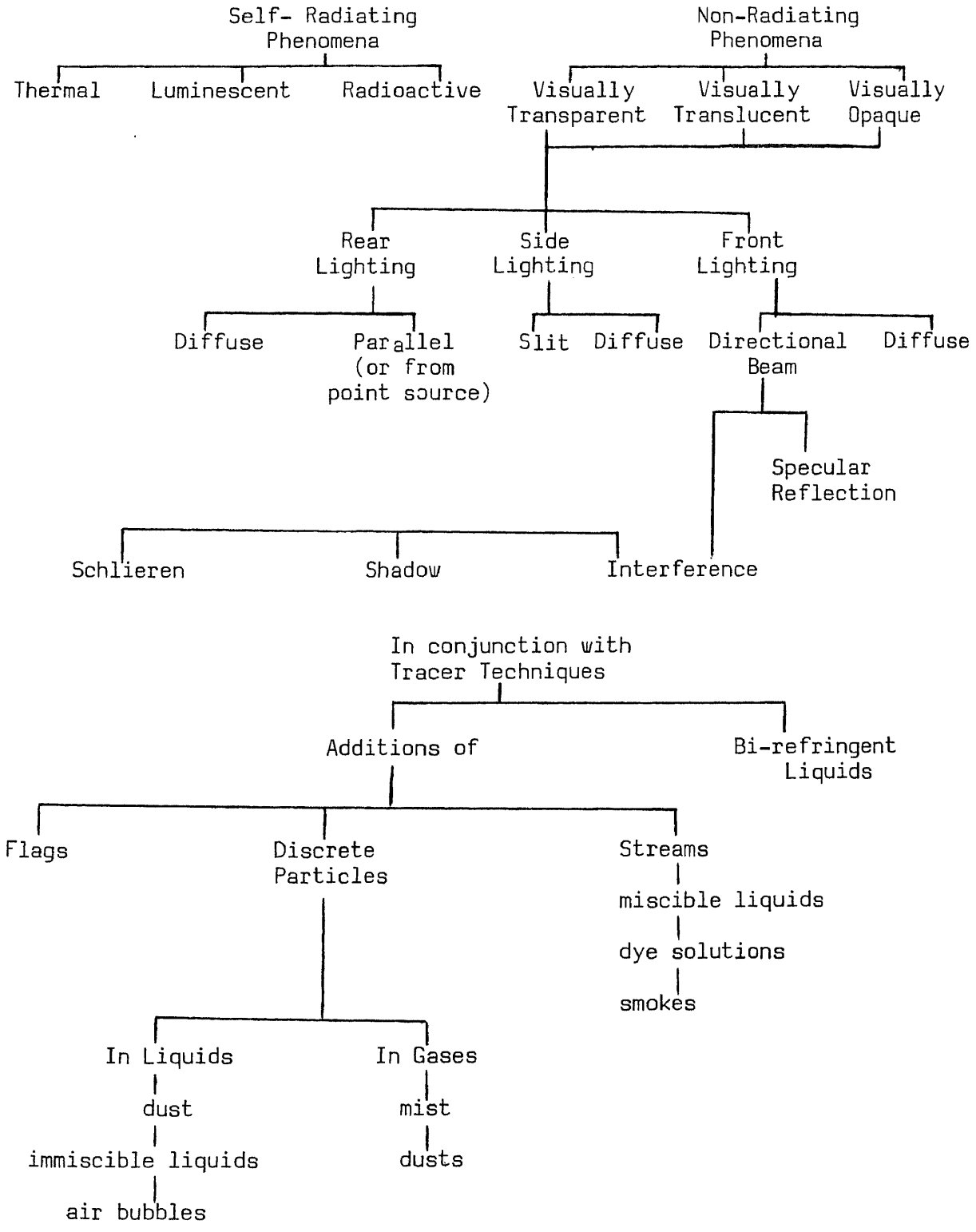

FIGURE 4.2

EXPOSURE METHODS TO STUDY MOVEMENT

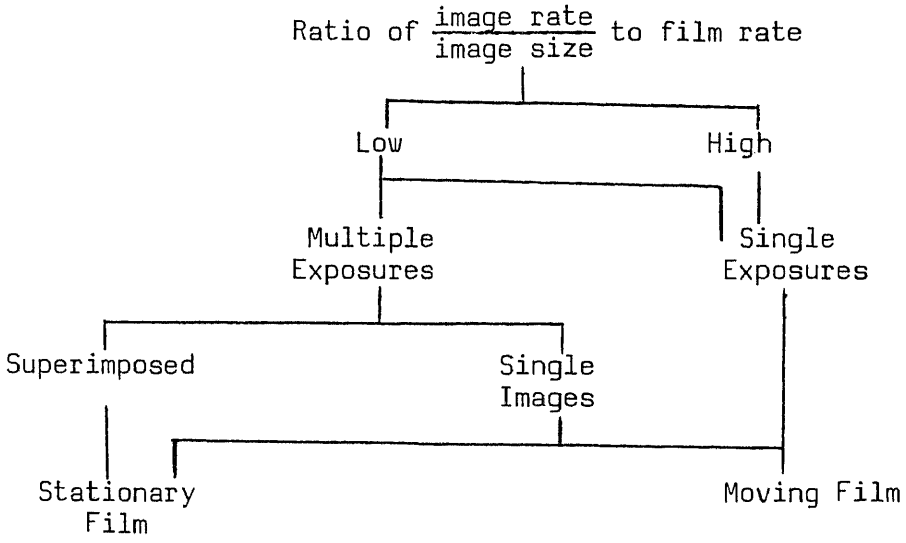

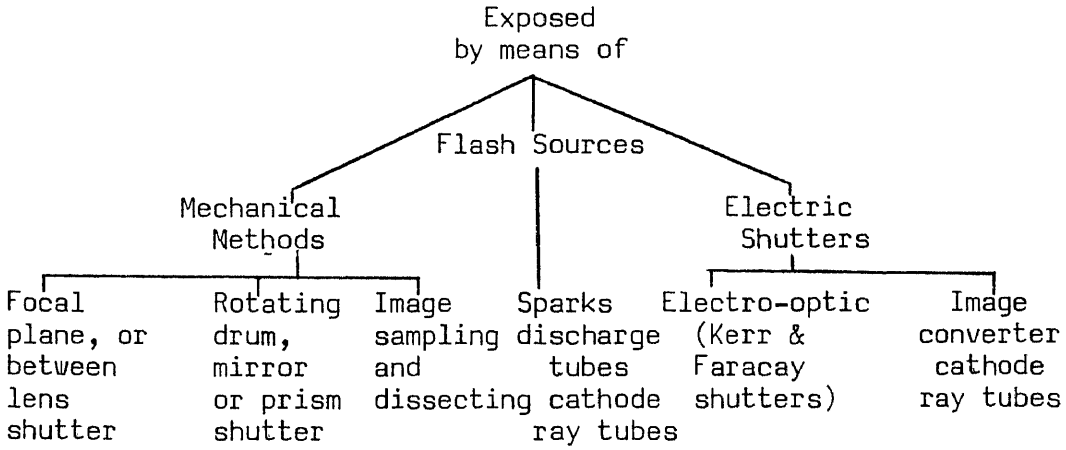

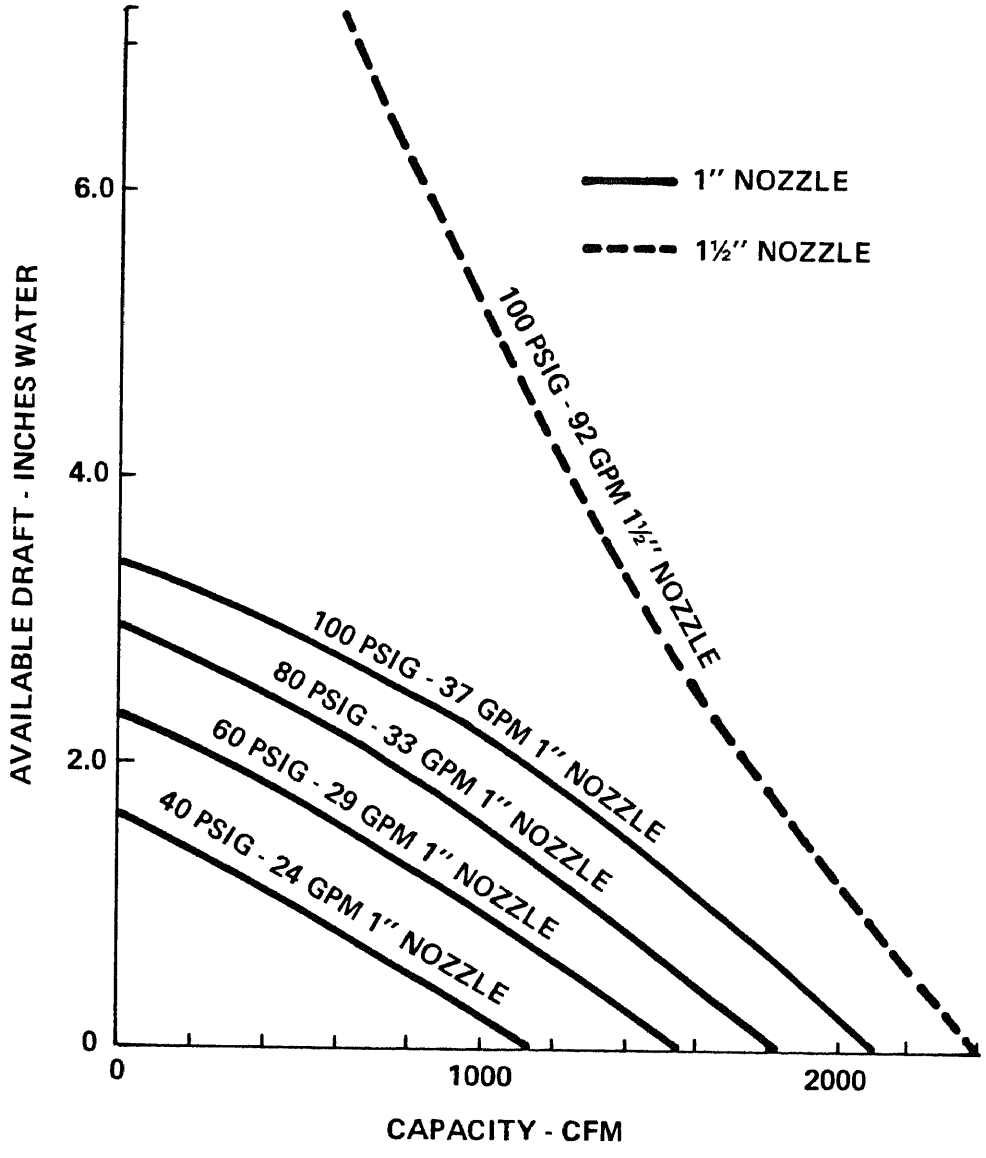

FIGURE 5.1
TYPICAL PUMPING CHARACTERISTICS OF A 12 INCH S&K EJECTOR VENTURI SCRUBBER, [FROM HARRIS (1965)]

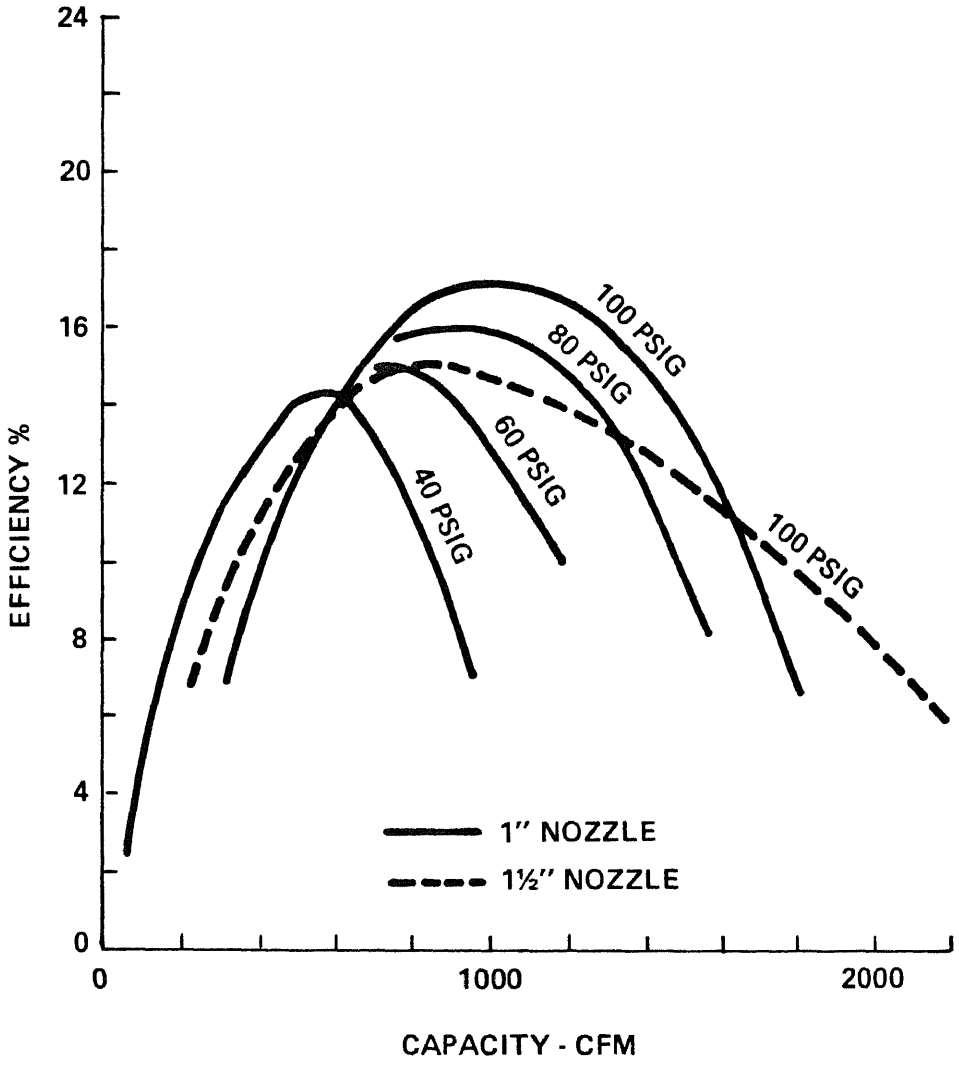

FIGURE 5.2
PUMPING EFFICIENCY OF 12 INCH S&K EJECTOR VENTURI SCRUBBER [FROM HARRIS (1965)]

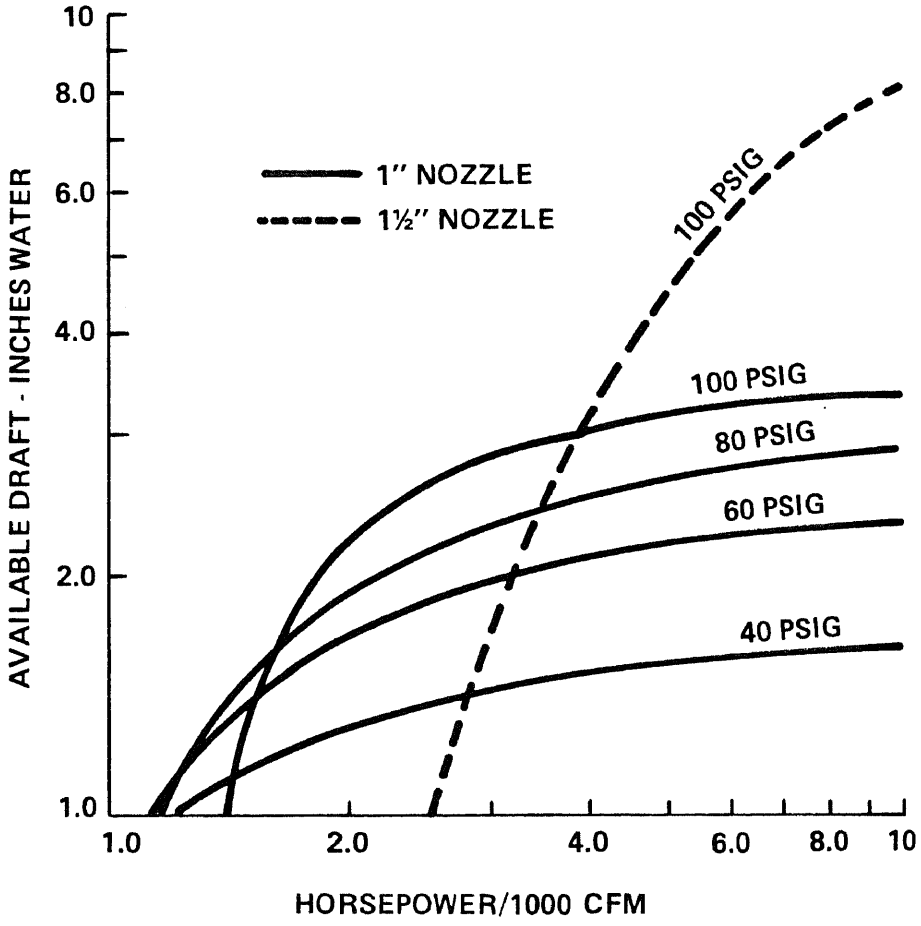

FIGURE 5.3
PUMPING ENERGY REQUIREMENTS FOR 12 INCH S&K EJECTOR VENTURI SCRUBBER. [FROM HARRIS (1965)]

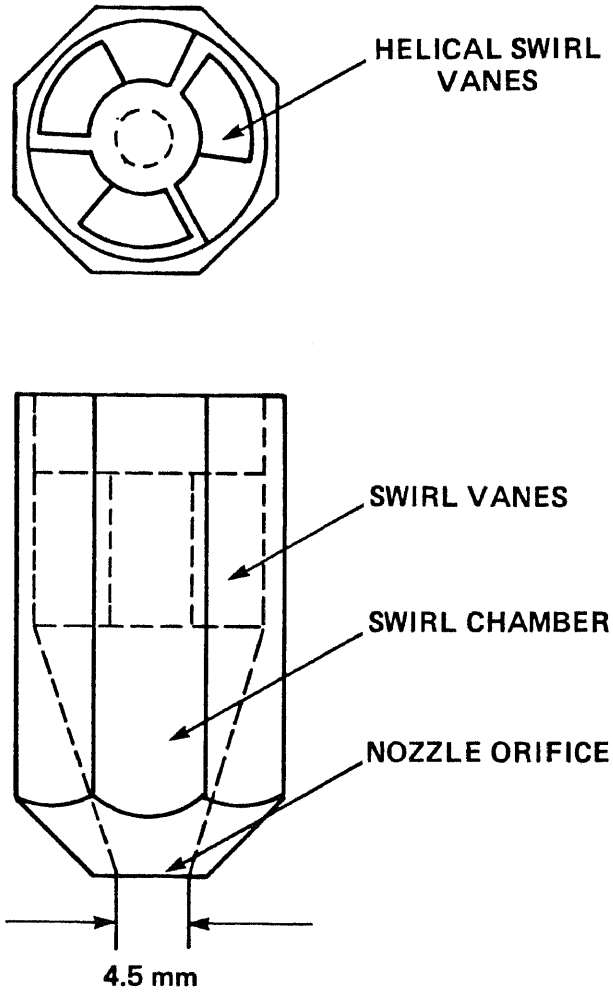

FIGURE 7.1.
3/8 INCH SCHUTTE & KOERTING MODEL 622-L NOZZLE

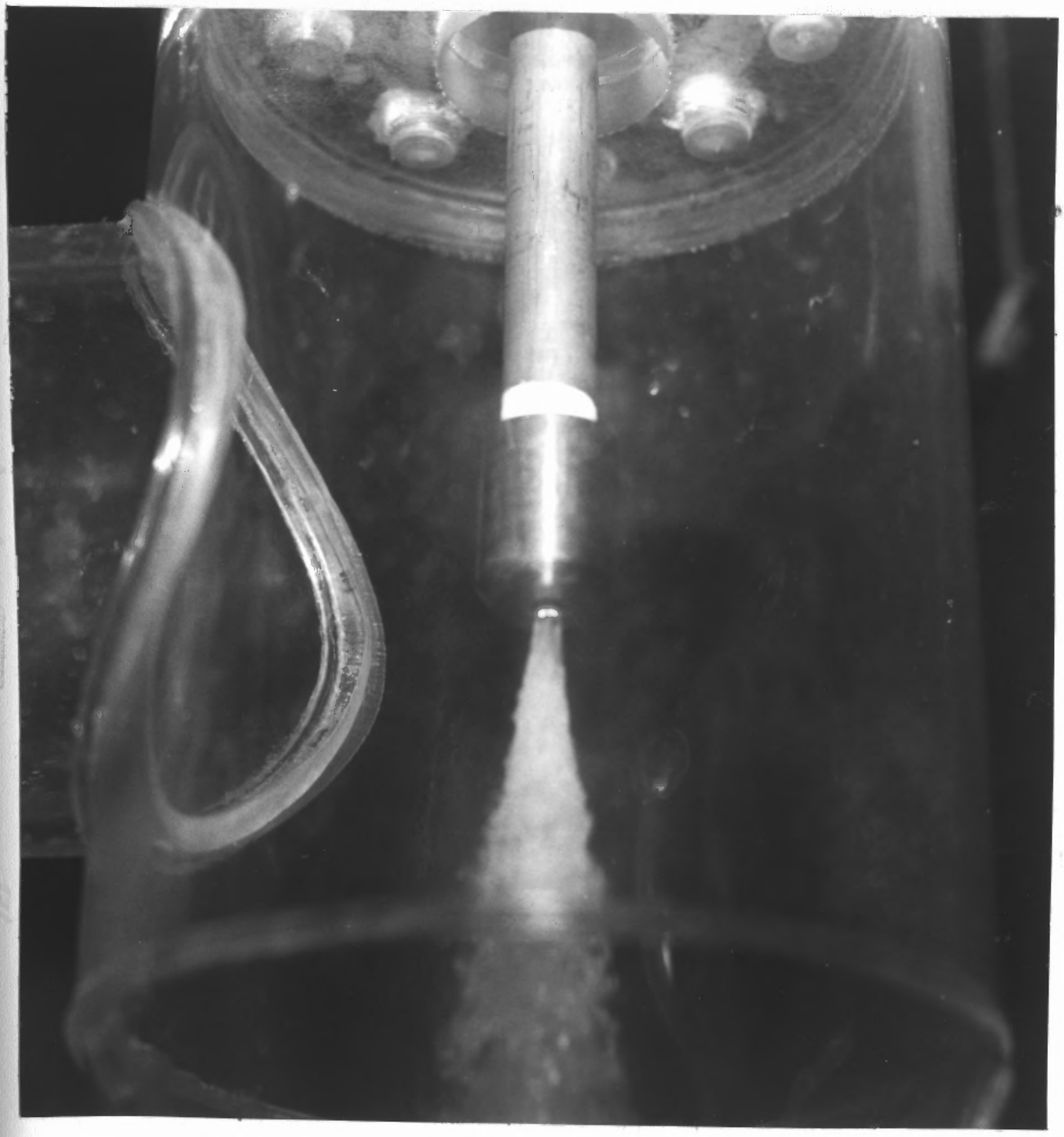

Figure 7.2 Spray Exiting 3/8 inch S&K 622-L Nozzle

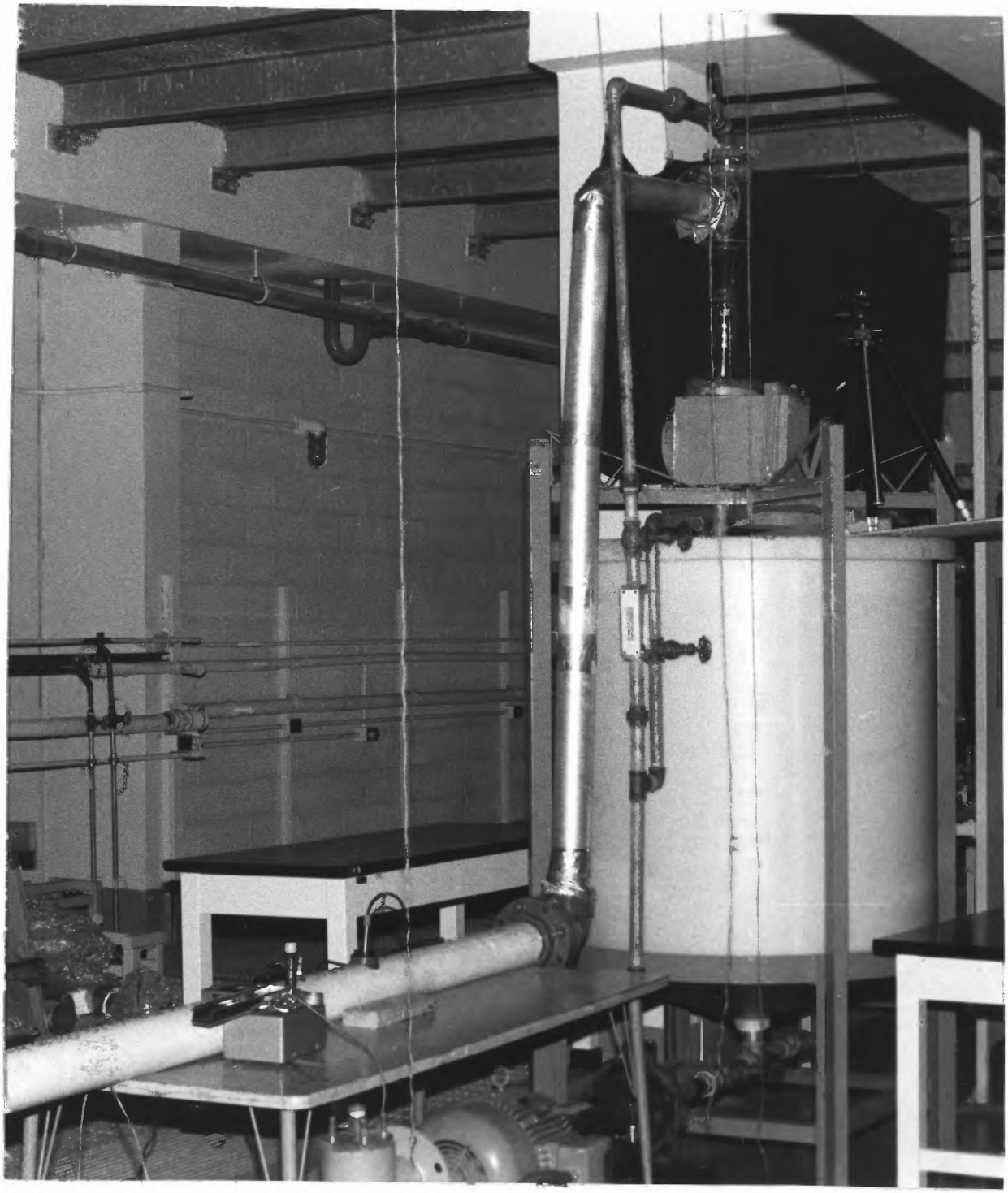

Figure 7.3 Ejector Venturi Scrubber System

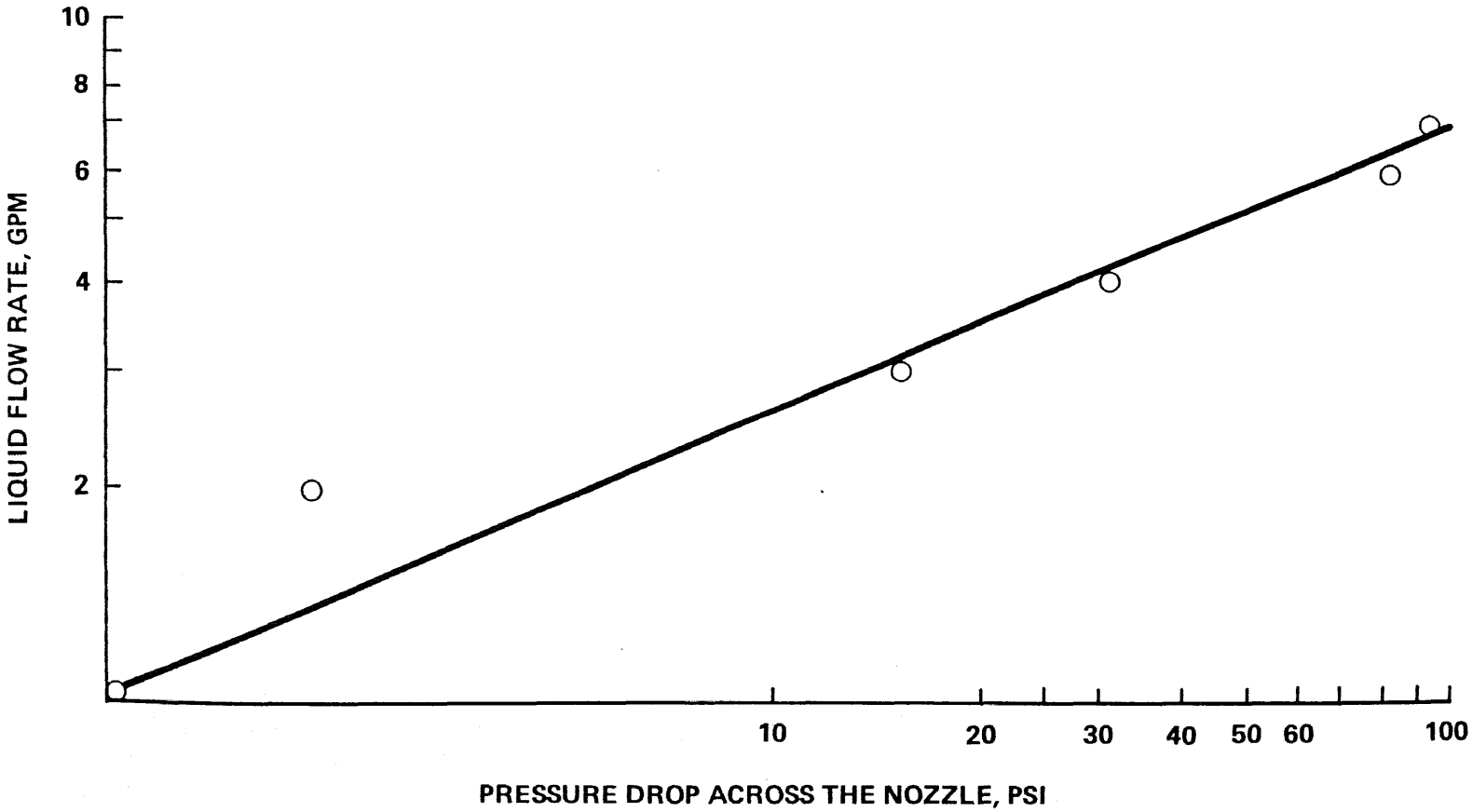

FIGURE 7.4
CAPACITY OF SCHUTTE & KOERTING 622-L 3/8 INCH NOZZLE

Figure 7.5 Photograph of the throat section of the ejector venturi scrubber taken with Minolta SRT-201 camera and Vivitar 285 flash at manual on Kodak Tri-X film

Figure 7.6 Photograph taken with Minolta SRT-201 camera and Vivitar 285 flash at yellow mode on Kodak Plus-X film (side lighted, flash at 1 ft, f/11)

Figure 7.7 Photograph taken with Minolta SRT-201 camera, Vivitar 285 flash at yellow mode on Kodak Plus-X film (back lighted, flash at 1 ft., f/11)

Figure 7.8 Photograph taken with Minolta SRT-201 camera, Vivitar 285 flash at yellow mode on Plus-X film(front lighting, flash at 1.5 ft., f/4)

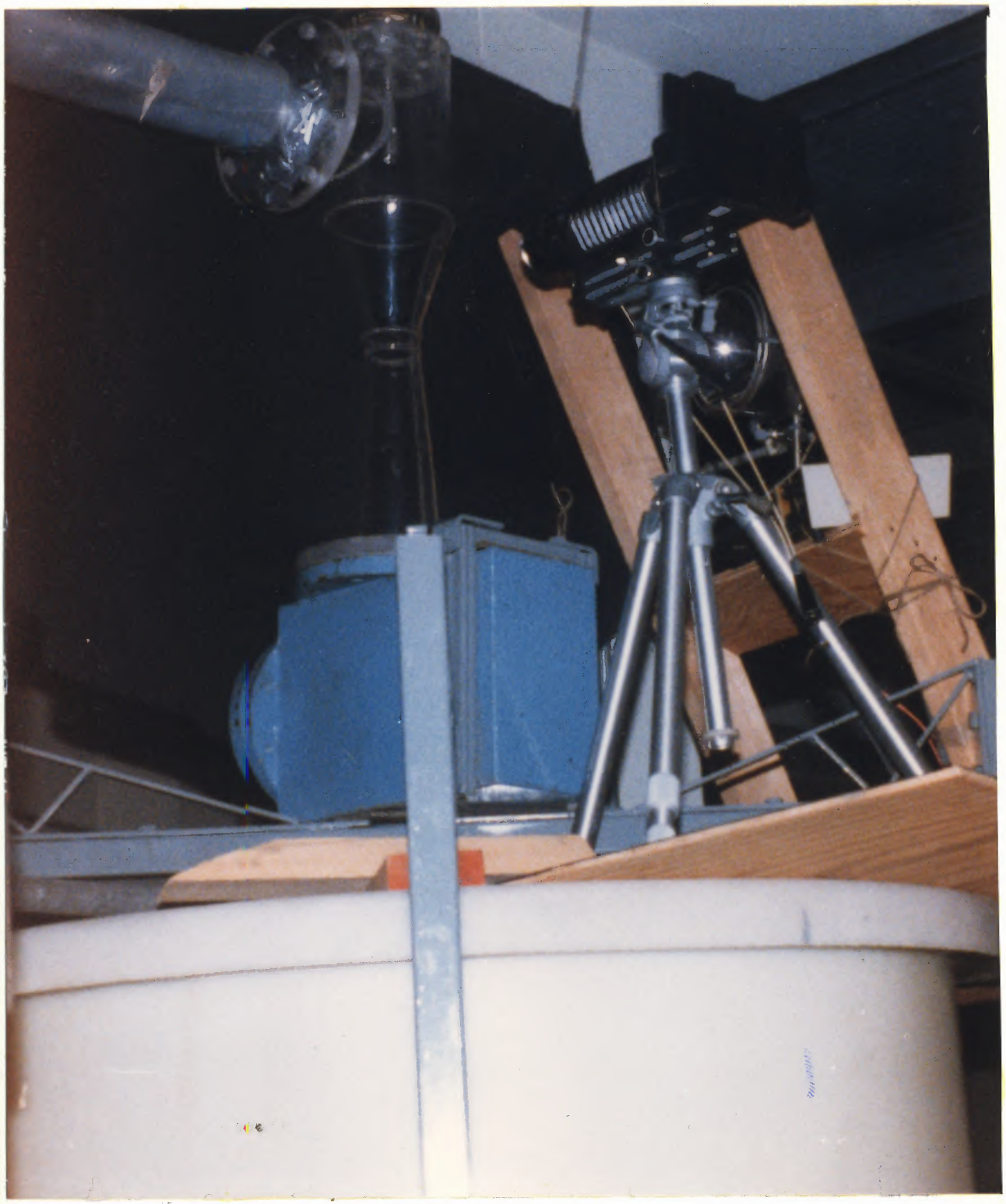

Figure 7.9 Hasselblad 500 C/M camera installed

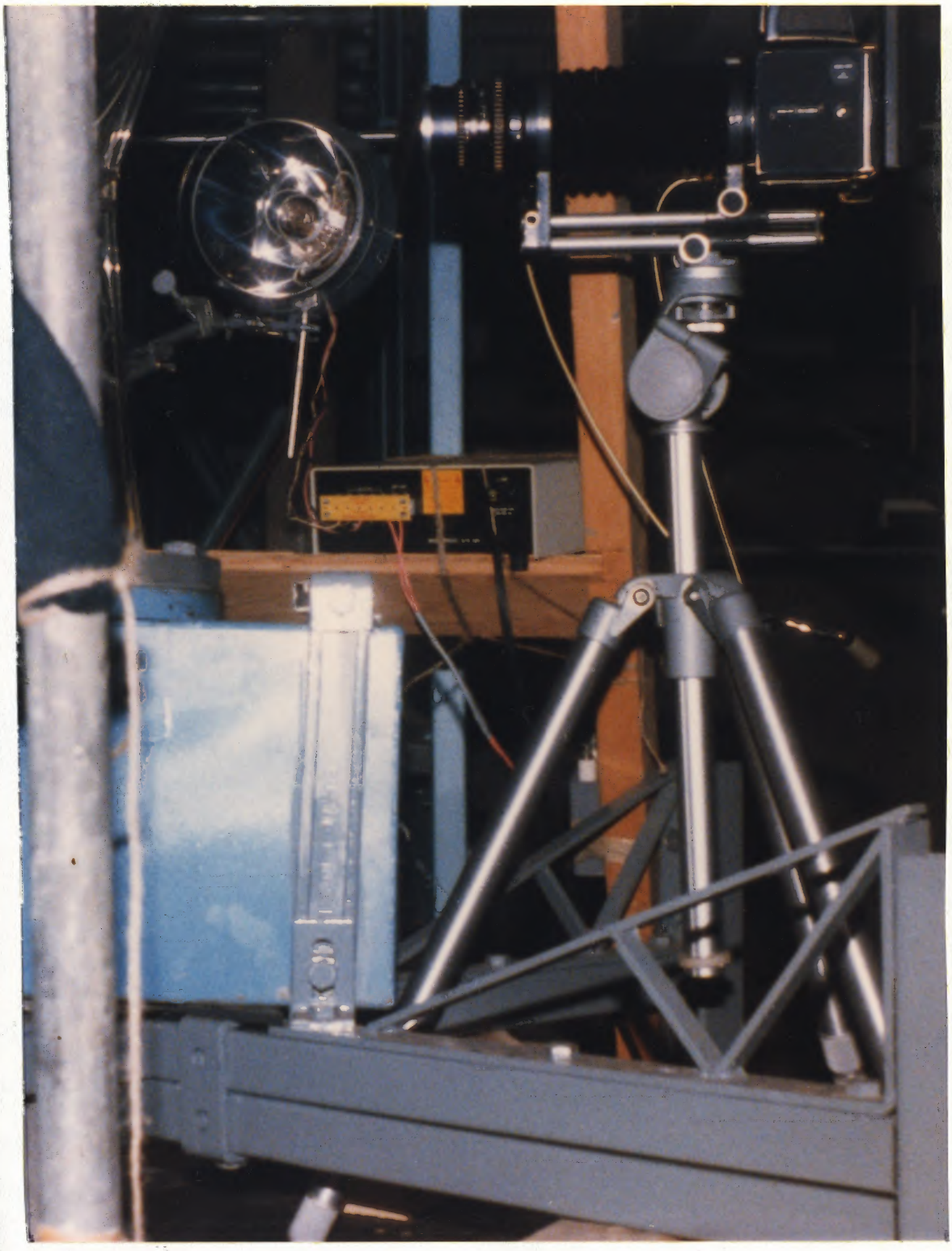

Figure 7.10 Xenon flash lamp (FX199 from EG&G) installed

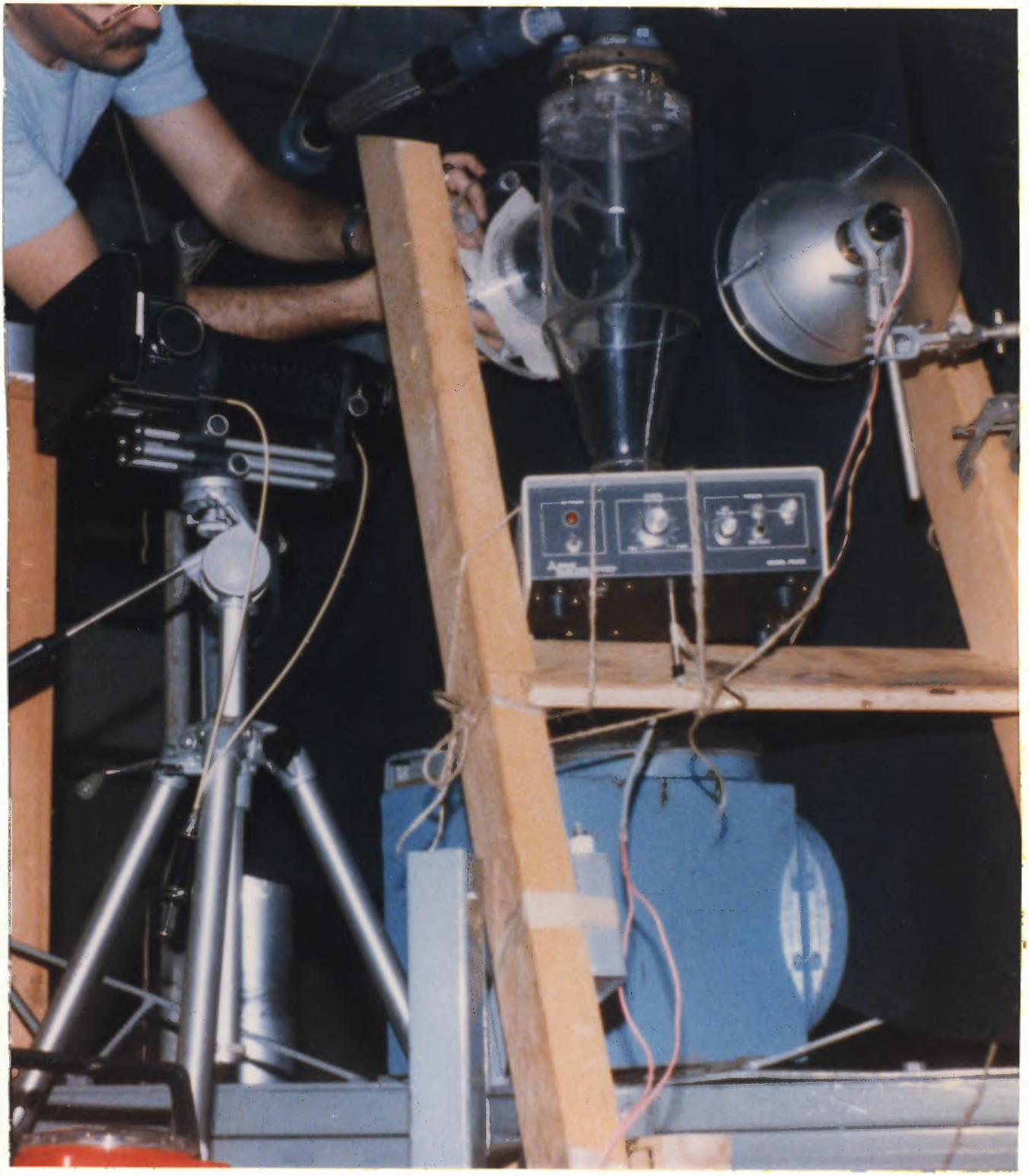

Figure 7.11 FYD-505 Lite Pack and PS-302 power supply trigger module from EG&G installed

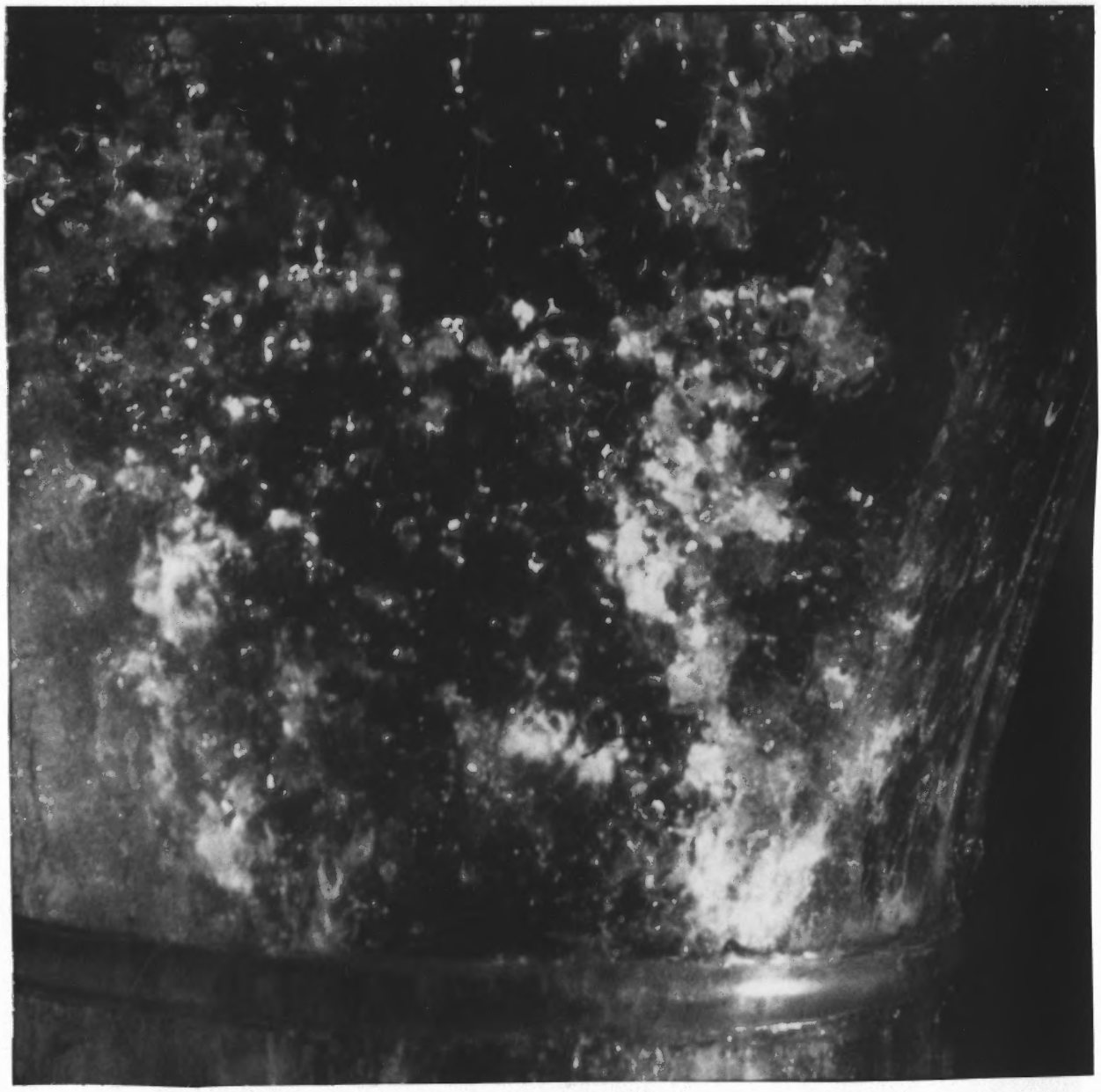

Figure 7.12 Photograph taken with Hasselblad 500C/M camera and Xenon flash lamp on Polaroid 667 film (f/27, 2μf external capacitor, Q_1=6 gpm).

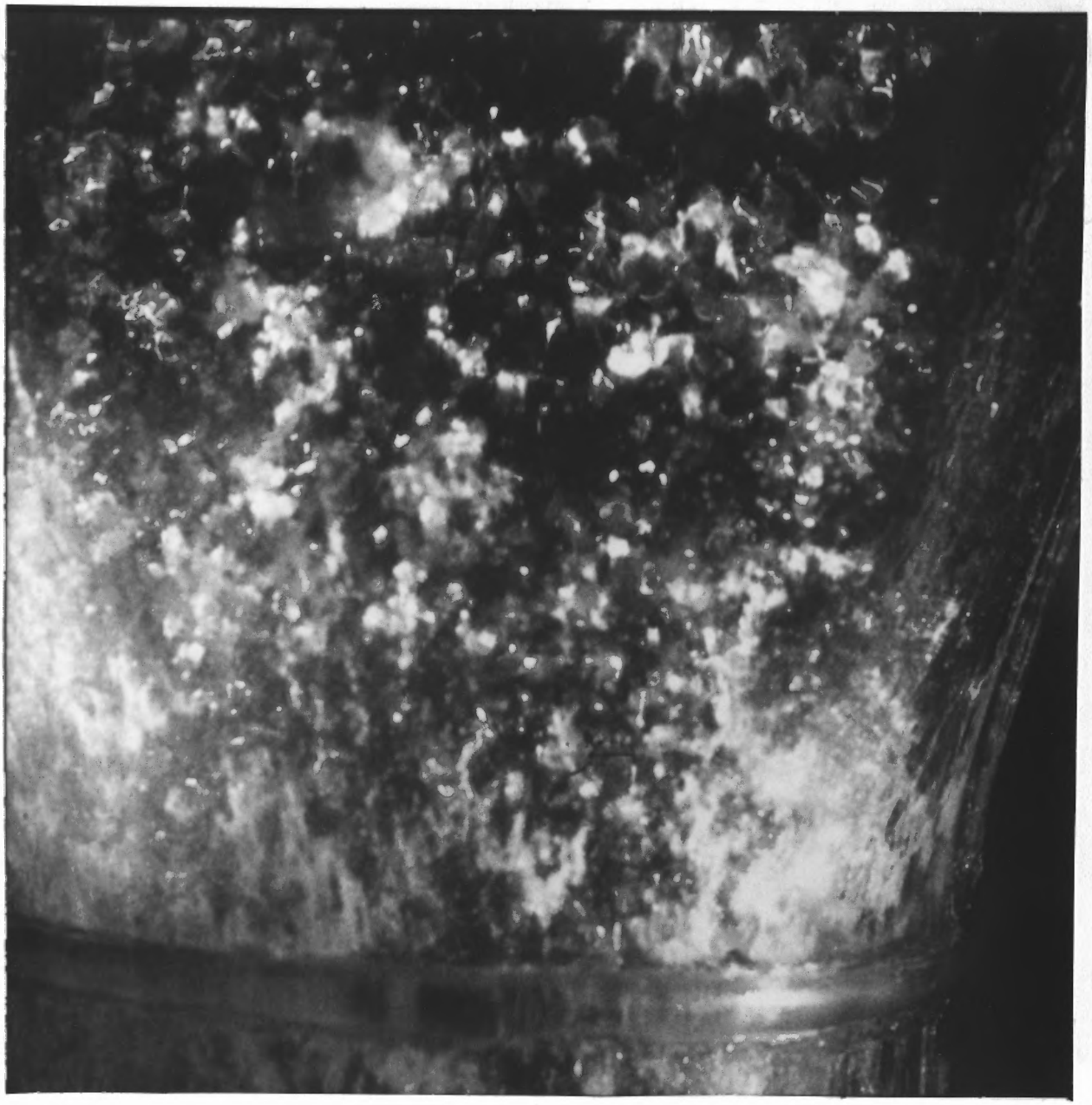

Figure 7.13 Photograph taken with Hasselblad 500 C/M camera and Xenon flash lamp on Polaroid 667 film (f/22, 2 μf external capacitor, Q_1=6 gpm)

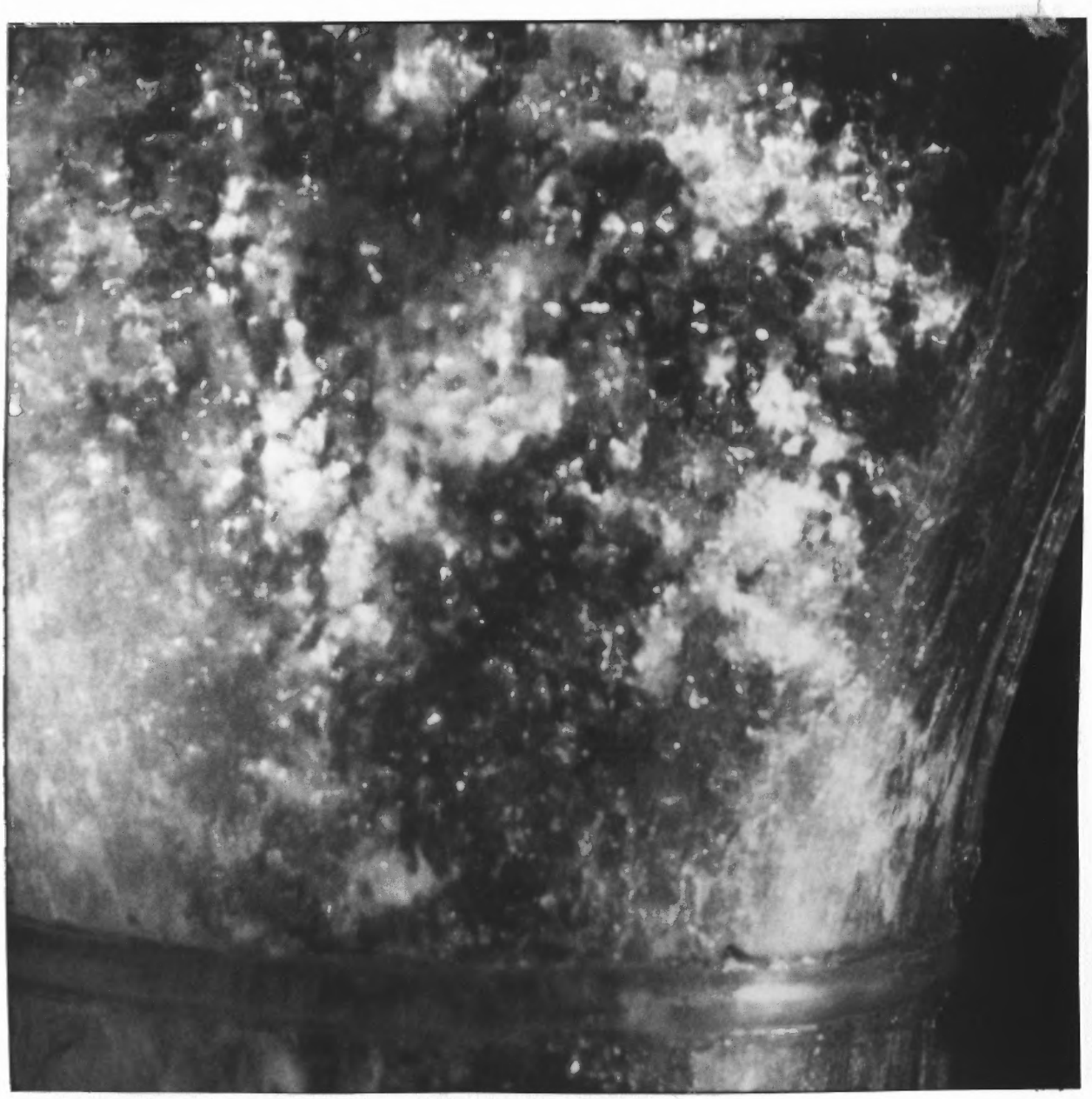

Figure 7.14 Photograph taken with Hasselblad 500 C/M camera and Xenon flash lamp on Polaroid 667 film (f/22, 2 μf external capacitor, Q_1= 8 gpm

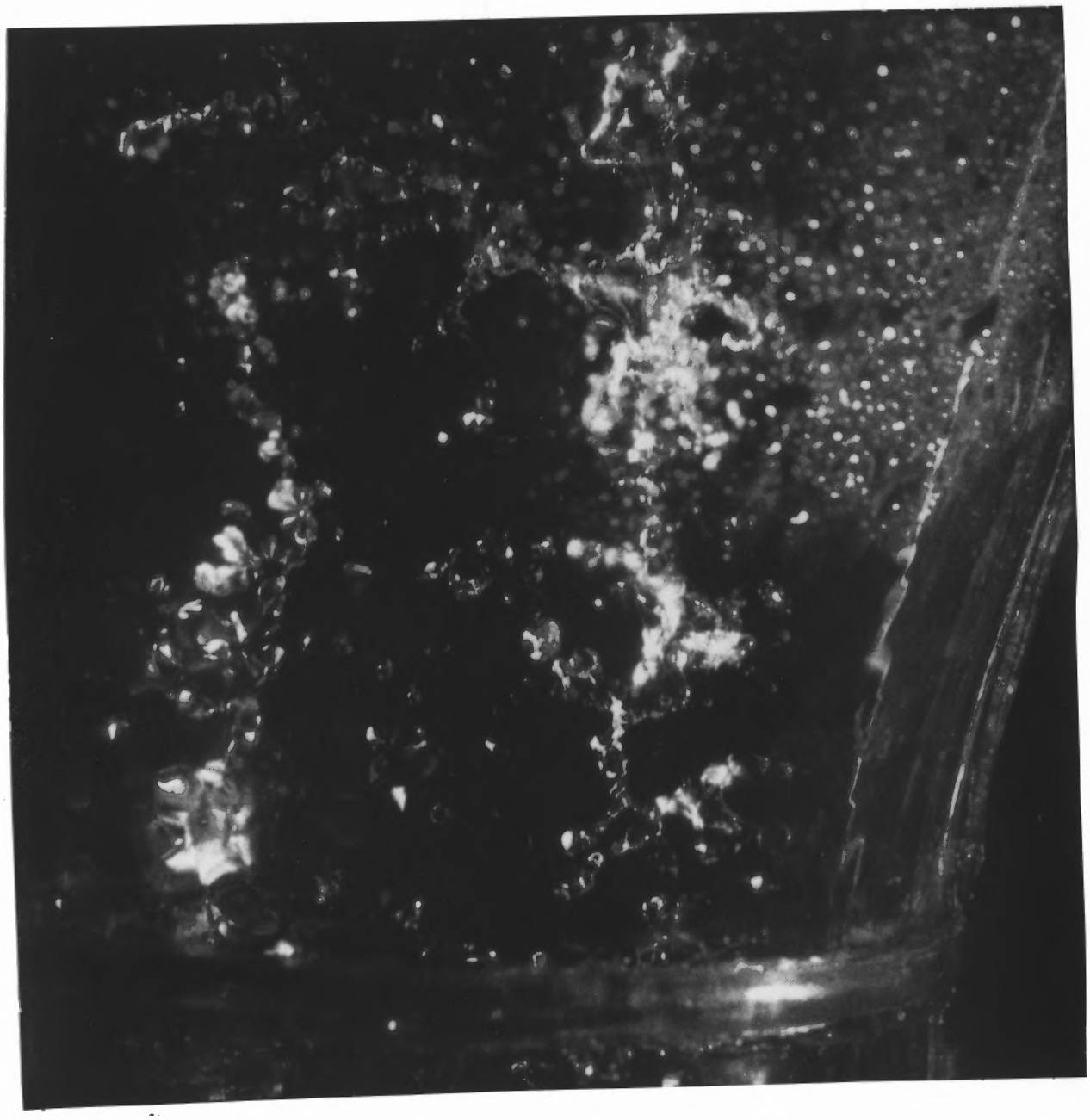

Figure 7.15 Photograph taken with Hasselblad 500 C/M camera and Xenon flash lamp on Polaroid 667 film (f/22, 2 μf external capacitor, Q_1= 3 gpm)

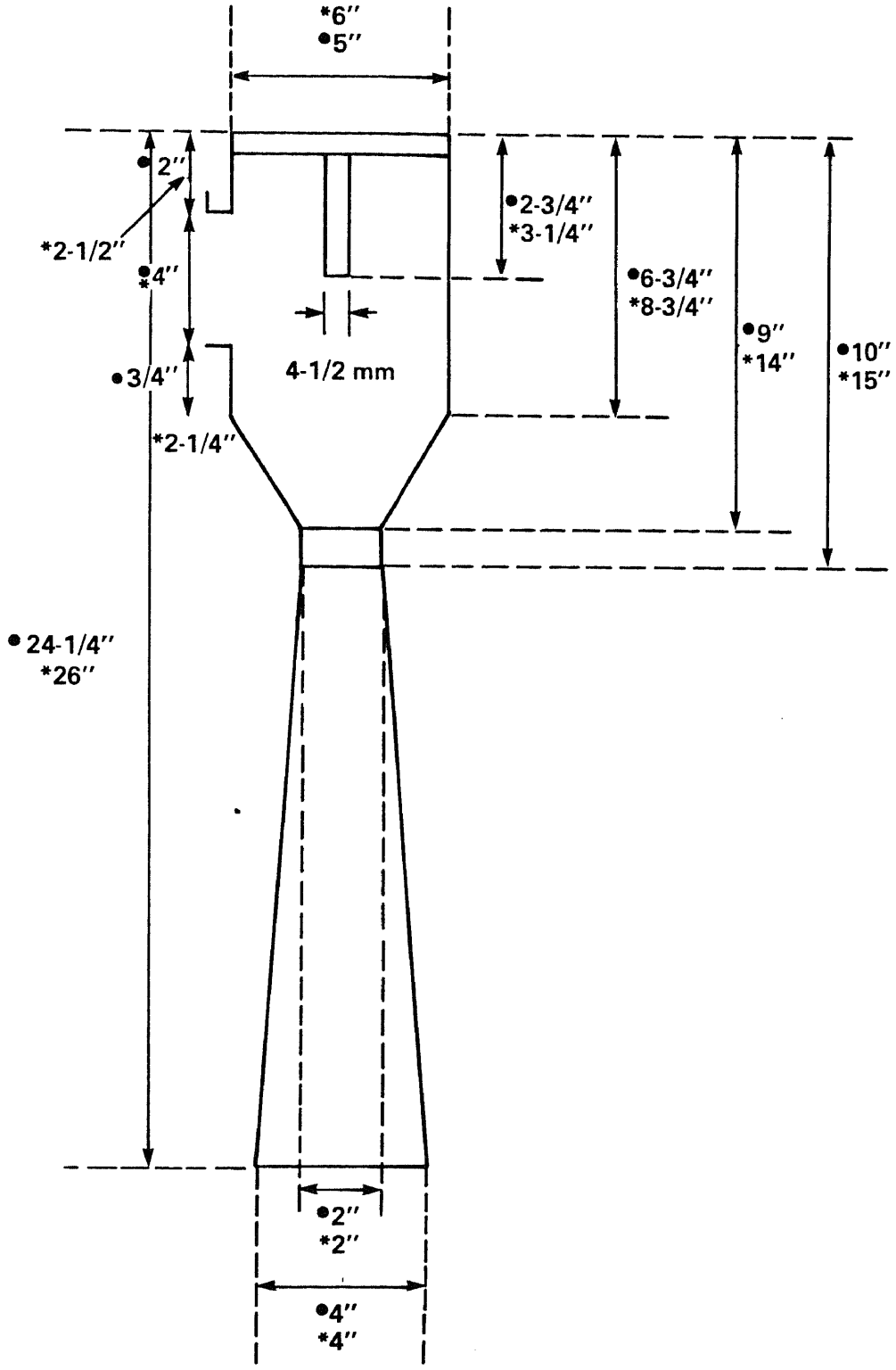

FIGURE 9.1
DIMENSIONS OF THE VARIOUS SECTIONS OF THE EJECTOR VENTURI SCRUBBER

•4" AMETEK 7010

*PLASTIC SCRUBBER

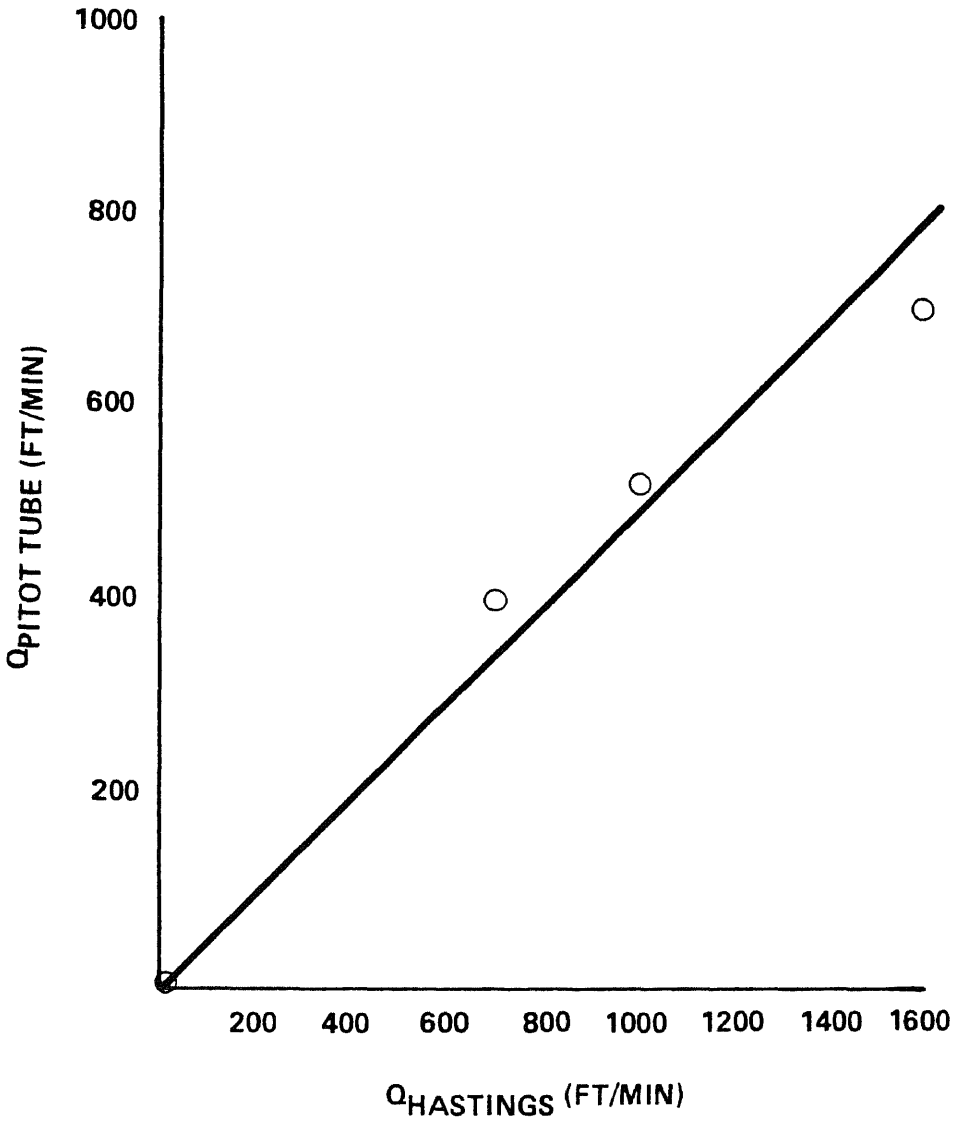

FIGURE 9.2
CALIBRATION OF HASTINGS METER WITH PITOT TUBE

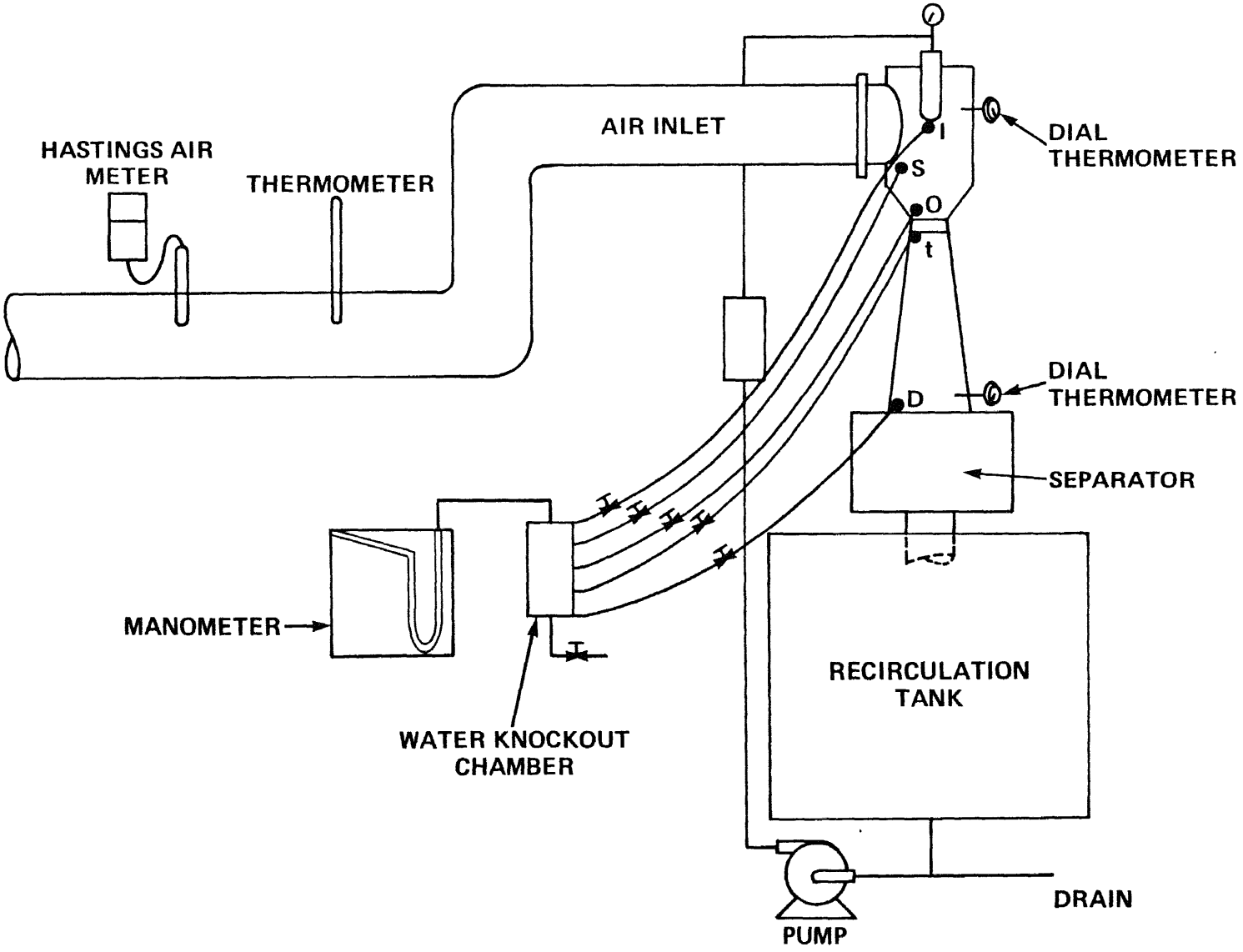

FIGURE 9.3.
EXPERIMENTAL SETUP FOR FLUID FLOW EXPERIMENTS

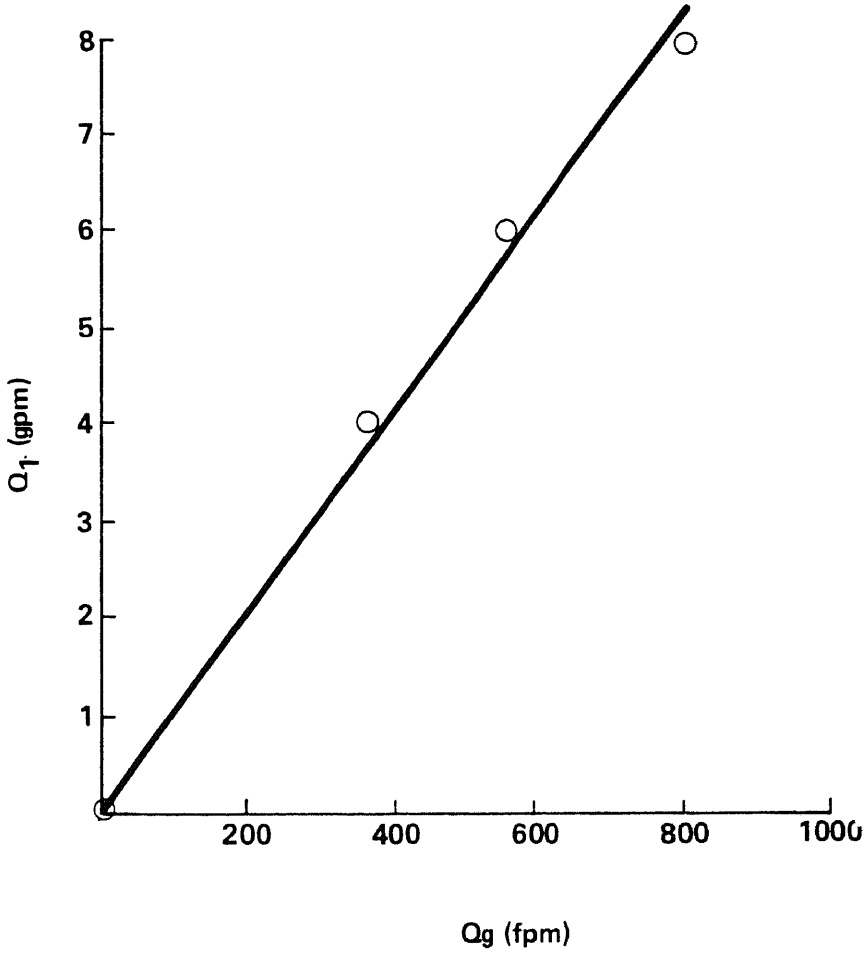

FIGURE 9.4
LIQUID FLOW RATE (ROTAMETER READING) VERSUS GAS FLOW RATE
(HASTINGS AIR METER READING) AMETEK 7010 EJECTOR
VENTURI SCRUBBER

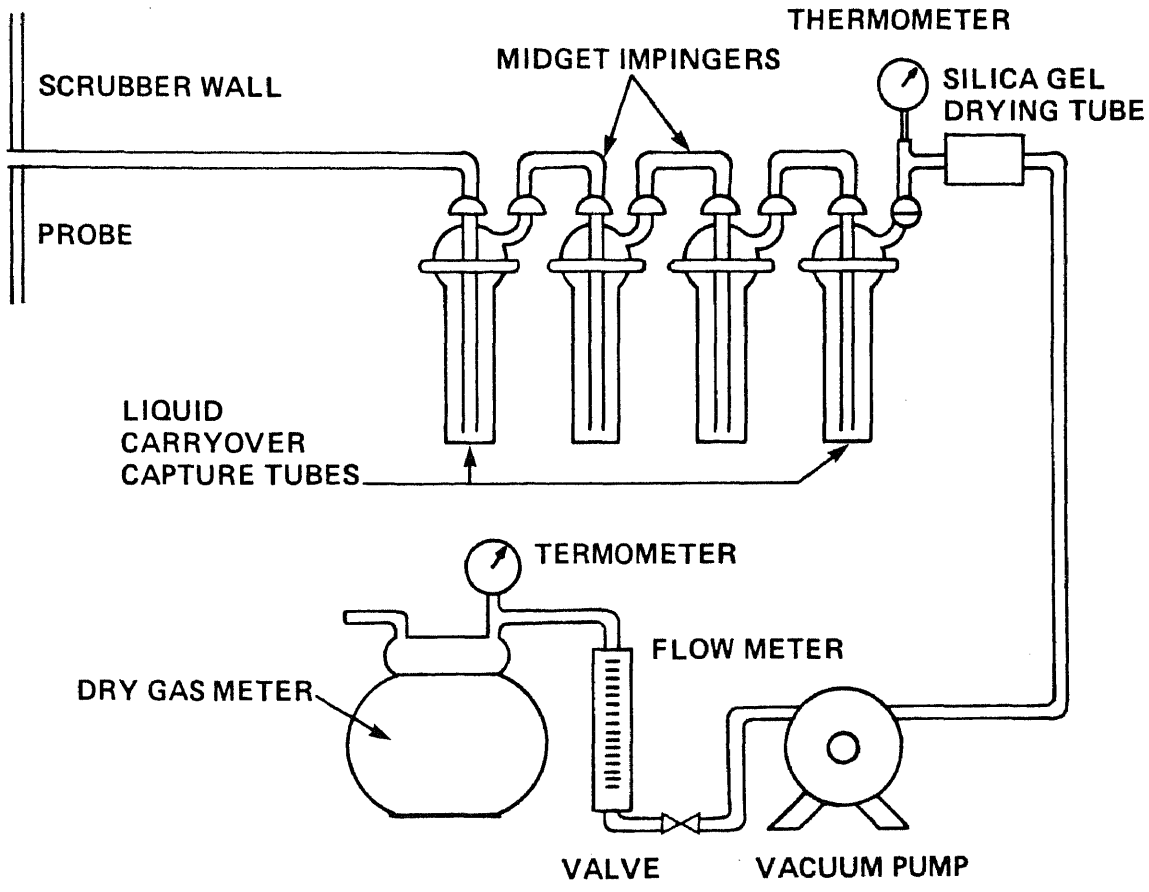

FIGURE 10.1
SO_2 SAMPLING TRAIN

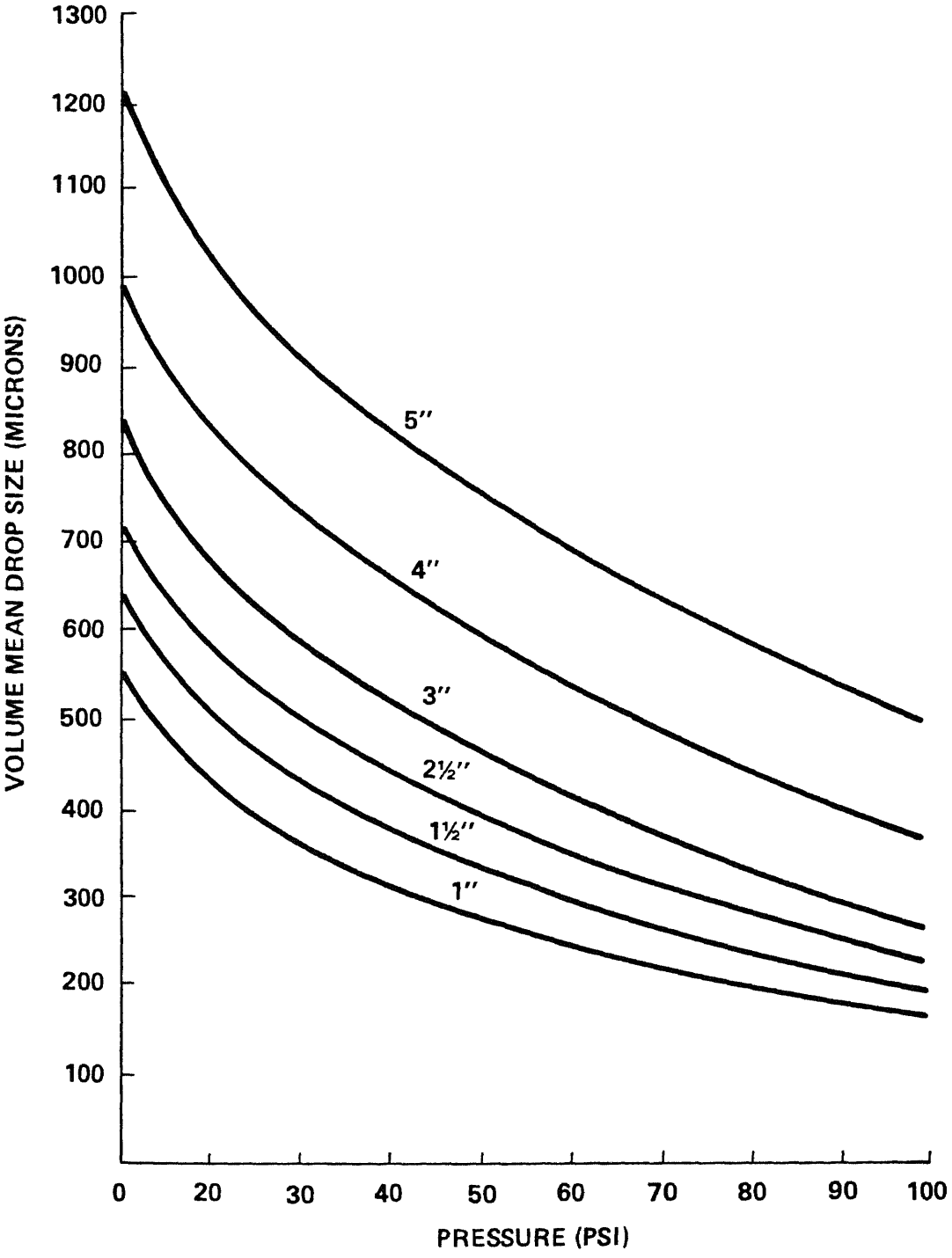

FIGURE 11.1
MEDIAN DROP SIZE VERSUS PRESSURE DROP ACROSS NOZZLE
(OBTAINED FROM SPRAYING SYSTEMS CO., NORTH AVE. AT
SCHMALE RD., WHEATON, ILL. 60187)

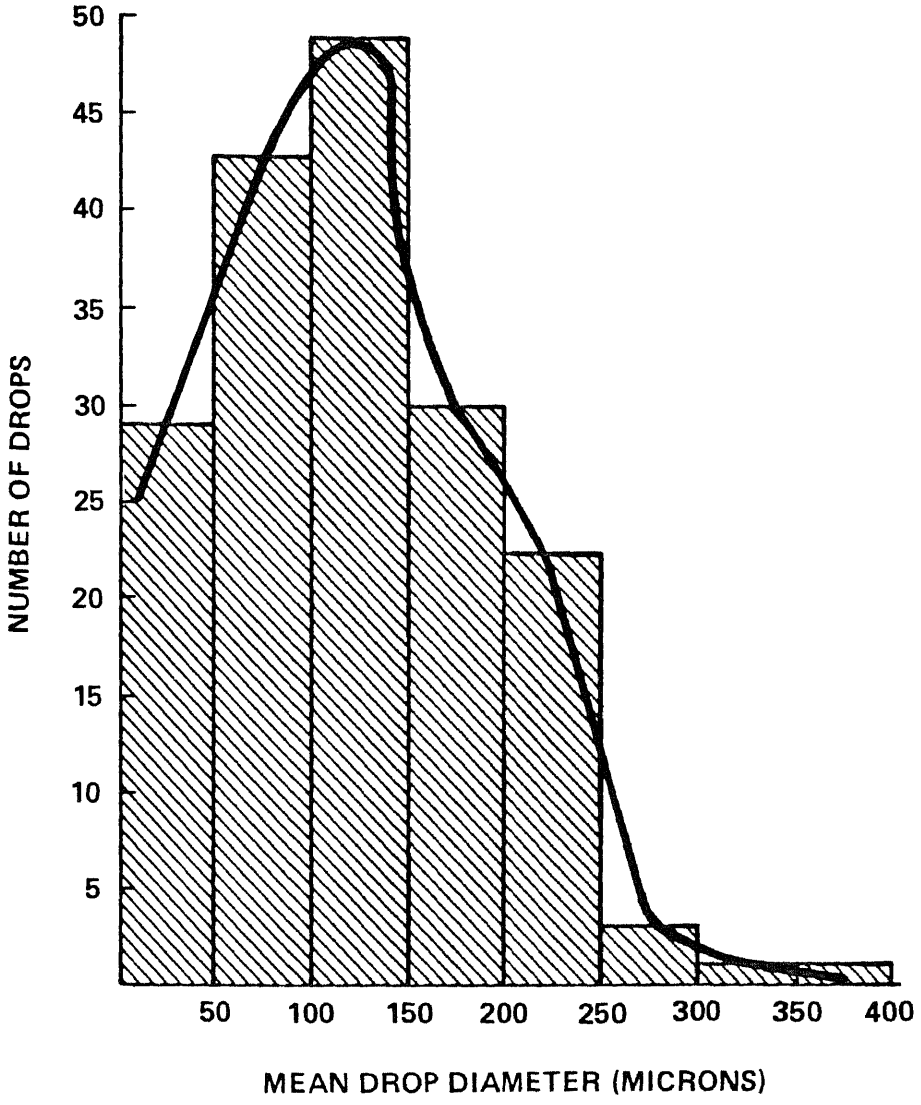

FIGURE 11.2
SIZE DISTRIBUTION OF DROPLETS IN 4" AMETEK 7010 EJECTOR VENTURI SCRUBBER WITH 3/8" S&K 622-L NOZZLE

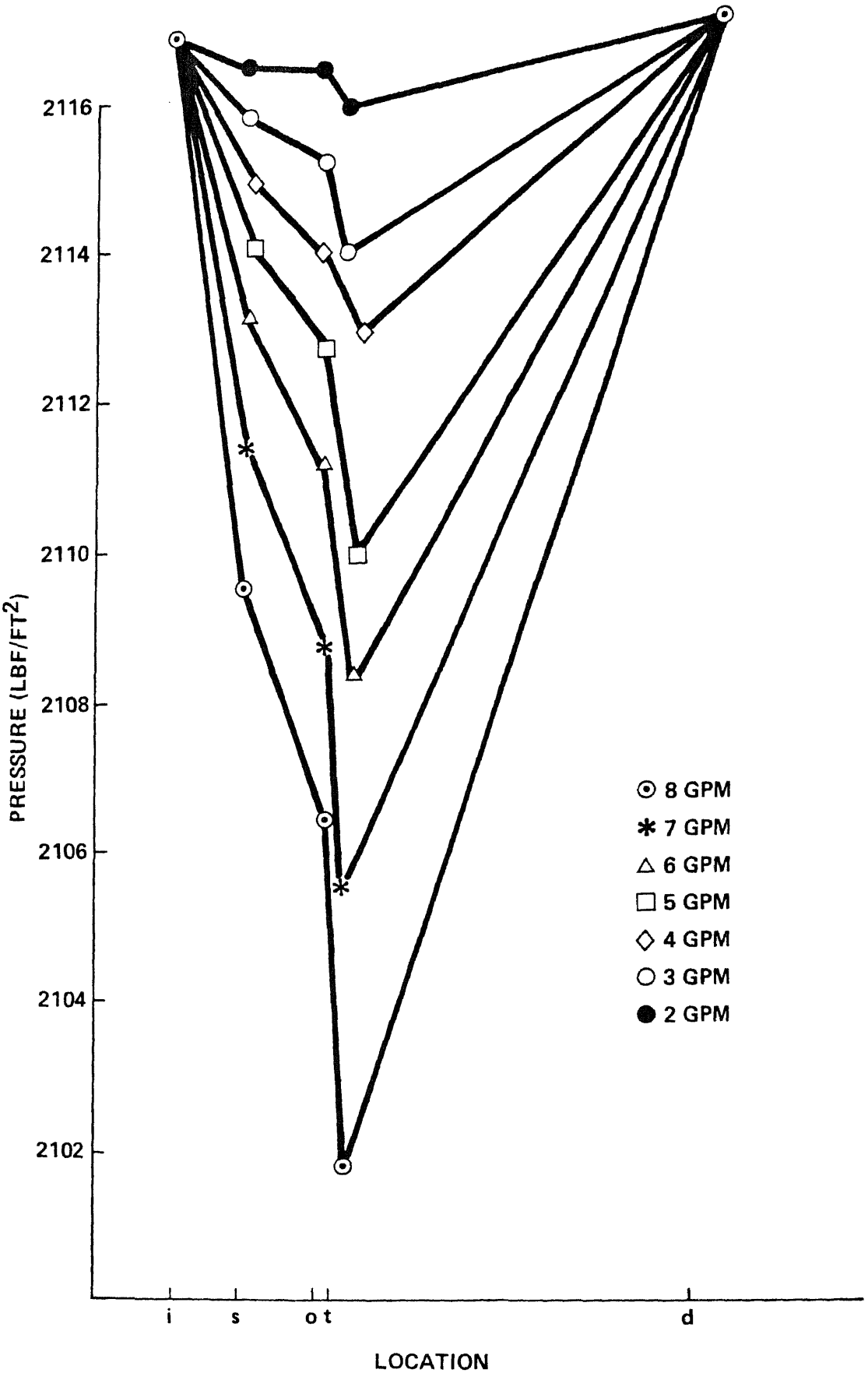

FIGURE 11.3
EJECTOR VENTURI SCRUBBER PRESSURE DISTRIBUTION

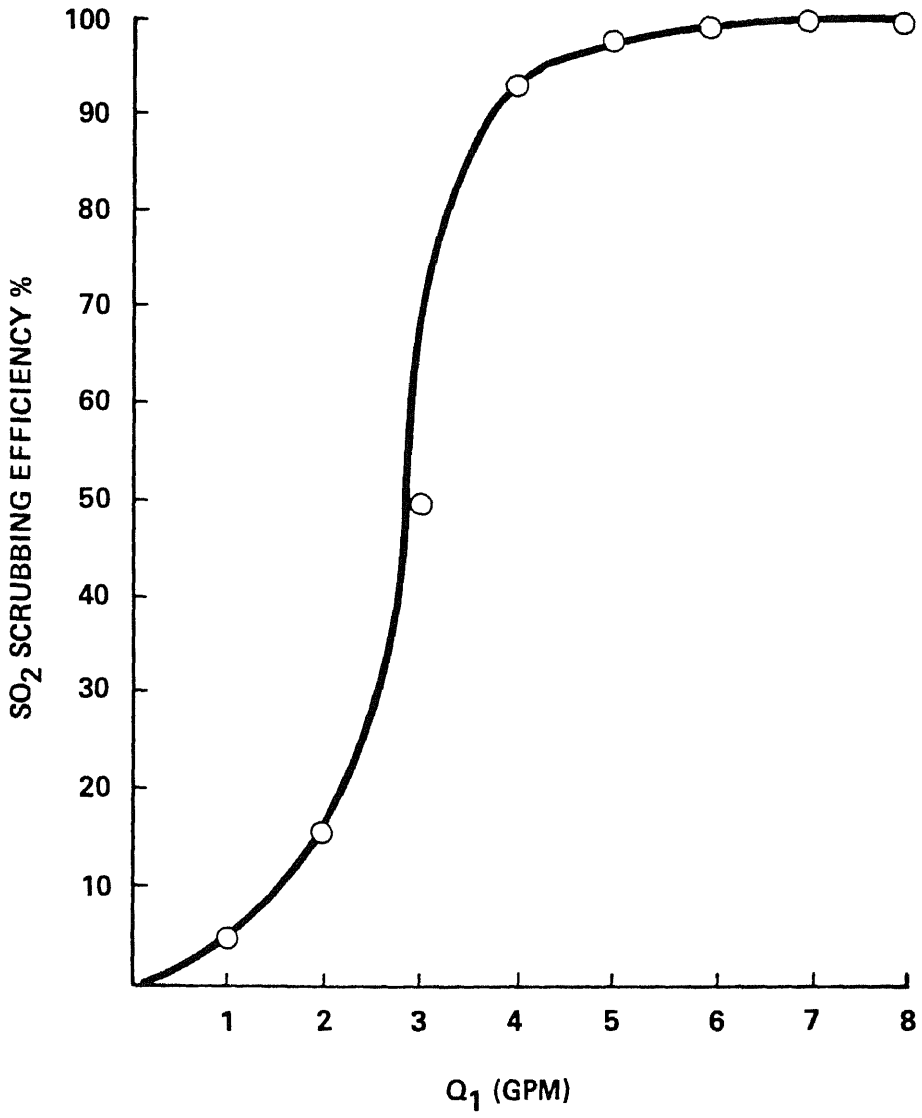

FIGURE 11.4
OVERALL SO_2 SCRUBBING EFFICIENCY (WITH 0.0001 M NaOH SOLUTIONS IN 4" AMETEK 7010 EJECTOR VENTURI SCRUBBER WITH 7040 SEPARATOR)

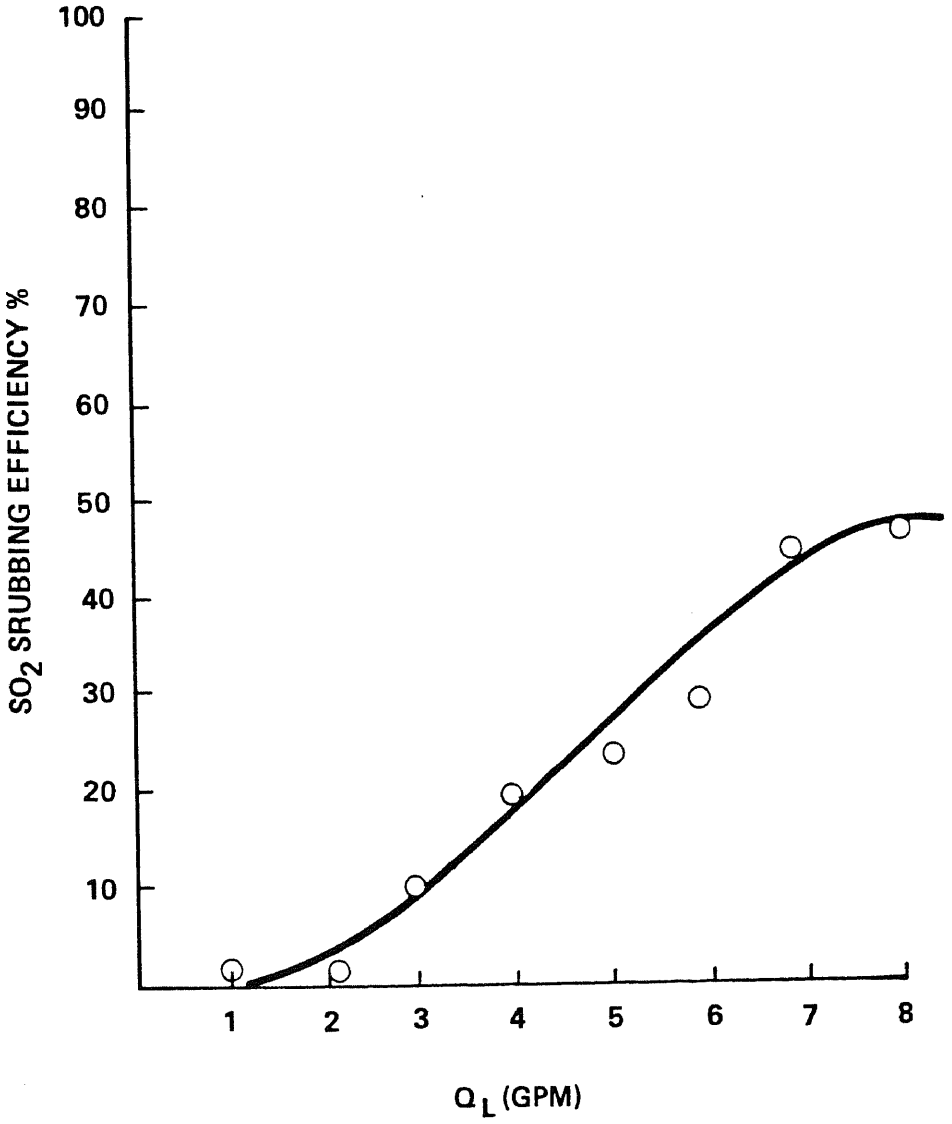

FIGURE 11.5
SO_2 REMOVAL EFFICIENCY IN AMETEK 7040 SEPARATOR

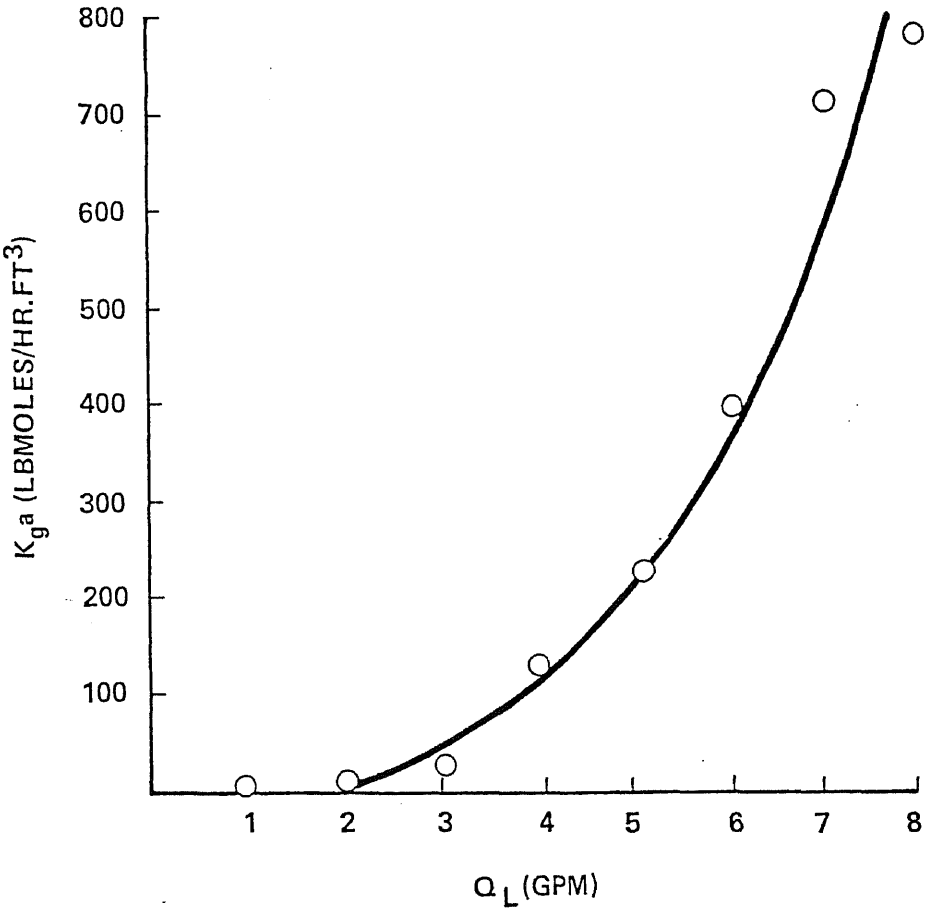

FIGURE 11.6
VARIATION OF VOLUMETRIC MASS TRANSFER COEFFICIENT (Kga) WITH LIQUID FLOW RATE [IN 4" AMETEK 7010 EJECTOR VENTURI SCRUBBER WITH 3/8" S&K 622-L NOZZLE (SO_2 ABSORBED IN 0.0001 M NaOH SOLUTION)]

REFERENCES

Atkinson, D.S.F. and Strauss, W., "Droplet Size and Surface Tension in Venturi Scrubbers", JAPCA, Vol 20, p. 1114 - 1118, (1978)

Arbel, S. and Manheimer-Timnat, Y., "The Performance of Multinozzle Ejectors" Israel Journal of Technology, Vol 12, p. 212 - 220, (1974)

Astarita, G., Mass Transfer with Chemical Reaction Elsevier, Amsterdam, (1966)

Batchelor & Davis (1956) Cited in Fox, G.E. "An Experimental Study of the Relaxation Zone Behind Shock Waves in Water-Air Mixtures with Emphasis in Drop Breakup". Ph. D. Dissertation, The University of Connecticut, (1976)

Bayvel, L. P. and Jones, A. R., Electromagnetic Scattering and its Applications, Applied Science Publishers, London, (1981)

Bayvel, L. P., "The Effect of the Polydispersity of Drops on the Efficiency of a of a Venturi Scrubber", Transactions of the Institute of Chemical Engineers, Vol 60, p. 31 - 34, (1982)

Bayvel, L.P., Veziroglu, Y. N., Multiphase Transport: Fundamentals, Reactor Safety, Applications, Hemisphere Publishing Coporation, Washington, D.C. p.2549, (1980)

Benjamin, T. B., "Shearing Flow Over a Wavy Boundary", Journal of Fluid Mechanics, Vol 6, p. 161, (1959)

Bergwerk, W., "Flow Pattern in Diesel Nozzle Spray Holes" Proceedings of the Institution of Mechanical Engineers, Vol 173, p. 655, (1959)

Betzler, R. L., "The Liquid-Gas Jet Pump Analysis and Experimental Results" M. S. Thesis, The Pennsylvania State University, (1969)

Bhat, P.A., Mitra, A. K., Roy, A. N., "Momentum Transfer in a Horizontal Liquid Jet Ejector" The Canadian Journal of Chemical Enginering Vol 50, p. 313-317, (1972)

Bird, Stewart, Lightfoot, Transport Pheomena, John Wiley, (1960)

Blanchard, D.C., "The Behavior of Water Drops at Terminal Velocity in Air" Transactions of the American Geological Society, p. 386, (1950)

Blanchard, D.C., "Comments on the Breakup of Raindrops", Journal Atmospheric Sciencies, p. 119, (1962)

Boll, R. H., "Particle Collection and Pressure Drop in Venturi Scrubbers", Industrial Engineering Chemistry Fundamentals, Vo. 12, p. 40, (1973)

Boll, R. H., et al. "Mean Drop Size in a Full Scale Venturi Scrubber Via Transmissometer", JAPCA, Vol 24, p. 934 - 938, (1974)

Bonnington, S. T., "Water Jet Ejectors", BHRA Publication, RR540, (1956)

Bonnington, S. T., "Water Driven Air Ejectors", BHRA Publication, SP664, (1960)

Bonnington, S. T. and King, A. L., "Jet Pumps and Ejectors, a State of the Art Review and Bibliography", Published by BHRA Fluid Engineering, Cranfield, Bedford, England, (1972)

Borman, G. L., Myers, P. S. and Vyehors, O.A., "Studies of Oscillatory Combustion and Fuel Vaporization" National Aeronoutics and Space Administration, Contractor, Report 120974, (1972)

Born, M. and Wolf, E., Principles of Optics, Fifth Ed., Pergamon Press, Oxford, (1975)

Borodin, V. A. and Yagodkin, V. I., "Stability of Motion of the Plane Boundary Separating Two Fluids", Journal of Applied Mechanics and Techniques Physics, p. 46, (1965)

Boyadhzhiev, K., "On the Optimal Flow of Liquid During Chemisorption in a Venturi Tube", "Int. Chem. Eng., Vol 4, p 22 - 26, (1964)

Burkholder, H.C. and Berg, J.C., "The Effect of Mass Transfer on Liquid Jet Breakup", AICLE, Vol 20, p. 863, (1974)

Calvert, S., "Venturi and Other Atomizing Scrubbers Efficiency and Pressure Drop", Vol 16, p. 392-396, (1970)

Castleman, R.A., "Mechanism of Atomization of Liquids", U.S. Natl. Bureau of Std. J.Res, Vol 6. p. 281, (1931)

Chraplyvy, A.R., "Nonintrusive Measurements of Vapor Concentrations Inside Sprays", Applied Optics, Vol 20, p. 2620, (1981)

Chilton, T. H. and Colburn, A. P., "Pressure Drop in Packed Tubes" Transactions of the American Institute of Chemical Engineers, Vol 26, p. 178, (1931)

Chin, J. H., Sliepcevich, C.M., and Tribus, M., "Determination of Particle Size Distributions in Polydispersed Systems", Journal of Physical Chemistry, Vol 57, p. 845, (1955)

Chow, T. S. and Hermans, J.J., "Stability of a Cylindrical Viscous Jet Surrounded by a Flowing Gas", The Physics of Fluids, Vol 14, p. 224, (1971)

Clark, C. J. and Dombrowski, N., "On the Photographic Analysis of Sprays", Aerosol Science, Vol 4, p. 27, (1973)

Cleeves, V. and Boelter, L.M.K., "Jet Mixing of Compressible Fluids", Chemical Engineering Progress, Vol. 43, No.3, pp. 123-134, (1947)

Collins, R. and Charwat, A. F., "The Deformation and Mass Loss of Liquid Drops in a High Speed Flow Gas", Israel Journal of Technology, p. 453, (1971)

Cox, D. R. and Miller, H. D., The Theory of Stochastic Processes, Methuen, London (1970)

Cullen, E. J. and Davidson, J. F., "Gas Absorption into Liquid Jets", Transactions of the Faraday Society, Vol 53, p. 113, (1957)

Cunningham, R. G., "Gas Compression with the Liquid Jet Pump", ASME Publication, 74-FE-18, (1974)

Cunningham, R. G., Dopkin, R. J., "Jet Breakup and Mixing Throat Lengths for the Liquid Jet Gas Pump", ASME Publications, 74-FE-17, (1974)

Curtet, R., "Confined Jets and Recirculation Phenomena with Cold Air", Combustion and Flame, London, Vol 2, p. 4, (1958)

Danckwerts, P. V., Significance of Liquid Film Coefficient in Gas Absorption" Industrial Engineering Chemistry, Vol. 43, p. 1460, (1951)

Danckwerts, P. V. and Sharma, M. M., "The Absorption of CO_2 into Solutions of Alkalis and Amines", Chemical Engineering, Vol 73, p. 244-281, (1966)

DeJuhasz, K. J., "Dispersion of Sprays in Solid Injection Oil Engines", Transactions of American Society of Mechanical Engineers, (OGP), Vol 53, p. 65, (1931)

DeJuhasz, K. J., Spray Literature Abstracts, New York, American Society of Mechanical Engineers, Vols 1, 2, 3, 4, (1960)

Dobbins, R. A., Crocco, L., Glassman, I., "Measurement of Mean Particle Size of Sprays from Diffractively Scattered Light", American Institute of Aeronautics and Astronautics Journal, Vol 1, p 1882, (1963)

Dombrowski, N., and Hooper, P. C., "The Effect of Ambient Density on

Drop Formation in Sprays", Chemical Engineering Science, Vol 17, pp 291-305, (1962)

Dombrowski, N. and Mundy, G., "Spray Drying", Biochemical and Biological Engineering Science, Vol 22, Academic Press, New York, (1968)

Downs, W. and Atwood, G.A., "Mathematical Model for Gas Absorption in a Venturi Scrubber", Paper Presented at AIChE National Meeting, Detroit, (1973)

Duda, J. L. and Vrentas, J.S., "Fluid Mechanics of Laminar Liquid Jets", Chemical Engineering Science, p. 855, (1966)

Duda, J. L. and Vrentas, J. S., "Laminar Liquid Jet Diffusion Studies", AICLE, p. 286, (1968)

Elenkov, D., "Hydrodynamics and Mass Transfer in a Venturi Absorber without an Atomizer", Isv, Inst., Obshta., Neorg. Khim., Bulgar, Akad. Nauk, Vol 2 pp. 109-117, 1964, cited in Downs, W. and Atwood, G.A. "Mathematical Model for Gas Absorption in a Venturi Scrubber", Paper Presented at AIChE National Meeting, Detroit, (1973)

Elkotb, M.M., "Fuel Atomization for Spray Modelling", Prog. Energy Combustion Science, Vol 8, p. 61, (1982)

Engdahl, R. B. and Holton, W. C., "Overfire Air Jets" Transactions of the American Society of Mechanical Engineers, Vol 65, p. 741-754, (1943)

Engel, O. G., "Fragmentations of Water Drops in the Zone Behind an Air Shock", Journal of Research of the National Bureau of Standards, Vol 60, p. 245, (1958)

Fabri, J. and Siestrunk, R., "Supersonic Air Ejectors", Advances in Applied Mechanics V, Academic Press, New York, (1958)

Fenn, R. W. and Middleman, S., "Newtonian Jet Stability - the Role of Air Resistance", AIChE, Vol 15, p. 379, (1969)

Flinta, J., Hernborg, G., Stenback, A., "A Water Jet Driven Two Phase Flow Ejector Pump Performance Test", Symposium on Jet Pumps and Ejectors BHRA Fluid Engineering in Conjunction with the Institute of Chemical Engineers, London, p. 19-25, (1972)

Folsom, R. G., "Jet Pumps with Liquid Drive", Chemical Engineering Progress, Vol 44, p. 765-770, (1948)

Fraser, R. P. an Eisenklam, P., "Liquid Atomization and the Drop Size of Sprays", Transactions of the Institution Chemical Engineers, Vol 34, p. 294-319, (1956)

Froessling, N., Gerlands Bertu Geophys, Vol 32, p. 170, 1938, cited in Raman, (1983)

Fymat, A. L., "Remote Monitoring of Environmental Particulate Pollution. A Problem in Inversion of First Kind Integral Equations", Applied Mathematical Computations, p. 131, (1975)

Giffen, E. and Muraszew, A., The Atomization of Liquid Fuels, John Wiley and Sons, New York, (1953)

Gleason, R. J. and McKenna, J. D., Technical Paper Presented at 69th National Meeting of AIChE, Cincinnati, (1971)

Goedde, E. F. and Yuen, M.C., "Experiments on Liquid Jet Instability", Journal of Fluid Mechanics, Vol 40, p. 495, (1970)

Goff, J. A. and Coogan, C. H., "Some Two Dinensional Aspects of the Ejector Problem", Transactions of the American Society of Mechanical Engineers, Vol 64, p. A151-154, (1942)

Goldshmid, Y. and Calvert, S., "Small Particle Collection by Supported Liquid Drops", AIChE, Vol 9, p. 352-358, (1963)

Gordon, G. D., "Mechanism and Speed of Breakup of Drops", Journal of Applied Physics, Vol 30, p. 1759, (1959)

Goren, S. L. and Wronski, S., "The Shape of Low-Speed Capillary Jets of Newtonian Liquids", Journal of Fluid Mechanics, Vol 25, p. 185, (1966)

Gosline, J. E., and O'Brien, M. P. , University of California Publications, Vol 3, No. 3, p. 167-190, (1934)

Gould, T. R. "Absorption of Ammonia with Water in a Venturi Scrubber", Masters Thesis, Newark College of Engineering, (1952)

Grant, R. P. and Middleman, S. "Newtonian Jet Stability", AICLE, Vol 12, p. 669, (1966)

Gretzinger, J. and Marshall Jr., W. R., Characteristics of Pneumatic Atomization", AIChE, Vol 7, p. 312-318, (1961)

Haenlein, A., "On the Disruption of a Liquid Jet", National Advisory Committee Aeronautics, Technical Memorandum 659, (1932)

Harmon, D. B., "An Equation for Predicting a Mean Drop Size in a High Speed Spray", Univeristy of California Publications in Engineering, Vol 5, (1955)

Harris, L. S., "Energy and Efficiency Charactheristics of the Ejector Venturi Scrubber", JAPCA, Vol 5, p. 302, (1965)

Hass, F. C., "Stability of Droplets Suddenly Exposed to a High Velocity Gas Stream", AIChE, Vol 10, p. 920, (1964)

Hatta, S., Technical Reports, Tohoku Imperial University, Vol 8, p. 1, (1928)

Hedges, K. R. and Hill, P. G., "Compressible Flow Ejectors, Part I - Development of a Finite - Difference Flow Model", Transactions of the American Society of Mechanical Engineers, p. 272-276, (1974)

Hesketh, H. E., "Fine Particle Collection Efficiency Related to Pressure Drop, Scrubbant and Particle Properties, and Contact Mechanism", Journal of Air Pollution Control Association, Vol 24, p. 939-942, (1974)

Hickman, K. E., Hill, P. G., and Gilbert, G. B., "Analysis and Testing of Compressible Flow Ejectors with Variable Area Mixing Tubes", Journal of Basic Engineering, Transactions of the American Society of Mechanical Engineers, p. 407, (1972)

Higbie, R. L., "Rate of Absorption of a Pure Gas Into a Still Liquid During Short Periods of Exposure", Transactions of the American Institute of Chemical Engineers, Vol 31, p. 365-370, (1935)

Higgins, H. W., "Water Jet Air Pump Theory and Performance", M.S. Thesis, The Pennsylvania State University, (1964)

Hinze, J. O., "Forced Deformations of Viscous Liquid Globules", Applied Scientific Research, p. 263, (1949)

Hinze, J. O. and Rijnders, J. D., "The Mixing Shock in a Water Jet Gas Pump", Ph.D. Thesis, Department of Mechanical Engineering, Delft University of Technology, The Nehterlands, (1971)

Hiroyasu, H., "Mathematical Expression for Drop Size Distribution in Sprays", National Aeronautics and Space Administration, Contractor Report - 72272, (1967)

Hiroyasu, H. and Kadota, T., "Fuel Droplet Size Distribution in Diesel Combustion Chamber", SAE Paper 740715, (1974)

Holroyd, H. B., "On the Atomization of Liquid Jets", Journal of Franklin Institute, Vol 215, p. 93, (1933)

Houghton, H. G., "The Size and Size Distribution of Fog Particles", Physics, Vol 2, p. 267, (1932)

Hrubecky, H. F., "Experiments in Liquid Atomization by Air Streams", Journal of Applied Physics, Vol 29, p. 572-578, (1958)

Huang Yung-Fu, "Mass Transfer During Drop Formation Under Jetting Conditions", Ph. D. Disseration, University of Kentucky, (1976)

Johnstone, H. F. and Anderson, L. B., "Gas Absorption and Oxidation in Dispersed Media", AIChE, Vol 1, p. 135-141, (1951)

Johnstone, H. F., Tassler, M. C., and Feild, R. B., "Gas Absorption and Aerosol Collection in a Venturi Atomizer", Industrial and Engineering Chemistry, Vol 46, p. 1601-1608, (1954)

Kenthe, A. M., Journal of Applied Mechanics, p. A87-A95, (1935)

Kerker, M., The Scattering of Light and Other Electromagnetic Radiation, Academic Press, New York, (1969)

Kim, K. Y. and Marshall Jr., W. R., "Drop Size Distribution from Pneumatic Atomizers", American Institute of Chemical Engineers Journal, Vol 17, p. 575-584, (1971)

Ko-Jen Wu, "Atomizing Round Jets", Ph.D. Dissertation, Princeton University, p. 13, (1983)

Krauss, W. E., "Water Drop Deformation and Fragmentation Due to Shock Wave Impact", Ph.D. Thesis, University of Florida, (1970)

Kuznetsov, M. D. and Ortawski, V. I., "Rate of Chemisorption in a Venturi Type Apparatus", Ph.D. Thesis, University of Florida, (1970)

LaFrance, P., "Non-Linear Breakup of a Laminar Liquid Jet", The Physics of Fluids, Vol 18, p. 428, (1975)

Lane, W. R., "Shatter of Drops in Streams of Air", Industrial and Engineering Chemistry, Vol 43, p. 1312, (1951)

Lapple, C. E., Henry, A., and Blake, D. E., "Atomization Survey and Critique of the Literature", Stanford Research Institute Report, No. 6, AD 831-314, (1967)

Lee, D. W. and Spencer, R. C., "Photomicrographic Studies of Fuel Sprays", National Advisory Committee for Aeronautics, Technical Report 454, (1933)

Levich, V. G., Physicochemical Hydrodynamics, Prentice Hall, (1962)

Levich, V. G. and Krylov, V. S., 1969, "Sufrace Tension Driven Phenomena", Annual Review of Fluid Mechanics, Vol 1, p. 293, (1969)

Lewis, H. C., Edward, D. G., Goglia, M.J., Rice, R. I., and Smith, L. W., "Atomization of Liquids in High Velocity Gas Streams", Industrial Engineering Chemistry, Vol 40, p. 67-74, (1948)

Levy, E. K. and Brown, G. A., "Liquid Vapor Interactions in a Constant-Area Condensing Ejector", Journal of Basic Engineering, ASME, p. 169-175, (1972)

Licht, W. and Radhakrishnan, E., "Some Basic Concepts in Modeling of Venturi Scrubbers", Presented at the 82nd National Meeting American Institute of Chemical Engineers, Atlantic City, New Jersey, August 29 - September 1, (1976)

Licht, W., Air Pollution Control Engineering - Basic Calculations for Particulate Collection, Marcel Dekkor, Inc., New York, (1979)

Longwell, J. P., "Fuel Oil Atomization", Ph.D. Thesis, Massachusettes Institute of Technology, (1943)

Mayfield, F. W. and Church, Jr., W. L., "Mass Transfer under Jetting Conditions", Industrial Engineering Chemistry, Vol 44, p. 2253, (1952)

McCabe, W. L. and Smith, J. C., Unit Operations in Chemical Engineering, 4th Edition, McGraw Hill, (1985)

McCarthy, M. J. and Molloy, N.A., "Review of Stability of Liquid Jets and the Influence of Nozzle Design", The Chemical Engineering Journal, Vol 7, p. 1, (1974)

Meister, B. J. and Scheele, G. F., "Generalized Solution of the Tomotika Stability Analysis for a Cylindrical Jet", American Institute of Chemical Engineers Journal, Vol 13, p. 682, (1967)

Mehlig, H., "On the Physics of Fuel Sprays in Diesel Engines", A.T.Z., Vol 37, No. 16, 1934, Cited in Giffen and Muraszew, (1953)

Mellanby, A. L., "Fluid Jets and Their Practical Applications", Transactions of the Institute of Chemical Engineers, London, Vol 6, p. 66-84, (1928)

Merrington, A. C. and Richardson, E. G., "The Breakup of Liquid Jets", Proceedings of the Physics Society, London, Vol 59, p. 1, (1947)

Miesse, C. C., "Correlation of Experimental Data on the Disintegration of Liquid Jets", Industrial Engineering Chemistry, Vol 47, p. 1960, (1955)

Mikhail, S., "Mixing of Coaxial Streams Inside a Closed Conduit", Journal of Mechanical Engineering Science, Vol 2, p. 50-68, (1960)

Minner, G. L., "A Study of Axisynmetric, Incompressible, Ducted Jet Entrainment", Ph.D. Thesis, Purdue University, January (1970)

Monk, G. W., "Viscous Energy Dissipated during the Atomization of a Liquid", Journal of Applied Physics, Vol 23, p. 288, (1952)

Mugele, R. A. and Evans, H. D., "Droplet Size Distribution in Sprays", Industrial Engineering Chemistry, Vol 43, No. 6, p. 1317, (1951)

Mugele, R. A., "Maximum Stable Droplets in Dispersoid", AIChE, Vol 6, p. 3-10, (1960)

Nayfeh, A. H. and Hassan, A. J., "The Method of Multiple Scales and Non-liner Dispersive Waves", Journal of Fluid Mechanics, Vol 48, p. 463, (1971)

Northrup, R. P., "Flow Stability in Small Orifices", A.R.S. Paper, pp. 49-51, (1951)

Nukiyama, S. and Tanasawa, Y., "Experiments on the Atomization of Liquids in an Air Stream", Transactions of the Society Mechanical Engineers, Japan, Vols 4-6, Reports 1-6, 1938-40. Translated by E. Hope for Defense Research Board, Department of National Defense, Canada 10 M-9-47 (393), H. Q. 2-0-254-1, March 18, (1950)

Nurick, W. H., "Orifice Cavitation and Its Effect on Spray Mixing", Journal of Fluids Engineering, Vol 98, p. 681, (1976)

Obert, E. F., Internal Combustion Engines and Air Pollution, Harper and Row, New York, (1973)

O'Brien, V., "Why Raindrops Breakup - Vortex Instability", Journal of Meteorology, Vol 18, p. 549, (1961)

O'Brien, M. P. and Gosline, J., University of California Publication in Engineering, Vol 3, p. 167, (1934)

Ohnesorge, W., "Formation of Drops by Nozzles and the Breakup of Liquid Jets", Z. Angew. Math. Mech., Vol 16 p. 335, Cited in Miesse, (1955)

Orr, C. J., Particulate Technology, MacMillen Co., (1966)

Overcamp, T. J., and Bowen, S. R. J., "Effect of Throat Length and Diffuser Angle on Pressure Loss Across a Venturi Scrubber", JAOCA, Vol 33, p. 600-604, (1983)

Panasenkov, N. S., "Effect of the Turbulence of a Liquid Jet on its Atomization", Zh. Tekh. Fiz., Vol 21, p. 681, (1976), Cited in Reitz (1978)

Paulon, J. and Fabri, J., "Theory an Experiments on Supersonic Air-to-Air Ejectors", National Advisory Commitee on Aeronautics, Technical Memorandum 1410, (1958)

Pavitt, K. W., Jackson, M. C. and Adams, R. J., "Holography of a Fast

Moving Cloud of Droplets", J. Phys., E. Scientific Instruments, Vol 3, p. 971, (1970)

Peters, C. E., "Theoretical and Experimental Studies of Ducted Mixing and Burning of Coaxial Streams", Journal of Space Craft, Vol 12, p. 1435-1441, (1969)

Phinney, R. E., "Stability of a Laminar Viscous Jet - The Influence of the Initial Disturbance Level", AIChE, Vol 18, p. 432, (1972)

Phinney, R. E., and Humphries, W., "Stability of a Laminar Jet of Viscous Liquid - Influence of Nozzle Shape", AIChE, Vol 19, p. 655, (1973)

Phinney, R. E., "Stability of a Laminar Viscous Jet - The Influence of Ambient Gas", The Physics of Fluids, Vol 16, p. 193, (1973a)

Phinney, R. E., "The Breakup of a Turbulent Liquid Jet in A Gaseous Atmosphere", Journal of Fluid Mechanics, Vol 60, p. 689, (1973b)

Placek, T. D. and Peters, L. K., "Analysis of Particulate Removal in Venturi Scrubbers - Effect of Operating Variables on Performance", AIChE, Vol 27, No. 6, p. 984-993, (1981)

Popov, M., "Model Experiments on Atomization of Liquids", National Aeronautics and Space Administration, Technical Transaction F-65, Ad 260-000, (1961)

Quenzel, H., "Determination of Size Distribution of Atmoshperic Aerosol particles from Spectral Solar Radiation Measurements", Journal of Geophysics Research, Vol 75, No. 15, p. 2915, (1970)

Quinn, B. "Ejector Performance at High Temperatures and Pressures", J. Aircraft, Vol 13, p. 948-952, (1976)

Raman, S., "Experimental Optimization of Liquid Injection Parameters in Venturi Scrubber", M.A.Sc. Thesis, University of Windsor, (1977)

Raman, S., "Gas Absorption in a Low Energy Venturi Scrubber", Ph.D. Dissertation, University of Akron, (1983)

Ranger, A. A., and Nicholls, J. A., "Aerodynamic Shattering of Liquid Drops,", AIAA Journal, Vol 7, p. 285, (1969)

Ranz, W. E., "On Sprays and Spraying", Department of Engineering Resources, Pennsylvania State University Bulletin 65, (1956)

Ranz, W. E., "Some Experiments on Orifice Sprays", Canadian Journal of Chemical Engineering, Vol 36, p. 175, (1958)

Rayleigh, W. S., "On the Stability of Jets", Proceedings of the London Mathematical Society, Vol 4, p. 10, (1878)

Razinsky, E. and Brighton, J. A., "A Theoretical Model for Nonseparated Mixing of a Confined Jet", Journal of Basic Engineering, Vol 94 Series D, p. 551-558, (1972)

Rehm, T. R., Moll, A. J. and Babb, A. L., "Carbon Dioxide Absorption by a Jet of Dilute Sodium Hydroxide", AIChE, Vol 9, p. 760, (1963)

Reinecke, W. G. and Waldman, G. D., "Shock Layer Shattering of Cloud Drops in Reentry Flight", AIAA, 13th Aerospace Sciences Meeting, Pasadena, California, AIAA Paper, p. 75-152, January (1975)

Reitz, R. D., "Atomization and Other Breakup Regimes of a Liquid Jet", Ph. D. Dissertation, Princeton University, (1978)

Retel, R., "Contribution to the Study of Injection in Diesel Engines", Pub. Sci. et Tech. du Ministaire de L'Air, B.S.T., No. 81, Cited in Giffen and Murassew, (1953)

Rosin, P. and Rammler, E., "The Laws Governing the Fineness of Powdered Coal", Journal of the Institute of Fuel, p. 29, (1933)

Rowe, P. N., Claxton, K. T., and Lewis, J. B., "Heat and Mass Transfer from a Single Sphere in an Extensive Flowing Fluid", Transaction Instrument Chemical Engineering, Vol 43, p. T14-T31, (1965)

Rupe, J. H., "On the Dynamic Charactheristics of Free Liquid Jets and a Partial Correlation with Orifice Geometry", J.P.L. Technical Report, No. 32, p. 207, (1962)

Ruscello, L. V. and Hirleman, E. D., "Determining Droplet Size Distributions of Sprays with a Photodiode Array", Paper No. WWS/C1-81-49, Fall meeting, Western States Section, The Combustion Institute, (1981)

Rutland, D. F. and Jameson, G. J., "Theoretical Prediction of the Sizes of Drops Formed in the Breakup of Capillary Jets", Chemical Engineering Science, Vol 25, p. 1698, (1970)

Sadek, R., Communication to Bergwerk (1959), Proceedings of the Institution of Mechanical Engineers, Vol 173, p. 671, (1959)

Sauter, J., "Investigation of Atomization in Carburators", National Advisory Committee on Aeronautics, Technical Memorandum 518, (1929)

Schweitzer, P. H., "Mechanism of Disintegeration of Liquid Jets", Journal of Applied Physics, Vol 8, p. 513, (1937)

Scriven, L. E. and Pigford, R. L., "Absorption of Carbon Dioxide in a Rod Like Water Jet", AIChE, Vol 4, p. 439, (1958)

Shifrin, K. S., 1956, Cited in Ko Jen Wu "Atomizing Round Jets", Ph. D. Dissertation, Princeton University, (1983)

Shkadov, V., Ya. "Wave Formation on the Surface of a Viscous Liquid Due to Tangential Stress", Fluid Dynamics, Vol 5, p. 473, (1970)

Skelland, A. H. P., Diffusional Mass Transfer, John Wiley and Sons, New York, (1974)

Slattery, J. C. and Schowalter, W. R., "Effect of Surface Tension in the Measurement of the Average Normal Stress at the Exit of a Capillary Tube through an Analysis of the Capillary Jet", Journal of Applied Polymer Science, Vol 8, p. 1941, (1964)

Sterling, A. M and Sleicher, C. A., "The Instability of Capillary Jets", Journal of Fluid Mechanics, Vol 68, pp. 477, (1975)

Switenbank, J., "Measurement of Unsteady Fluid Dynamic Phenomena", V.K.I. Lecture Series, (1975)

Swithenbank, J., Beer, J. M., Taylor, D. S., Abbot, D., and McCreath, G. C., "A Laser Technique for the Measurement of Droplet and Particle Size Distribution", AIAA Paper 76-69, (1976)

Takashima, Y., "Studies on Liquid Jet Gas Pumps", Journal of Scientific Research Institute, (Tokyo), Vol 46, p. 230-246, (1952)

Tanasawa, Y. and Toyoda, S., "On the Atomization Charactheristic of Injectors for Diesel Engines", Technical Report Tohoku University Vol 21, p. 117, (1956)

Tate, R. W. and Marshall, W. R., "Atomization by Centrifugal Nozzles", Chemical Engineering Progress, Vol 49, p. 169, (1953)

Tate, R. W., "Sprays" Encyclopedia of Chemical Technology, Vol 18, p. 634, (1969)

Taylor, C. F., The Internal Combustion Engine in Theory and in Practice, MIT Press, Cambridge, Massachusettes, (1968)

Tollmien, W., ZAMM, Vol 6, pp. 468-478, (1926), Translated in National Advisory Committee for Aeronautics Technical Memorandum 1085

Tomotika, S., Proceedings of the Royal Society of London, A., Vol 870, p. 322, (1935)

Torda, T. P., "Evaporation of Drops and Breakup of Sprays", Astronautica Acta, Vol 18, p. 383, (1973)

Trolinger, J. D., "Particle Field Holography", Journal of Optical Engineering, p. 22, (1975)

Van Krevelen, D. W. and Hoftijzer, P. J., "Kinetics and Simultaneous Absorption and Chemical Reaction", Chemical Engineering Progress, Vol 62, p. 529-536, (1968)

Virkar, P. D. and Sharma, M. M., "Mass Transfer in Venturi Scrubbers", Canadian Journal of Chemical Enginering, Vol 53, p. 512-516, (1975)

Volgin, B. P., et al., "Absorption of Sulfur Dioxide by Ammonium Sulfite-Bisulfite Solution in a Venturi Scrubber", Industrial and Chemical Enginering, p. 113-118, (1969)

Vyrubov, D. N., Journal of TechnicalPhysics, U.S.S.R., p. 1923, (1939)

Wang, D. P., "Finite Amplitude Effect on the Stability of a Jet of Circular Cross-Section", Journal of Fluid Mechanics, Vol 34, p. 299, (1968)

Wang, T., Lerfald, G. M. and Derr, V. E., "Simple Inversion Technique to Obtain Cloud Droplet Size Parameters Using Solar Aureole Data", Applied Optics, Vol 20, p. 1511, (1981)

Watson, F. R. B., "The Production of a Vacuum in an Air Tank by Means Steam Jet", Proceedings of the Institute of Mechanical Engineers, London, Vol 124, p. 231-300, (1933)

Weber, C., "On the Breakdown of a Fluid Jet", Z.A.M.P., Vol 11, p. 136, (1931)

Wen, C. Y. and Uchida, S., "Absorption of Sulfur Dioxide by Alkaline Solutions in Venturi Scrubber Systems", Ind. Eng. Chem. Process Des. Develop, Vol 12, p. 437, (1973)

Wetzel, H., Ph.D. Dissertation, Unversity of Wisconsin, Madison, (1951)

Whitman, W. G., "The Two Film Theory of Gas Absorption", Chemical and Metallurgical Engineering, Vol 29, No.4, (1923)

Witte, J. H., "Mixing Shocks in Two Phase Flow", Journal Fluid Mechanics, Vol 36, Part 4, p. 639-655, (1969)

Wright, W. A. and Shahrokhi, F., "Investigation of High Mass Ratio Multiple-Nozzle, Air Ejector System", Journal of Space Craft, p. 1489-1491, (1970)

Yamamoto, G. and Tanka, M., "Determination of Aerosol Size Distribution from Spectral Attenuation Measurements", Applied Optics, Vol 8, p. 447, (1969)

York, J. L. and Stubbs, H. E., "Photographic Analysis of Sprays", Transactions of American Society of Mechanical Engineers, p. 1157-1162, October (1952)

Yuen, M. C., "Non-linear Capillary Instability of a Liquid Jet", Journal of Fluid Mechanics, Vol 33, p. 151, (1968)